Mechanisms underlying relapses and remissions in a model of multiple sclerosis: indications for therapy

Woojin Lee

Supervisor: Prof. Kenneth John Smith
Secondary supervisor: Dr. Raj Kapoor

Submitted in partial fulfilment of the requirements to
University College London
for the degree of Doctor of Philosophy

July, 2011

Declaration of contribution

I, Woojin Lee confirm that the work presented in this thesis is my own. Where information has been derived from other sources, I confirm that this has been indicated in the thesis.
Resin embedding and sectioning was carried out by Dr. Daniel Morrison, and half of the workload of processing frozen sections for histology was performed by Dr. Damineh Morsali.

Abstract

Multiple sclerosis (MS) is an inflammatory demyelinating disease of the central nervous system that causes a range of neurological deficits expressed in a series of relapses separated by remissions. Surprisingly, our understanding of the mechanisms responsible for both relapses and remissions remains incomplete, even for the expression of major deficits.

To explore the mechanisms, a model of MS (experimental autoimmune encephalomyelitis, EAE) has been studied neurologically, electrophysiologically and histologically at five time points along the course of the disease, i.e., 'preinduction', 'predisease, 'peak disease', 'remission', and 'relapse'. The animals were assessed daily to determine the magnitude of any neurological deficit, and electrophysiological techniques were developed to permit serial measures of axonal conduction, synaptic transmission, and the excitability of motor neurons. Also, to investigate whether inflammatory factors can modulate the expression of neurological deficits, a pro-inflammatory agent, lipopolysaccharide (LPS) was injected systemically in animals at the 'remission' phase to explore whether systemic inflammation exacerbates the disease. A selective inhibitor of inducible nitric oxide synthase (iNOS), 1400W, was also administered into animals with EAE at the onset of disease expression to examine whether inhibition of nitric oxide (NO) production ameliorates the disease.

The findings have revealed that no electrophysiological deficits were detected before the onset of neurological deficits, but axonal conduction and synaptic transmission were significantly impaired at the 'peak disease'. These measures remained reduced during the 'remission' and 'relapse', at which time motor neuronal excitability was also significantly decreased. It is intriguing that none of the electrophysiological measures have so far revealed changes that correlate closely with the expression of, *and recovery from*, neurological deficit.

Present data also show that systemic inflammation induced by an injection of LPS in animals with EAE caused an acute relapse that peaked 3.5 hours post injection. However, no electrophysiological changes occurring at this peak were detected that could be responsible for the transient neurological deficits, and so the exact mechanisms underlying the deficits remain unknown. Also, based on the histological analysis revealing an exclusive expression of iNOS at 'peak disease' in animals with EAE, the consequences of selective inhibition of iNOS using 1400W were explored. This treatment significantly reduced the severity of the neurological deficits, implicating NO in their production. Importantly, electrophysiological and histological examination of 1400W-treated animals revealed that the inhibition of iNOS also provided significant protection from the loss of function, and degeneration, of axons, again implicating NO in a pathogenic role.

In conclusion, these findings add further weight to the evidence that inflammation plays a key role in the pathogenesis of EAE, although the exact mechanisms underlying the production of the neurological deficits remain unknown. Potential explanations are discussed, including the possibility that the deficits may arise from spinal hypoxia. In addition, the inhibition of NO production may provide an effective protection from both the functional and pathological consequences of neuroinflammatory diseases such as MS.

Acknowledgement

I thank God for helping me throughout my PhD studies, providing me with everything I needed.

I am most grateful to my supervisor Professor Kenneth J Smith, for his support and guidance through my PhD, teaching me how to experiment, write, present and discuss, all in an accurate and responsible manner. Invaluable help was also furnished by current lab members; Amber Hill, Dr Andrew Davies, Dr Daniel Morrison, Diogo Trigo, Dr Norman Gregson, Gregory Delattre, Dr Marianne Kasti, Dr Marija Sajic, Dr Mona Sadeghian, Dr Peter Anderson, Rahda Desai, Roshni Desai, Dr Rouslan Sitnikov, Viorica Robu, and former colleagues; Dr Fengfeng Bei, Dr Frida Laulund, Dr Peter McKintosh, Dr Angelina Mosley by providing me with helpful comments and ideas through lab meetings and research presentations. I would also like to send my special gratitude to Dr Damineh Morsali who has not been only a great colleague, but a wonderful friend. I will not forget the late night experiments and the walk to the Kings Cross station!

I also would like to take this opportunity to thank my loving family for being there for me all the time. Yangsoon Oh, my grandmother and Dr Duckrog Lee, my father who has always provided me with unfailing encouragements and motivation. Mother, Eunsil Joo, who has prayed for me in all circumstances, sister, Dr Woojoo Lee, thank you for your caring advice and preparing for our Christmas gatherings every year, and finally to her husband James Kang. And to all of my friends especially to Jungyoun Yang, for the valuable prayers and support for me. My special thanks go to Jaewon Yoon, you were wonderful throughout, I would never forget the times shared together. Finally, I am extremely grateful for receiving Korean Governmental Overseas Scholarship Grant in Biological studies, and University College London Research Studentship, which enabled me to finish the course without financial difficulties.

Table of contents

List of figures

List of tables

Abbreviation

AG	aminoguanidine
ATP	adenosine-5'-triphosphate
BBB	blood-brain barrier
CDP	cord dorsum potential
CNS	central nervous system
CSF	cerebro-spinal fluid
DA	dark agouti
DAB	diaminobenzidine
DPX	di-n-butyl phthalate xylene
DREZ	dorsal root entry zone
EAE	experimental autoimmune encephalomyelitis
ED1	ectodermal Dysplasia 1
EDSS	expanded disability status scale
EMG	electromyography
eNOS	endothelial nitric oxide synthase
EP	evoked potential
F wave	foot wave
fMRI	functional magnetic resonance imaging
Gd-DTPA	diethylenetriaminepentaacetic acid−gadolinium
GFAP	glial fibrillary acidic protein
H reflex	Hoffmann reflex
IFA	incomplete Freund's adjuvant
IFN-γ	interferon-gamma
IL-10	interleukin-10
IL-18	interleukin-18
iNOS	inducible nitric oxide synthases
L-NAME	N-nitro-L-arginine-methylester
L-NMA	N-methyl-L-arginine

LPS	lipopolysaccharide
M response	muscle response
MBP	myelin basic protein
MCP-1	monocyte chemotactic protein-1
MHC	major histocompatibility complex
MOG	myelin oligodendrocyte glycoprotein
MS	multiple sclerosis
NADPH	nicotinamide adenine dinucleotide phosphate
NMDA	*N*-methyl *D*-aspartate
NMMA	N-monomethyl-L-arginine
NNA	N-nitroarginine
nNOS	neuronal nitric oxide synthase
NO	nitric oxide
NOS	nitric oxide synthase
PBS	phosphate buffered saline
PD	peak disease
PI	preinduction
PLP	proteolipid protein
PNS	peripheral nervous system
PP-MS	primary progressive multiple sclerosis
PreD	predisease
PVG	Piebald Virol Glaxo
REL	relapse
REM	remission
RP-MS	progressive relapsing multiple sclerosis
RR-MS	relapsing remitting multiple sclerosis
SAM	synaptic activation of motor neurons
SCAP	sensory compound action potential
SEP	sensory evoked potential
SP-MS	secondary progressive multiple sclerosis
TCR	T cell receptor

TNF-α	tumour necrosis factor-alpha
VEP	visual evoked potential

Chapter 1

Introduction

Chapter 1. Introduction

1.1. Multiple sclerosis (MS)

Multiple sclerosis (MS) is a disease of the central nervous system, characterised by inflammation, demyelination and axonal degeneration. It is the most common disabling neurological disease among young adults and it affects around 85,000 people in the UK and approximately 2.5 million people between 17 and 65 years old worldwide, with an incidence of approximately 7 new cases per 100,000 person years at risk (Compston and Coles 2002;Kantarci and Wingerchuk 2006). Many attempts have been made to identify the cause of MS, and to date, a number of complex genetic, environmental factors have been suggested to be involved. Among the genetic factors, MHC class II genes have been reported to be strongly involved (Ramagopalan et al. 2009), which was amongst the earliest studied in the field of MS genetics. Environmental factors related to MS include gender (Eikelenboom et al. 2009), vitamin D intake (Solomon and Whitham 2010), and viral infections (Lipton et al. 2007).

1.1.1. Clinical manifestations and disease course of MS

MS is a chronic debilitating disease that reduces the lifespan by an average of seven to eight years (Trapp and Nave 2008), and the clinical symptoms and disease course are widely variable. The common clinical symptoms involved are loss of vision, motor weakness, sensory loss, gait impairment, cognitive impairment, bladder dysfunction, mood disorders, sexual dysfunction, pain and fatigue (Boissy and Cohen 2007). In 1996 the terminology used to describe the pattern and course of MS was standardised under the auspices of the National Multiple Sclerosis Society of the USA (Lublin and

Reingold 1996), which classified the disease course in four different categories. These categories are described below.

1) Relapsing-remitting (RR) MS : clearly defined disease relapses with full recovery or with sequelae and residual deficit upon recovery; periods between disease relapses characterised by a lack of disease progression.

2) Primary-progressive (PP) MS : disease progression from onset with occasional plateaus and temporary minor improvements allowed.

3) Secondary-progressive (SP) MS : initial RR disease course followed by progression with or without occasional relapses, minor remissions, and plateaus.

4) Progressive-relapsing (RP) MS : progressive disease from onset, with clear acute relapses, with or without full recovery; periods between relapses characterised by continuing progression.

Approximately 15% of MS patients experience a primary-progressive (PP) disease course, and 85% exhibit a relapsing-remitting (RR) disease course, later going through periodic exacerbations and entering the progressive phase (Compston and Coles 2002). As relapse and remissions have been the characteristic features of MS, they have long been used as a tool to study the aetiology and pathogenesis of MS, and to assess the therapeutic efficacy of potential treatments. However, the exact cause and mechanisms underlying the disease phases are not fully understood. The next section describes the potential mechanisms responsible for relapse and remissions in MS and EAE that have been reported so far.

1.1.2. Possible mechanisms of relapse and remissions in MS

1.1.2.1. Mechanisms of relapse

The types and duration of symptoms that MS patients experience from the occurrence of relapses are heterogeneous. The reason for this heterogeneity is not fully revealed, but it may be due to a combination of different pathological events ranging from infection, psychological stress, molecular characteristics, inflammation, and demyelination.

Infection

A number of studies have suggested the association of clinical symptoms and viral or bacterial infections (Edwards et al. 1998;Confavreux 2002;Giovannoni et al. 2006). The authors generally propose that relapse can occur through epitope mimicry between microbial and self-antigens inducing the activation of the immune system, followed by migration of immune cells into the CNS. These cells such as blood-born mononuclear cells and autoreactive T cells secrete inflammatory cytokines and inflammatory mediators which contribute to local inflammation. Secondary effects such as fever from the infection have also been found to induce pseudo-relapse. This has been reported both clinically (described as Uhthoff's phenomenon (Uhthoff 1890)) and experimentally, that hyperthermia may exacerbate the symptoms by causing conduction block in peripheral and central axons (Davis and Jacobson 1971;Bajada et al. 1980;Pender and Sears 1984).

Stress

The description of the potential link between stress and MS symptoms was first made by Charcot (Charcot JM 1877) who noted that grief, vexation and changes in social circumstances may relate to exacerbations. More recently, a number of studies have appeared reporting a positive correlation between psychological stress and symptoms (Rabins et al. 1986;Mohr et al. 2004;Artemiadis et al. 2011). A systematic and quantitative meta-analysis performed by Mohr *et al*, reported a consistent association suggesting that stress management may be of therapeutic value (Mohr et al. 2004). However, controversies have arisen due to the uncertain nature of any biological mechanisms, and due to the variability in measurement of stress, both of which encourage limitations in interpreting the results. Indeed, a recent study from Riise et al (Riise et al. 2011) reported that there was no increased risk of MS associated with severe stress. At present, further analyses are required to explore whether stress causes relapses in patients with MS and, if so, research is needed to determine the mechanisms involved.

Molecular characteristics

Recent studies employing molecular biological techniques have improved our knowledge of MS pathophysiology. The molecular characteristics of MS may be used as biomarkers for predicting the onset and duration of relapses, and may also help selecting the accurate therapeutical interventions. MHC class II genes (Ramagopalan et al. 2009) and IL-7 receptor (Lundmark et al. 2007) genes have been found to be associated with higher risk of developing MS. Also, a molecular trio has been reported which explains the mechanism behind relapse and remissions. The binding of α4β1 integrin on T lymphocytes with osteopontin expressed on inflamed endothelium induces relapses by stimulating the expression of pro-inflammatory cytokines (Chabas

et al. 2001;Jansson et al. 2002) and by inhibition of apoptosis of autoreactive immune cells (Hur et al. 2007). However, αB crystallin is the molecule that acts as a chaperone to this pair, which inhibits NF- κB mediated transcription of pro-inflammatory cytokines therefore contributing to remission (Ousman et al. 2007).

Inflammation

A number of clinical studies reported the key role of inflammation in causing deficits. Youl and others found that the leakage of Gd-DTPA was associated with exacerbation of clinical symptoms such as abnormal visual acuity and reduction of the visual evoked potentials in patients with optic neuritis (Youl et al. 1991). The role of cytokines such as TNF-α and IFN-γ have also been reported in patients with MS as the increased levels correlated with significant worsening of the symptoms or re-awakening of pre-existing symptoms (Moreau et al. 1996). In addition, although axonal injury was generally considered to be a sequel of demyelination, it was reported that axonal injury could be mediated by inflammatory cells such as macrophages, microglia, and CD8 + T lymphocytes, independent of demyelination from autopsy tissues of MS patients (Bitsch et al. 2000).

The exact mechanisms of the neurological deficits induced by inflammation remain speculative, but it has been generally accepted that the autoreactive T lymphocytes and their soluble mediators play an important role in the pathogenesis of MS. Infiltration of these T lymphocytes occurs in MS lesions through penetration of the blood-brain barrier (BBB) and mediates damage of the myelin sheaths. These cells may also be responsible for axonal injury (Booss et al. 1983;Bitsch et al. 2000;Fletcher et al. 2010), and CD8+ T lymphocytes have been implicated in the production of neurological deficits via mechanisms involving perforin (Murray et al. 1998;Friese and Fugger 2009). The cytokines produced by the T cells such as TNF-α and IFN-γ may also induce the production of a powerful inflammatory mediator, inducible nitric oxide

synthase (iNOS), for which a role has been implied in impairing neurological functions in both MS and EAE (MacMicking et al. 1992;Bo et al. 1994;Willenborg et al. 2007). It has been reported that increased level of nitric oxide (NO) produced by its induced synthase may cause axonal degeneration at physiological frequencies of impulse conduction (Smith et al. 2001), and also that it has an effect on the sodium and potassium channels upon which conduction depends (Ahern et al. 1999;Ahern et al. 2000). Furthermore, mitochondrial activity can also be impaired by NO, which could lead to lack of ATP in axons preventing them from maintaining their normal functions (Bolanos et al. 1997). Further detailed role of NO in lesions of MS and EAE are described in a later section.

Synaptic dysfunction

Inflammation has also been reported to affect synaptic transmission, causing impaired function in the grey matter. Several factors including IL-2 (Park et al. 1995), TNF-α (Tancredi et al. 1992), IFN-γ (D'Arcangelo et al. 1991) and especially NO were reported to disturb synaptic transmission in the grey matter (Fossier et al. 1999), which may lead to axonal degeneration in combination with impaired sodium channels (Smith 2007), NMDA receptors (Piani et al. 1991), and raised glutamate release (Pitt et al. 2000).

Demyelination

Demyelination is a hallmark of MS pathology, which is the most well known cause of conduction block responsible for the neurological deficits. Demyelination can happen segmentally, when the myelin is lost between the two adjacent nodes (i.e. segmental demyelination), or by nodal widening occurring from the loss of myelin from the paranodes (Waxman 1989;Smith and Hall 2001;Wolswijk and Balesar 2003). This

conduction failure is due to lack of sodium channels in the exposed axolemma, as the density of the channels is much lower for normal conduction (Waxman 1989;Waxman and Ritchie 1993). In addition, it has been reported that demyelinated axons have a low safety factor for conduction (near 1 in demyelinated axons, whereas in normal myelinated axons it is around 3-5) (Smith 1994). This implies that any subtle changes to the environment which might affect the safety factor such as temperature (Davis 1970) can hinder normal conduction.

1.1.2.2. Mechanisms of remission

Remission occurs in patients with MS for variable time periods, often followed by another relapse. This remission may occur by means of counterbalancing some of the factors listed above, such as through remyelination or resolution of inflammation. Remyelination occurs in response to demyelination by the recruitment of oligodendrocyte precursor cells (Sim et al. 2002), where these cells restore myelin sheaths engaging the axon (Watanabe et al. 2002), and enabling recovery of saltatory conduction of action potentials (Smith et al. 1979;Nave and Trapp 2008). However, this restoration of conduction may also occur in the absence of remyelination, when new sodium channels appear in the denuded axons. It has been reported that aggregations of sodium channels were found along the demyelinated axolemma enabling slow conduction (Black et al. 1991;Felts et al. 1997). The appearance of sodium channels has also been found in astrocytes in lesions, which may support Na+/K+ ATPase-dependent ionic homeostasis in areas of injury (Black et al. 2010).

On the other hand, resolution of inflammation within the lesions can also influence the recovery in patients as reported by Youl and others (Youl et al. 1991). They have found that clinical recovery was associated with the cessation of leakage across the blood- optic nerve barrier. Also, the resolution of inflammatory mediators such as NO was found to reverse blocked conduction within experimentally demyelinated axons

(Redford et al. 1997).

Furthermore, adaptive changes in the cerebral cortex may contribute to the recovery of symptoms evidenced by fMRI studies in MS patients (Pantano et al. 2006;Cerasa et al. 2006). These adaptive changes could be comparable to cortical reorganisation occurring as a consequence of a CNS injury, by strengthened synaptic connections or regulation of neurotransmitters and their receptors (Endo et al. 2009).

1.2. Experimental autoimmune encephalomyelitis (EAE)

Animal models of multiple sclerosis are indispensable for understanding the aetiology and pathology of the disease, as there is limited access to human tissue from MS patients. The animal models reflect the different clinical courses and pathology of MS, depending on the method of disease induction. One common method is employing viral infection, based on the ground that viral infection plays an instrumental role in the development of CNS autoimmunity. For example, Theiler's murine encephalomyelitis virus and corona virus infect and damage oligodendrocytes resulting in destruction of myelin (Grigoriadis and Hadjigeorgiou 2006). Alternatively, neurotoxicants such as cuprizone have been used to induce demyelination by oral administration (Blakemore 1972;Matsushima and Morell 2001), to produce central demyelinating lesions. However, experimental autoimmune encephalomyelitis (EAE) is so far the most intensively studied models of MS that can be produced by active sensitization to particular tissue or protein components of the central nervous system, or by passive transfer of autoreactive T cells (Stromnes and Goverman 2006). The characteristics of the disease induced rely on the type of antigen used for sensitization, and the species or the strain of the animal used. The first actively induced EAE was developed in 1933 when Rivers *et al*. showed EAE was induced in primates when immunized with normal rabbit brain tissue (Rivers 1933). Additionally, the passively induced EAE model was developed subsequently in 1960 by transfer of lymph node

cells from rats immunised with spinal cord homogenates into naïve animals (Paterson 1960).

There are a number of types of EAE which reflect the heterogeneous pathology of MS depending on the method of induction (active or passive), type of antigen used for sensitization (e.g. myelin basic protein (MBP), proteolipid protein (PLP), and myelin oligodendrocyte protein (MOG) (Muller et al. 2000)), and the type of animal/strain used. Depending on these factors, animals express different types of neurological deficits. The classic neurological deficits are expressed by ascending flaccid paralysis, presented as having a flaccid tail leading to paralysed limbs (Stromnes and Goverman 2006). However, while a number of experimental models present an acute disease course, fewer models show a chronic progressive or relapsing pattern (Skundric 2005).

1.2.1. Relapsing-remitting EAE

Relapsing-remitting EAE is a useful model employed for understanding the aetiology and pathology of multiple sclerosis, as a high proportion of patients suffer from this relapsing form. However, the exact mechanisms causing the different stages of the disease are not clearly understood.

Recent research has elucidated a number of mechanisms underlying the relapses using various models of EAE exhibiting a relapsing remitting form (Skundric 2005). The role of mononuclear cells has been reported in EAE, that the reappearance of these cells was associated with relapses (Bjartmar and Trapp 2003). Furthermore, convincing evidence in EAE has demonstrated that the occurrence of epitope spreading also contributes to relapses, resulting from increased immune reactivity against an expanding array of myelin target epitopes (Tuohy et al. 1998;Miller and Eagar 2001;Steinman 2004). Also the role of chemoattractants such as chemokines or cytokines was implicated in the relapsing disease, inducing further inflammatory

attacks (Imitola et al. 2005;Engelhardt 2008). Macrophage chemoattractant protein-1 (MCP-1) which belongs to a CC family of chemokines regulates the influx of macrophages and memory T cells into the CNS (Mahad and Ransohoff 2003). It has been shown that the expression of MCP-1 correlated with the severity of the disease in EAE, and when these animals were treated with anti-MCP-1 antibodies the relapse rate was significantly reduced (Karpus and Kennedy 1997). Others reported the regulatory role of IL-16, a CD4+ T cell chemoattractant cytokine in the pathogenesis of EAE. The level of IL-16 in the CNS correlated positively with the number of infiltrating CD4+ and CD8+ T cells during the relapses, and animals that were treated with anti-IL-16 antibodies showed amelioration of the neurological deficits (Skundric et al. 2005).

1.2.2. rMOG-EAE induced in DA rats

Myelin oligodendrocyte glycoprotein (MOG) is a type I membrane glycoprotein exclusively expressed in the CNS (Linington and Lassmann 1987), which induces a type of EAE in animals when injected as an emulsion with an adjuvant. MOG is highly conserved between species including human, rat, mouse, and bovine species (Hilton et al. 1995), and it has been reported that the pathology occurring as a consequence of an injection of MOG in DA rats closely resembles Pattern Ⅱ lesions, which are arguably the most frequent type of MS lesions (Storch et al. 1998;Schubart A 2001). The lesions are characterised by infiltration of autoimmune T and B lymphocytes, perivenous phagocytic cells, widespread demyelination and relative sparing of axons, in the context of complement binding. Not only are the lesions similar to MS, but the incidence of the disease in DA rats is very high (95.28%) and reproducible (Storch et al. 1998). The rats can exhibit a chronic disease course, making the model an attractive tool for studying the mechanisms of relapsing-remitting MS: for these reasons the model was chosen for the present study. Although

the exact pathomechanisms responsible for the disease expression in this model remain to be elucidated, it has been reported that the first peak of disease may be driven by inflammation mainly by autoimmune CD4+ Th1 cells which induce the recruitment and activation of ED1+ macrophages. MOG-specific autoantibodies have been attributed as the driving force for inducing demyelination in the relapses during the progressive phase of the disease (Schubart A 2001).

1.3. Electrophysiological studies in EAE

In comparison with the number of studies on EAE (8348 articles in Pubmed), relatively few (only 13) have examined the disease electrophysiologically. Indeed few investigators appear to have wondered why the animals have a neurological deficit, and the assumption appears to have been that the deficits are due to demyelination. Prior to these electrophysiological investigations, it was widely believed that neurological deficits in EAE, such as tail or hindlimb weakness, were due to CNS lesions similar to MS. However, whilst chronic relapsing models of EAE showed large plaques of demyelination in the CNS, such plaques were rare or absent in acute EAE. It was hypothesised that the cause of neurological deficits in these animals were due to other factors such as oedema (Paterson 1976), or an impairment of monoaminergic neurotransmission (Carnegie 1971). However, histological evidence had challenged this hypothesis by reporting pathology in the PNS of acute EAE animals (WAKSMAN and ADAMS 1955). In light of these evidences, Pender *et al* conducted studies investigating the cause of neurological deficits and found evidence indicating that the conduction block was due to demyelination occurring in both the CNS and PNS. The reported sites of predilection for demyelination in the CNS were the dorsal root entry zones and the ventral root exit zones. In the PNS, the dorsal root ganglia and spinal roots were frequently affected.

The studies were conducted in rabbits (Pender and Sears 1982;Pender and Sears 1984) and Lewis rats (Pender and Sears 1986;Pender 1986a;Pender 1986b;Pender 1988a;Pender 1988b;Pender 1989;Stanley and Pender 1991;Deguchi et al. 1992;Chalk et al. 1994;Chalk et al. 1995) either inoculated with whole spinal cord, MBP or PLP to induce EAE. In the rabbits and rats inoculated with whole spinal cord to induce EAE, demyelination of the dorsal root ganglia and the dorsal root entry zone were suggested as the cause of conduction block (Pender and Sears 1982;Pender and Sears 1984;Pender and Sears 1986;Pender 1986a;Pender 1988b). In these rats the ventral root exit zones were also reported to be a site for demyelination (Pender 1986b). In the rats with EAE induced by inoculation with MBP, demyelination and nerve conduction abnormalities were demonstrated in the dorsal roots, dorsal root entry zones, ventral roots and ventral root exit zones (Pender 1986a;Pender 1988b;Pender 1989). Additionally a study on passively induced EAE in rats by transferring T lymphocytes activated against MBP showed that the impaired conduction was due to the slowing of afferent conduction within the dorsal column and spinal roots from demyelination (Heininger et al. 1989). On the other hand, in animals with PLP-induced EAE, the demyelination induced conduction block was restricted to the CNS which implies that PLP or other antigen confined to the CNS such as MOG could be the target antigen in MS (Chalk et al. 1994). In addition to these studies suggesting the cause of neurological deficits, the mechanism of clinical recovery in animals with acute EAE and chronic relapsing EAE was explained by remyelination in both CNS and PNS, by oligodendrocytes and Schwann cells respectively (Pender 1989;Stanley and Pender 1991). Notably, the incomplete recovery of conduction block in the chronic relapsing EAE animals exhibited at late remission were attributed to axonal degeneration (Stanley and Pender 1991).

Various electrophysiological methods were used in these studies to investigate the cause of neurological deficits. Recordings from the ‘volume conductor’ were used to reveal the site of axonal conduction block in some studies (Pender and Sears 1982;Pender and Sears 1984;Pender and Sears 1986;Pender 1986a;Pender

1986b;Pender 1988a;Pender 1988b;Pender 1989;Stanley and Pender 1991), and the monosynaptic reflex pathway was examined by recordings of the H reflex (Pender 1987;Pender 1988a;Pender 1989;Stanley and Pender 1991). Furthermore, to investigate the afferent conduction pathways, recordings were made of the spinal cord dorsal column compound action potential (Stanley and Pender 1991;Chalk et al. 1994;Chalk et al. 1995) and the cerebral cortical somatosensory potential, typically evoked by stimulation of the sciatic nerve (Deguchi et al. 1992).

In summary, these studies concluded that demyelination occurring both in the CNS and PNS is the main cause of the neurological deficits. This belief was further supported by observations that the axons had impaired ability to transmit trains of impulses and were susceptible to temperature changes, namely characteristics of demyelinated axons (Stanley and Pender 1991).

1.4. Nitric oxide (NO) in MS/EAE and implications for therapy

1.4.1. Nitric oxide (NO) and its dual role

Nitric oxide (NO) is a free radical, inorganic gas produced by the oxidation of the terminal guanidine nitrogen of arginine, and catalysed by an NADPH dependent enzyme, nitric oxide synthase (NOS) (Stuehr and Marletta 1987). It is produced in many types of cells in the body (Marletta 1993), and has been implicated in a variety of inflammatory mediated disorders occurring in the joint, gut, lung and brain (Moncada and Higgs 2006;Sharma et al. 2007). Under normal physiological conditions, neuronal cells and endothelial cells produce NO by neuronal NOS (nNOS or NOS1) and endothelial NOS (eNOS or NOS3) respectively, which are constitutively expressed and activated in response to intracellular calcium/calmodulin levels (Bredt and Snyder 1990). NO produced by nNOS acts as a neurotransmitter (Stuehr and Marletta 1987), whereas eNOS-derived NO regulates vascular tone (Ignarro 1989), adhesion of circulating blood cells and inhibits platelet aggregation (Kubes et al. 1991). In abnormal conditions however, such as in response to inflammatory stimuli for instance cytokines or lipopolysaccharide, the inducible isoform of NOS (iNOS or NOS2) is expressed in many cell types including macrophages, microglia, neutrophils, and it produces the NO in a calcium-independent manner, producing NO in large quantities (Salter et al. 1991).

Several reports suggest that NO may possess a dual role; a destructive or a protective role in an inflammatory environment. One study that supports the 'destructive' role of NO described that NO could down-regulate the synthesis of IL-6, yet up-regulate the production of TNFa in a macrophage cell line, exerting cytotoxic action on the cells, which may contribute to tissue destruction (Deakin et al. 1995). NO itself does not only act as a reactive radical, but also reacts with superoxide anion ($O_2^{\bullet-}$) to generate

the peroxynitrite anion ($ONOO^-$), which is an even stronger oxidant (Beckman et al. 1990). Also, NO derived from activated microglia and astrocytes has been implicated in the damage of myelin-producing oligodendrocytes (Merrill et al. 1993;Koprowski et al. 1993) in EAE models. Furthermore, in MS patients NO has been reported to affect the integrity of the blood-brain barrier (BBB) as the nitrite and nitrate concentrations in the cerebrospinal fluid correlated with BBB breakdown (Giovannoni 1998). NO has also been demonstrated to cause vasodilation which may also assist the inflammatory process (Xiao et al. 1996).

On the contrary, the 'protective' role of NO was introduced from reports showing that NO down-regulates immune responses by suppressing Ia expression of activated macrophages (Sicher et al. 1994), where increased expression of Ia molecules has been reported in EAE (Stoll et al. 1993). Moreover, NO produced by macrophages has been shown to inhibit lymphocyte (Denham and Rowland 1992), and also to inhibit the adhesion of leucocytes to the vascular endothelium (Kubes et al. 1991). The dual roles of NO described so far suggest that experiments which aim to explore the role of NO using inhibitors of nitric oxide synthases (NOS) may provide complex results.

1.4.2. Nitric oxide (NO) in MS

The presence of NO and induction of iNOS have been reported in the inflammatory demyelinating plaques of patients with MS. Bo *et al* demonstrated NADPH diaphorase histochemical staining in the brains of MS patients, and also concluded that the majority of these cells which produced NO were astrocytes since these cells showed immunoreactivity to glial fibrillary acidic protein (GFAP) (Bo et al. 1994). Furthermore, they showed that levels of iNOS mRNA were significantly higher in patients' brain with MS compared to control groups. Another group reported that nitrated proteins in MS lesions co-localised with mRNA of iNOS in macrophages or microglia (Bagasra et al. 1995). This finding suggests that not only NO exists in these

lesions, but also peroxynitrite anion ($ONOO^-$) could be present since protein nitration was observed. In addition, the presence of NO in patients was also detected by examining the concentration of nitrite and nitrate within the CSF (Cross et al. 1998;Brundin et al. 1999), and from the significantly raised nitrotyrosine levels (Zabaleta ME et al. 1998).

1.4.3. Nitric oxide (NO) in EAE

Numerous studies have attempted to detect the presence of NO or NOS in EAE to understand the pathological role of these molecules, and apply the knowledge for developing therapy. Macmicking *et al* first reported that NO and superoxide anion ($O2^{\bullet-}$) was released from neutrophils and mononuclear cells isolated from Lewis rats with acute guinea pig spinal cord homogenate-induced EAE (MacMicking et al. 1992). A year afterwards, Koprowski *et al*. described that iNOS mRNA was found broadly along the disease course of EAE in the brains of Lewis rats induced with MBP (Koprowski et al. 1993). Other studies followed, reporting the positive correlation of iNOS expression with the severity of neurological signs, in animals induced with EAE. For example, in the studies of Van Dam *et al*, the authors concluded that the altered functions of the brain in Lewis rats induced with EAE by guinea pig spinal cord homogenate may be due to the infiltration of iNOS positive peripheral macrophages (Van Dam et al. 1995). These cells were detectable at 15 days post induction of EAE coinciding with the symptoms such as paresis and paralysis of tail and/or hindlimbs. An interesting study by Okuda *et al* explored the presence of iNOS at different time points along the EAE disease course (induced in mice with rabbit MBP), and showed that iNOS was most highly expressed at the peak of the disease where animals showed severe or complete hindlimb paralysis (Okuda et al. 1995). Again, the iNOS positive cells were mostly macrophages, and the authors suggested that the excessive NO production by these cells could be responsible for the damage in the central nervous system in EAE.

1.4.4. Nitric oxide (NO) and loss of function

How inflammation impairs function is still not clearly understood, but there is growing evidence on the role of NO in the loss of neurological functions. An interesting study from Redford *et al* reported that NO caused a reversible conduction block in both normal and demyelinated axons (Redford et al. 1997), which implies that NO may contribute to clinical deficits in inflammatory diseases of the nervous system. A possible mechanism has been suggested, that NO may affect axonal conduction by directly impairing the function of axonal channels including sodium channels (Li et al. 1998;Ahern et al. 2000), potassium channels(Ahern et al. 1999) and calcium channels (Kurenny et al. 1994). NO may also impair conduction by inhibiting the Na^+/K^+ ATPase activity in an autocrine fashion causing depolarisation of the axons (Guzman et al. 1995). In addition, various redox forms of NO can also modify the NMDA receptors (Choi and Lipton 2000;Amitai 2010), therefore affecting synaptic transmission. Another role of NO has also been implied in causing axonal degeneration, known as a major cause of permanent deficits in MS. Smith *et al* described that the combination of normal impulse traffic and NO at sites of inflammation may cause axonal degeneration, as they observed early stages of wallerian degeneration in the dorsal roots stimulated at 50 or 100Hz, exposed to NO (Smith et al. 2001). NO has also been reported in hindering ATP production by mitochondria by outcompeting oxygen for binding at cytochrome C oxidase (Cleeter et al. 1994;Bolanos et al. 1997;Brown and Borutaite 2002). This inadequate ATP production prevents ATPase pumps, such as the Na^+/K^+ pump, from working properly, which may have a damaging effect on the axons, as it produces intra-axonal Na^+ accumulation leading to a build up of Ca^{2+} entry due to Na^+/Ca^{2+} exchanger activity, similar to what happens to axons in ischemia (Stys et al. 1991;Waxman et al. 1994;Lehning et al. 1996;Kapoor et al. 2003). Furthermore, the peroxynitrite anion ($ONOO^-$), produced from the combination of NO with superoxide anion ($O2^{\bullet-}$), may

induce cytochrome C release from the inter-membrane space causing apoptosis (Su et al. 2009).

1.4.5. Studies using inhibitors of nitric oxide synthase (NOS) in EAE

Based on the studies suggesting pathological roles of NO, a number of attempts were made to treat EAE using NOS inhibitors. Most of the studies using NOS inhibitors were performed during the late 1990s, starting with a study from Cross *et al* (Cross et al. 1994). They used aminoguanidine (AG) which is a selective iNOS inhibitor in SJL mice with adoptively transferred EAE, and showed that AG inhibited the expression of disease, suggesting a destructive role of NO. The use of AG was further proved to prevent EAE in adoptively transferred EAE in rats (Zhao et al. 1996) and actively induced EAE with MBP in mice (Brenner et al. 1997). Subsequently more studies emerged testing NOS inhibitors in animals with EAE, and the destructive role of NO was further supported by the positive correlation of the iNOS expression with the disease activity (Van Dam et al. 1995;Cross et al. 1996;Zhao et al. 1996;Brenner et al. 1997). Furthermore, nitrotyrosine, which is a marker for peroxynitrite-induced damage was detected in mononuclear inflammatory cells and CD4+ T cells in adoptive EAE in mice (van, V et al. 1997), and was also found to correlate with the peak of disease in the spinal cord lesions of mice with EAE (Okuda et al. 1997).

However, a study conducted by Zielasek *et al* reported that no amelioration of the disease was found using different types of NOS inhibitors such as AG, N-monomethylarginine (NMMA), N-nitroarginine (NNA), and in fact even that such therapy could exacerbate the neurological deficits in Lewis rats induced with MBP-EAE (Zielasek et al. 1995). It was suggested for the first time from this study that NO may possess a complex role in EAE. Another study using a non-selective NOS inhibitor N-nitro-L-arginine-methylester (L-NAME) and N-monomethyl-L-arginine (NMMA) in active EAE in Lewis rats, reported that the therapy aggravated the

neurological deficits, and supported an immunosuppressive role of NO in the disease process (Ruuls et al. 1996). In addition, iNOS knockout (-/-) mice with EAE were reported to show greater incidence and higher neurological scores than the wild type controls, and also were less able to recover from the deficits (only 19% of iNOS -/- mice had recovered compared with 82% of wild type animals) (Fenyk-Melody et al. 1998).

So far many authors speculated that the contradicting outcomes of the studies using NOS inhibitors in EAE may be due to the use of different methods of EAE induction, the type of the inhibitor, different administration routes and dosing schedules of the inhibitors. Indeed a paper from Okuda *et al* reported that the timing of treatment using AG in mice with active EAE at different times along the disease course of EAE can be crucial (Okuda et al. 1998). The administration of AG from day 2 to day 12 after immunization caused a significant delay in the onset of EAE, but administration for 10 days after the onset of EAE enhanced both the neurological deficits and the mortality rate, and also accelerated the onset of relapse significantly. The authors concluded that NO is a pathogenic factor in the induction phase but has an inhibitory role in the progression phase, and suggested that timing should be taken into consideration in designing treatments in both EAE and MS. Moreover, a few studies have suggested that the amount of NO that can be produced varies between strains or genders of animals, and this could influence the susceptibility of the disease and may explain the contradictory outcomes of experiments using NOS inhibitors. Cowden *et al* described that PVG rats, which have low susceptibility to EAE, had significantly increased serum NO levels after the induction of MBP-EAE, compared with Lewis rats (Cowden et al. 1998). When the PVG rats were treated with N-methyl-L-arginine (L-NMA) a NOS inhibitor, the rats acquired high susceptibility to EAE and showed decreased NO levels. Hence the authors reported a protective role of NO, as the lymph node cells isolated from the inhibitor-treated PVG rats with EAE showed higher proliferation rate than the controls. This finding implies that NO may down-regulate EAE by inhibition of T cell proliferation. On the contrary, female SJL/J mice expressed higher levels of

NO and developed more severe EAE compared with males, suggesting a destructive role of NO in the pathogenesis of EAE (Ding et al. 1997).
Altogether these studies imply that more intensive studies on the role of NO are required to understand the exact mechanisms underlying the disease course of EAE and are indispensable for future application of therapy in patients with MS.

- **1400W, a selective inhibitor of iNOS**

1400W dihydrochloride [N-(3-(Aminomethyl)benzyl)acetamidine.2HCl] identified by Garvey *et al*, is a highly selective iNOS inhibitor versus both eNOS (greater than 5000 fold) and nNOS (greater than 200 fold) in both human and rats (Garvey et al. 1997). 1400W inhibits NOS by binding at the arginine-binding site in competition with L-arginine (Alderton et al. 2001). It has been reported that no reversal of inhibition occurred after two hours of injection; hence 1400W is either irreversible or only very slowly reversible (Garvey et al. 1997). 1400W has been used in several animal models in the field of cancer studies (Thomsen et al. 1997), diabetes (Cheng and Pang 2004), traumatic brain injury (Jafarian-Tehrani et al. 2005), but so far no reports on EAE have been found.

Chapter 2
Aims of thesis

The first aim of this thesis is to optimise electrophysiological tests in naïve animals to obtain reliable and reproducible recordings, in order to detect any neurological dysfunction in animals induced with EAE. The second aim is to characterise the pathophysiology of animals with EAE at each five key stages along the disease course ('preinduction', 'predisease', 'peak disease', 'remission', 'relapse'), using neurological, electrophysiological and histological assessments. Finally, in order to explore whether modulation of inflammatory factors affect the disease course, a proinflammatory agent LPS and a selective iNOS inhibitor 1400W are used in these animals, and any changes will be detected by employing the set of assessments described above.

Chapter 3

Development of in vivo electrophysiological techniques

Chapter 3. Development of in vivo electrophysiological techniques

3.1. Introduction and aims

Serial *in vivo* electrophysiological examinations can be useful when testing neurological functions in live animals, as it may reduce experimental errors that are more prone when results are compared between different animals. In this chapter, I developed methods of electrophysiological tests in order to obtain serial recordings reliably. These techniques have been successfully applied to the animals with EAE and the results are described in the following chapter.

The aim of this chapter is firstly to introduce electrophysiological tests that were used to examine the animals. The electrophysiological tests were employed to examine 'axonal conduction', 'motor neuronal excitability', 'synaptic transmission', and 'synaptic activation of motor neurons' within the central nervous system. Secondly, each of these tests was optimised by looking at several factors which may contribute to the reliability of these recordings. For example, the type of anaesthesia used, frequency of stimulation, and limb temperature were explored on motor neuronal excitability. In addition, the effect of electrode positioning was investigated on recording synaptic transmission. Finally, I aimed to develop a new method of examining the synaptic activation of motor neurons in the ventral horn.

3.2. Methods

3.2.1. Animals

Female Dark Agouti rats weighing 150-180 grams were purchased from Harlan Laboratories (UK), and were housed for one week prior to induction of EAE. Rats were kept in groups of four to five per cage, and housed in the animal unit (Denny Brown Laboratories) at the Institute of Neurology, University College London. Animals were kept under controlled temperature (between 18~22°C) and maintained in a 12hr light/dark cycle in the unit. All procedures were carried out in accordance with the requirements of the Animals (Scientific Procedures) Act 1986 and with ethical committee approval under a UK Home Office License.

3.2.2. Anaesthesia

The rats were anaesthetised by inhaling 2 % isoflurane (Agar Scientific Ltd, UK) or by intraperitoneal injection of a combination of 90mg/kg of ketamine (Fort Dodge Animal Health Ltd, UK) and 10mg/kg of xylazine (Animal Care Ltd, UK). The ketamine/xylazine combination was made as a stock solution and kept for less than a week at room temperature.

3.2.3. In vivo electrophysiological assessments

The rectal temperature of the rat was monitored during anaesthesia for electrophysiological assessment, and was maintained in the range of 36-37 °C by a heated blanket or by radiant heat when necessary. The temperature of the foot was monitored by a thermistor attached to the plantar surface of the foot. Electrophysiological examination was performed using needle electrodes. Compound responses were evoked using a signal generator (Neurolog module NL300, Digitimer, UK) and an isolated stimulator (DS2, Digitimer, UK). Signals were recorded using a differential electrophysiological amplifier (Neurolog module NL104, Digitimer, UK), displayed on an oscilloscope (Sigma 60, Nicolet, UK), and saved as .wft files. For analysis, the recordings were exported to Impression (Nicolet, UK) and Origin 6.1 (Origin Coorporation, USA) for plotting as 3D 'waterfall' plots or superimposed recordings.

3.2.3.1. Examination of sensory compound action potentials (SCAP)

Sensory compound action potential (SCAP) was evoked with the stimulating cathode resting on the vertebrae in the paravertebral muscle at the level of T10/T11 vertebral junction with the stimulating anode located over the shoulder blade, and a ground electrode was inserted into the skin of the animal between the stimulating and recording electrodes. SCAP was recorded differentially with the active electrode at the base of the tail, and the indifferent through the tail tip. The recordings were averaged (n=10).

3.2.3.2. Examination of M responses, H reflexes and F waves

The direct motor response M response, monosynaptically-evoked H reflexes, and antidromically-evoked F waves were examined by stimulating the sciatic nerve at the sciatic notch and recording at the muscles on the dorsum of the unilateral hind limb. Two stimulating electrodes (cathode and anode inserted adjacent to the nerve) and recording electrodes (active inserted through the skin of the foot dorsum, indifferent through the tip of the middle digit of the same foot) were used, and a ground electrode was inserted into the skin of the animal between the stimulating and recording electrodes. At each stimulating site the stimulus intensity was gradually increased until the M response, and H reflex when present, could be recorded from the muscle. Following recording of the H reflex, the F wave could be observed by increasing the stimulus intensity up to supramaximal level.

3.2.3.3. Examination of cord dorsum potential (CDP)

Cord dorsum potentials (CDP) were evoked with the stimulating cathode and anode inserted through the ventral and dorsal side of the base of tail respectively. The responses were recorded by placing the active electrode on the vertebrae in the paravertebral muscle at the level of L4/L5, and the indifferent electrode into the skin of the animal parallel to the position of the active electrode. The ground electrode was inserted into the skin of the animal between the stimulating and recording electrodes. The recordings were averaged (n=10).

3.2.3.4. Examination of synaptic activation of motor neurons (SAM)

Synaptic activation of motor neurons (SAM) was evoked with the stimulating cathode resting on a vertebra in the paravertebral muscle at the level of T10/T11 vertebral junction, with the stimulating anode located over the shoulder blade, and a ground electrode inserted into the skin of the animal. SAM was recorded with recording electrodes (active inserted through the skin of the foot dorsum, indifferent through the tip of the middle digit of the same foot), and a ground electrode was inserted into the skin of the animal between the stimulating and recording electrodes.

3.2.4. Histology

3.2.4.1. Perfusion and fixation

The animals were anaesthetized under 2% isoflurane, and fixed by transcardial perfusion using rinse buffer (2000U/L heparin, 0.025% lidocaine, 0.002% $NaNO_2$ and 0.02M N-2-hydroxyethylpiperazine-NO-2-ethanesulphonic acid (HEPES; pH 7.4)) and 4% glutaraldehyde (4% in 0.15M phosphate buffer). The spinal cord of the rat was removed following laminectomy, and a transverse section (0.5mm) of the lumbar enlargement was processed into resin sections (see next section).

3.2.4.2. Resin section processing

The 0.5mm blocks of lumbar enlargement from different animals were kept in 4% glutaraldehyde, and then distributed in processing 'honeycombs' and washed with 0.15M phosphate buffer overnight. This 'honeycomb' with tissues was then placed in a container filled with 1.5% buffered osmium tetroxide solution, and left on an orbital shaker for 2 hours. The tissues were washed in 0.14M phosphate buffer for 10 minutes, three times. After the washes, the tissues were dehydrated by using a series of alcohols with ascending concentrations (15 minutes in 30% alcohol, 15 minutes in 50% alcohol, 15 minutes in 90% alcohol, 3 x 20 minutes in 100% alcohol). These dehydrated tissues were placed in 100% propylene oxide for 30 minutes twice, then in 50% propylene oxide with 50% resin for 60 minutes, and in 25% propylene oxide with 75% resin for another 60 minutes, and finally, in 100% resin overnight at 4 ˚C. Embedding of each tissue in the resin was carried out in a BEEM capsule to allow the cutting of transverse sections. The whole capsule with its content was then placed in an oven with a temperature of 60˚C for 24-36 hours for polymerization. For light microscopic examinations, transverse sections of the spinal cord with a thickness of 1µm were obtained using a microtome (Leica Microsystems (UK) Ltd., Knowlhill, Buckinghamshire, Milton Keynes). As the cut sections were initially floated on a water surface, they were dried on a hotplate at 60˚C after they were transferred onto the slides. The sections were stained with 0.1% thionin acetate (50% ethanol, basic) and 1% aqueous basic acridine orange, and mounted in DPX (BDH, Poole, UK). These sections were viewed using a light microscope (Zeiss Axiophot, Germany) and digital photographs were taken by a PC- connected camera (D300, Nikon, Japan).

3.3. Results

3.3.1. Introduction to *in vivo* electrophysiological examinations

The main purpose of performing electrophysiological examinations is to determine the functional integrity of the nervous system. To investigate the neurological functions within the central nervous system, I examined axonal conduction by recording the sensory compound action potential (SCAP), motor neuronal excitability by M response, the H reflex, and F wave. Also, synaptic transmission was examined by recording the cord dorsum potential (CDP), and synaptic activation of motor neurons (SAM) was monitored as well. The representative recording and positioning of the needle electrodes (stimulation, recording and ground) are illustrated and described in the table below.

Table 3.1. Battery of electrophysiological tests used in this study

Representative trace	Electrode positioning
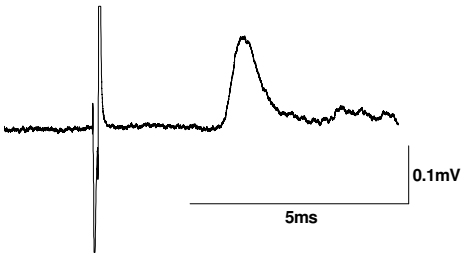	
Figure 3.1(a) Sensory compound action potential	***Figure 3.1(b) Illustration of electrode positioning for recording SCAP***
Figure 3.1(a) shows the representative recording of sensory compound action potential (SCAP) which was averaged 10 times to minimise noise. The SCAP is a result of antidromic conduction in sensory axons evoked by supramaximal stimulation of the spinal cord at vertebral levels T10/T11, and recorded from the base of the tail, vs. an indifferent at the tip of the tail, as shown in Figure 3.1(b). Ground electrode was placed between the stimulating and recording electrodes.	

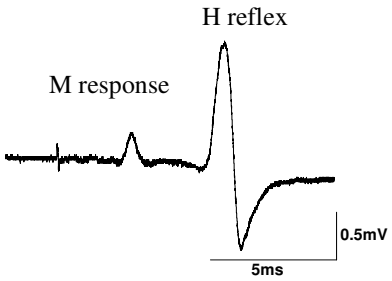

Figure 3.2(a) M response and H reflex

Figure 3.2(b) Illustration of electrode positioning for recording

Figure 3.2(a) shows a representative recording of an M response and H reflex. The M response is an orthodromically conducted motor response recorded, in this case from the foot muscles, and evoked by stimulation of the sciatic nerve (as illustrated in Figure 3.2(b)). The H reflex results from the monosynaptic reflex from the activation of Ia sensory fibers and motor neurons. The M response and H reflex in this trace were recorded at the threshold level of stimulation.

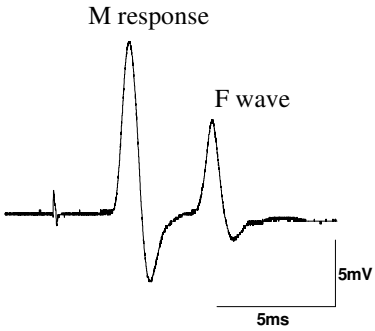

Figure 3.3(a) M response and F wave

Figure 3.3(b) Illustration of electrode positioning for recording

Figure 3.3(a) shows a representative recording of an M response and F wave, and Figure 3.3(b) illustrates the positioning of the electrodes. The M response is as previously described in Figure 3.2(a), whereas the F wave results from the 'reflection' of antidromic motor impulses from ventral horn motor neurons. The M response and F wave in this trace were recorded at the supramaximal level of stimulation.

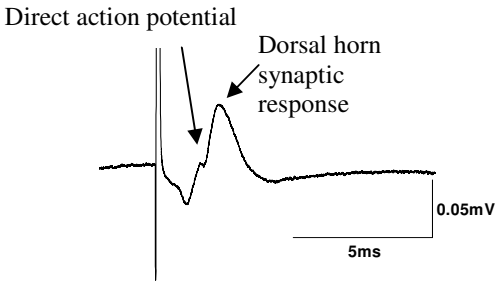

Figure 3.4(a) Cord dorsum potential (CDP)

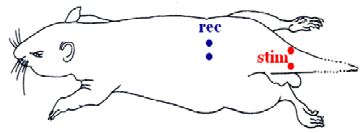

Figure 3.4(b) Illustration of electrode positioning for recording

The cord dorsum potential is composed of two peaks which are the directly conducted action potential and the dorsal horn synaptic response (Figure 3.4(a)). The responses are evoked by stimulating the tail and recorded at the vertebral level of L4/L5 (Figure 3.4(b)). The directly conducted action potential appears with short latency, and the synaptically-mediated responses from the dorsal horn appear in the records obtained from the location of the dorsal root entry zone (DREZ) of the tail roots.

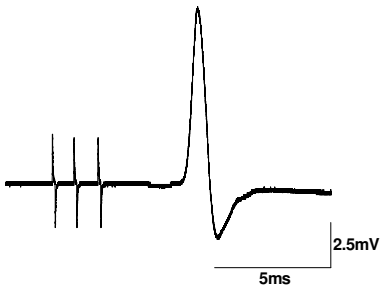

Figure 3.5(a) Synaptic activation of motor neurons (SAM)

Figure 3.5(b) Illustration of electrode positioning for recording

The synaptic activation of motor neurons (Figure 3.5(a)) was obtained by giving a triple supramaximal stimulation separated by 1 millisecond at the vertebral level of T10/T11, and recorded from the foot muscles (Figure 3.5(b)). This recording is a sum of both 'H reflex-like response', and the corticospinal tract response (validation method is described in section 3.3.2.4.)

3.3.2. Optimisation of electrophysiological examinations

Electrophysiological recordings are affected by several factors, including the type of anaesthetic agent used, the temperature of recording site of the animal, the frequency of stimulation, and positioning of the electrodes. As the aim was to obtain serial recordings reliably, optimisation of these parameters is required.

Here, the effects of different anaesthetic agent by using isoflurane and ketamine/xylazine, frequency of stimulation, and temperature of the foot were explored on recordings of M responses, F waves and H reflexes. Also, positioning of recording electrodes was shown to affect the amplitude of the cord dorsum potential (CDP). Furthermore, recordings of synaptic activation of motor neurons (SAM) were developed and validated by cutting the dorsal roots to eliminate 'H reflex- like response'.

3.3.2.1. The effect of different anaesthesia and frequency on M response, F wave and H reflex

F waves and H reflexes are recognised measures of motor neuronal function, but they are also well known for being inherently variable. Therefore, in order to obtain reliable and reproducible F waves and H reflexes, I tested two types of anaesthesia, namely isoflurane and ketamine/xylazine, and also applied different frequencies to obtain the best recordings. Rats were anaesthetised either by the inhalation of 2% isoflurane, or by the intraperitoneal injection of a combination of 90mg/kg of ketamine and 10mg/kg of xylazine, and prepared for electrophysiological examination. H reflexes and F waves were recorded under each anaesthetic agent using different frequencies of stimulation (0.1Hz, 1Hz, 2Hz and 5Hz). Both the H reflex and the F wave showed larger response amplitudes under ketamine/xylazine than under isoflurane, whilst the M responses were not influenced (Figure 3.6). Furthermore, when the stimulations were given at different frequencies, the H reflexes and F waves were best elicited at

the lowest frequency of 0.1Hz, and their amplitude decreased as the frequency increased. Again, the M responses were not affected by the change of stimulation frequencies. From these data, ketamine/xylazine was selected as the anaesthetic agent for subsequent electrophysiological examinations, and a frequency of 0.1 Hz was chosen when recording the H reflexes and F waves.

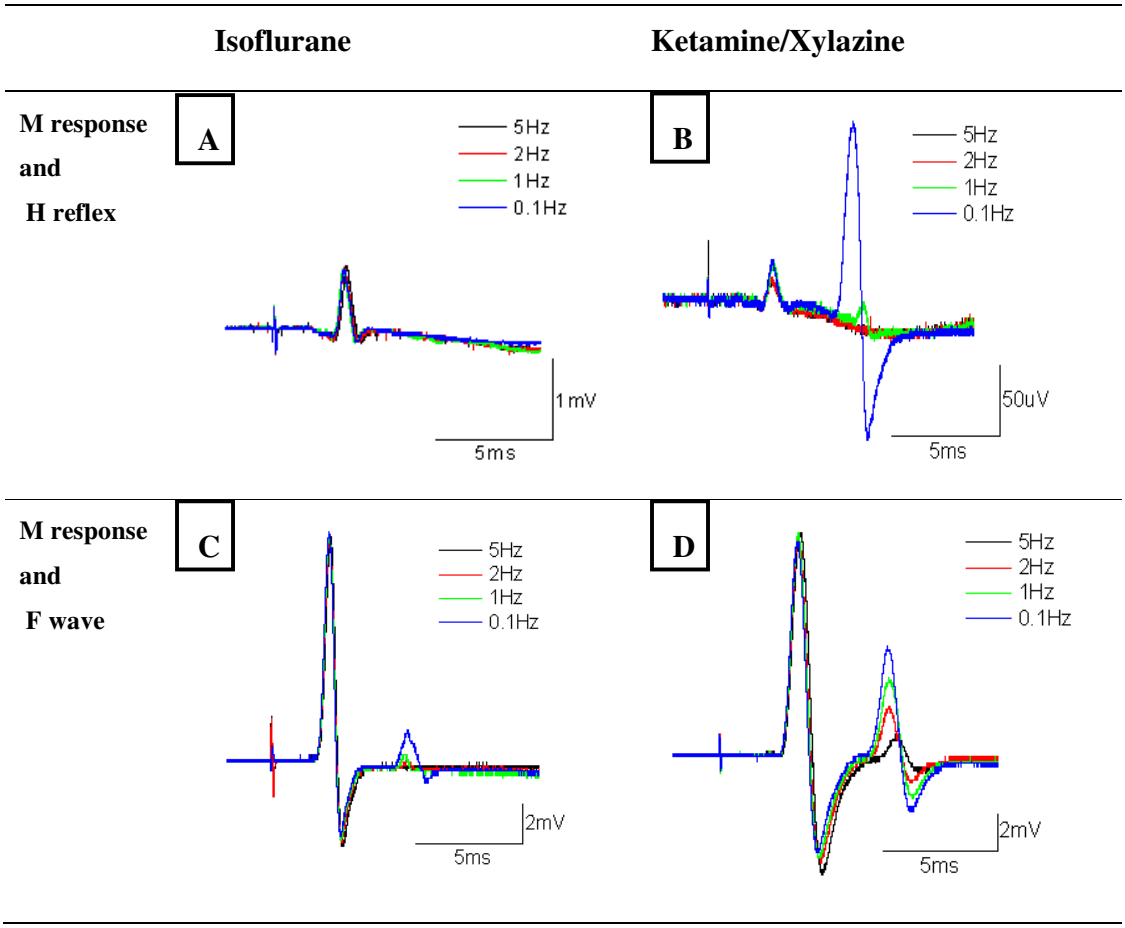

Figure 3.6. M response, H reflex and F wave recorded under isoflurane and ketamine/xylazine anaesthesia at different frequencies

Figure shows that the M response, H reflex and F wave were elicited under isoflurane and ketamine/xylazine anaesthesia. The H reflexes and F waves were recorded at the threshold level and the supramaximal level of stimulation respectively. Both H reflexes and F waves showed the largest amplitude under ketamine/xylazine, and at the low frequency of 0.1Hz (b, d). Under isoflurane anaesthesia, the H reflex could not be recorded at all (a), and F waves showed a smaller response amplitude (c). However, the M response was not affected by the type of anaesthesia, nor the change in frequency.

3.3.2.2. The effect of temperature on F waves and H reflexes

Although the rectal temperature of the animals was monitored and maintained to be in the range of 36-37˚C under anaesthesia, during winter times the animals presented cooler extremities due to cooler air in our poorly heated laboratory. In these cases, a prolonged latency and duration of the recorded M responses, H reflexes and F waves were noticeable, so a radiant heat lamp was used to keep the limbs warm. In order to assess the need to maintain the limb temperature within a certain range, I have investigated the effects of temperature on M responses, H reflexes and F waves. An ice bag was used to cool the hindlimb temperature, and a thermistor was attached to the plantar surface of the foot for monitoring. It is realised that the practice of recording the temperature in the foot will have exaggerated the apparent changes in temperature of the leg, but the foot provides a convenient and indicative temperature. The temperature of the plantar surface was between 31–32˚C in naïve rats. The recordings of the M response, H reflex and F wave were taken at this temperature and at every 1˚C decrease of the temperature. Figure 3.7 and 3.8 show the recordings obtained. When the latency (time till onset of the ensuing action potential) of each recording was measured and plotted against the temperature, a positive correlation was shown (Figure 3.9 and 3.10). The latency of the M response evoked by supramaximal stimulus of the sciatic nerve increased approximately 0.2ms per 1˚C decrease of temperature. Also the latency of the H reflex and F wave increased approximately 0.17ms and 0.4ms per 1˚C decrease of temperature respectively. These data show that maintaining consistenty of the hindlimb temperature when recording the M response, H reflex and F wave is crucial when accurately analysing consecutive recordings of EAE animals over days.

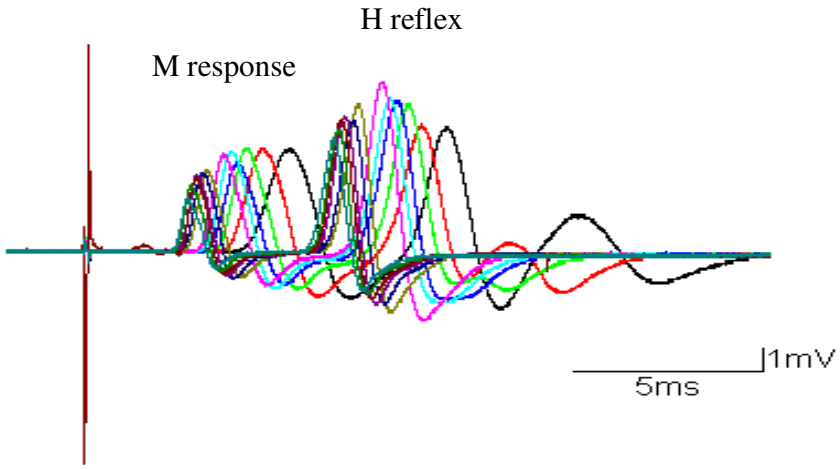

Figure 3.7. Superimposed recordings of M responses and H reflexes taken at different temperatures

M responses and H reflexes were recorded at every 1˚C decrease of temperature of the foot from normal status (recordings are superimposed but in practice appear to start from left to right in different colours). Both M response and H reflex show increased latency, duration, and amplitude as the temperature cools.

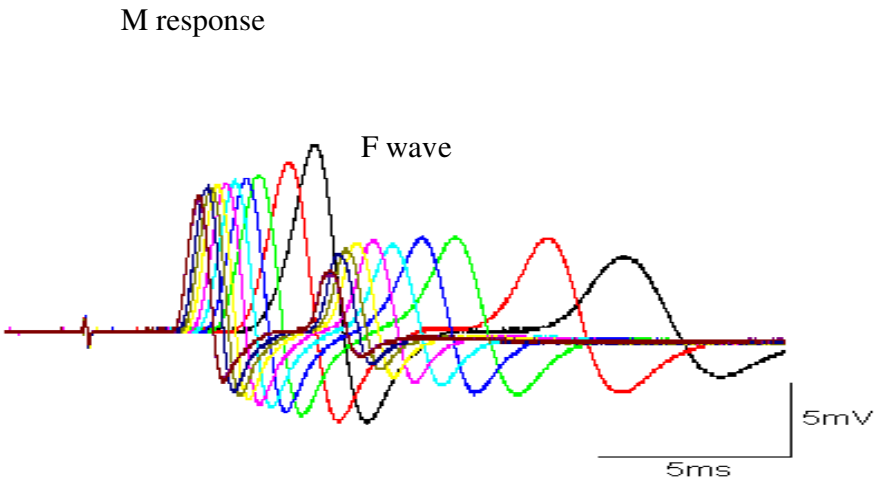

Figure 3.8. Superimposed recordings of M responses and F waves taken at different temperatures

M responses and F waves were recorded at every 1˚C decrease of temperature of the foot from normal status (Recordings start from left to right in different colours). Both M response and F wave show increased latency, duration, and amplitude as the temperature cools.

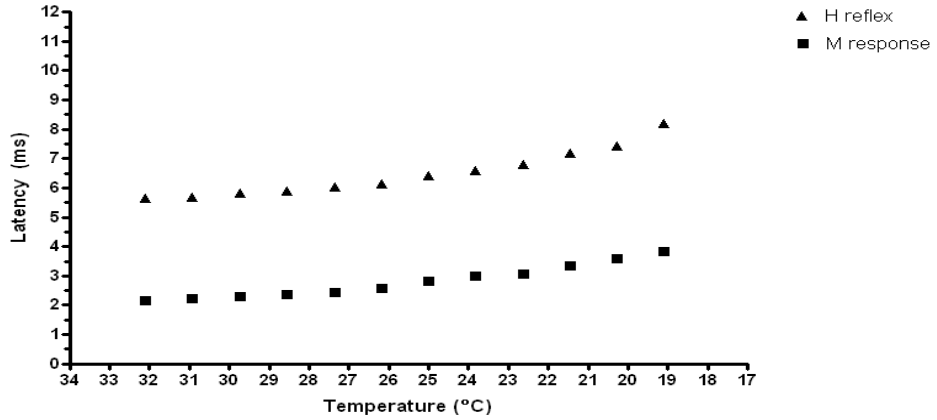

Figure 3.9. Latency (ms) of M response and H reflex, plotted against temperature decrement

The latency of M response and H reflex from each recording in Figure 3.7 was measured and plotted against temperature decrement by 1˚C. The latency of the M response increased approximately 0.2ms per 1˚C decrease of temperature. The latency of the H reflex was increased by approximiately 0.17ms per 1˚C decrease of temperature.

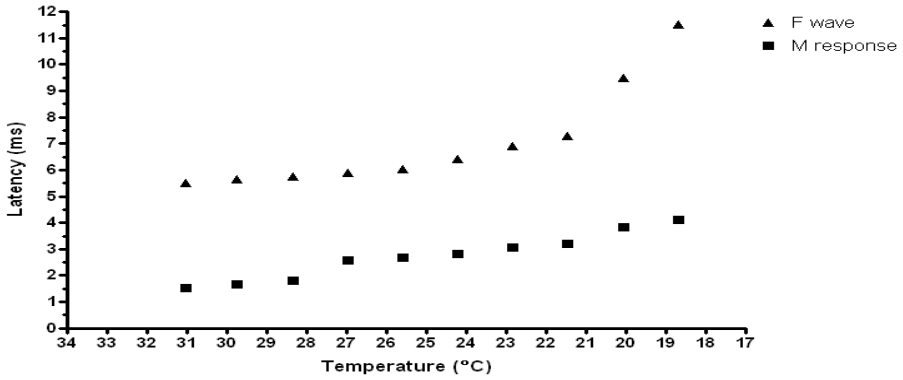

Figure 3.10. Latency (ms) of M response and F wave, plotted against temperature decrement

The latency of M response and F wave from each recording in Figure 3.8 was measured and plotted against temperature decrement by 1˚C. The latency of the M response increased approximately 0.2ms per 1˚C decrease of temperature. The latency of the F wave was increased by approximiately 0.4ms per 1˚C decrease of temperature.

3.3.2.3. Developing recording methods for the cord dorsum potential (CDP) to examine synaptic transmission

The cord dorsum potential (CDP) can be recorded by stimulating the peripheral tail nerves and recording rostro-caudally along the dorsal surface of the spinal cord (Figure 3.4(b) illustrates electrode positions). Figure 3.11 is a 'waterfall' plot showing a series of compound action potentials recorded at different locations along the spinal cord in response to supramaximal stimulation applied at the base of the tail. The most caudal recording is shown at the front (lowest record shown). The responses are recorded from the level of the L6/S1 vertebral junction, up to the level of T12/T13. The directly conducted action potential appears with short latency, and the synaptically-mediated responses from the dorsal horn appear in the records obtained from the location of the dorsal root entry zone (DREZ) of the tail roots. This response becomes larger than the primary volley due to an amplification process occuring in the cord, and it reaches a maximum over the lumbar enlargement, i.e. the location of the DREZ. The recording shown in red was made at vertebral level L4/L5, and it was chosen for analysis as it showed a clear distinction between the two responses.

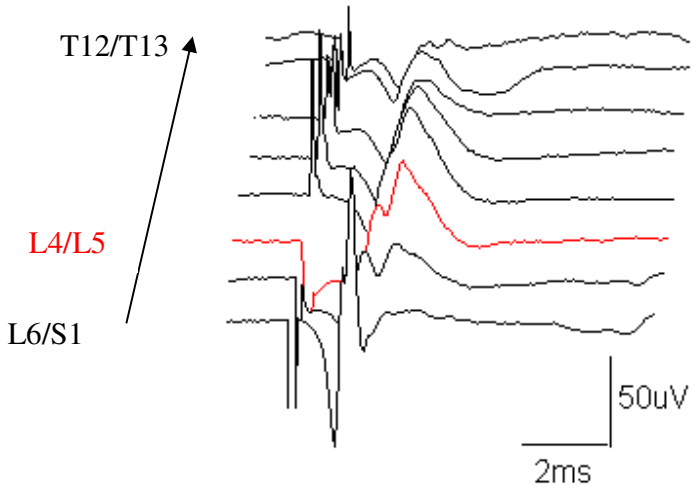

Figure 3.11. 'Waterfall' plot of the cord dorsum potential (CDP) recorded from L6/S1 to T12/T13

The cord dorsum potential (CDP) was recorded by stimulating the peripheral tail nerves and recording at the dorsal surface of the spinal cord. The 'waterfall' plot shows the most caudal recording at the front (lowest recording) at the vertebral junction of L6/S1 and up to the level of T12/T13. The primary peak is the direct action potential that travelled along the fibers of the spinal roots to the dorsal column. The second peak is a result of post-synpatic activation primarily from the dorsal horn cells, and it shows the largest volley at the L4/L5 vertebral level (shown in red), with a clear distinction from the direct action potential peak.

As shown in Figure 3.11, the amplitude of the synaptic potential was the largest, and also clearly distinct from the direct action potential (short latency peak), at the vertebral level of L4/L5, and accordingly this junction was chosen as the recording site. Next, I aimed to map the traces accurately by recording at every 1mm from L4 up to the L5 vertebra within the junction, so that one can accurately position the active recording electrode within the junction for recording the CDP. Figure 3.12 shows that there was an increase of the amplitude of the synaptic transmission when the recording electrode was placed 2mm rostral to the L5 vertebrae. However, the amplitude of the direct action potential was stable regardless of the electrode position.

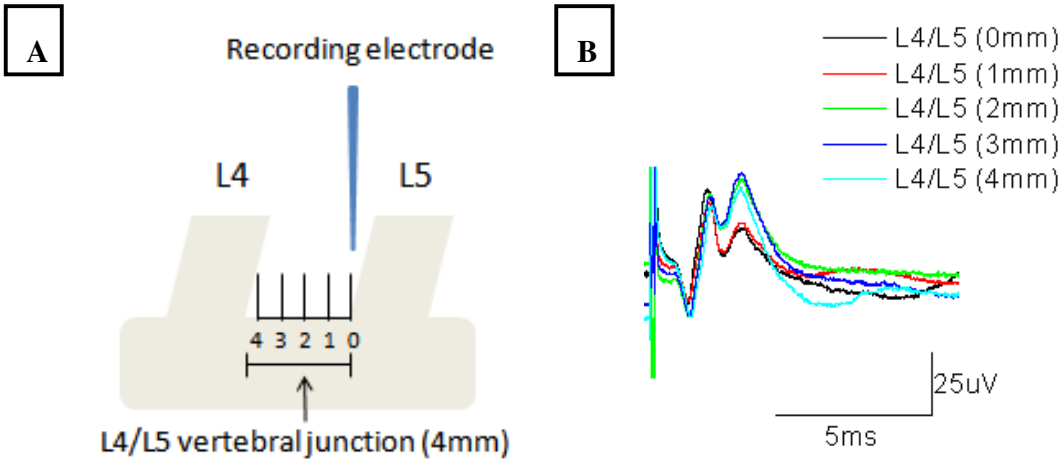

Figure 3.12. Diagram of L4/L5 vertebral junction and 'superimposed' plot of spinal cord dorsum potentials (CDP)

The spinal cord dorsum potential (CDP) was recorded within the L4/L5 vertebral junction by stimulating the base of the tail. The diagram (a) shows the L4 and L5 vertebrae and the 5 points within the junction where the cathodic needle electrode were positioned for recording. The 'superimposed' plot (b) shows CDP recordings made at these 5 points. The potential resulting from synaptic transmission (the second peak) increased when the electrode was positioned 2mm rostral to the L5 vertebra, and remained at a similar amplitude up to the L4 vertebra.

3.3.2.4. Developing recording methods of synaptic activation of motor neurons (SAM)

The H reflex has been previously described as a means of examining synaptic transmission between the Ia sensory axons and α motor neurons. Here, another method of examining the synaptic activation of motor neurons has been developed. Whilst the H reflex recording involves threshold stimulation of the sciatic nerve, this new method uses supramaximal or near supramaximal stimulation to activate the dorsal horn axons at the T10/T11 vertebral junction (as illustrated in Figure 3.5(b)). When this region is stimulated, both the corticospinal tract axons and the dorsal column sensory axons are activated which both synapse on the motor neurons that innervate the foot muscles. Hence this recording was named 'synaptic activation of motor neurons (SAM)' (illustrated in Figure 3.14). The sensory axons of the dorsal column elicit an 'H reflex-like response', as they synapse on the motor neurons likewise to the Ia sensory axons as a result of sciatic nerve stimulation.

In order to explore the contribution of this 'H reflex-like response' to SAM, we severed the left L4, L5 and L6 dorsal roots (surgery performed by Professor Kenneth Smith) which convey the sensory signal through sensory Ia fibres under general anaesthesia (illustrated in Figure 3.13). After the surgery, the animal did not show a pinch withdrawal reflex in the left leg, which correlated with a sensory pathway dysfunction due to the dorsal root cut. SAM, H reflex, and F wave recordings were made at both the left and right side of the animal, before and after severing the roots, and at four days after the surgery when the sensory axons would have been degenerated. The EMG recordings of these tests are shown in Figure 3.15. None of the recordings taken from the right side were affected throughout the examinations, whilst the recordings from the left side were profoundly affected. The left H reflex amplitude had decreased after the surgery, which indicates the dorsal roots were cut successfully, as the dorsal roots convey the afferent sensory signals (Figure 3.15 (c)). Interestingly, the decrease in the amplitude of left SAM at day four (Figure 3.15 (a)) after the surgery suggests that SAM is likely to be composed of both the 'H reflex-like response', and

corticospinal tract response. The 'H reflex-like response' may have diminished as a result of axonal degeneration in the dorsal column occurring from the severance of the dorsal roots. The F wave had also decreased at day four post surgery, which may be due to inflammation around the motor neurons occurring due to the degeneration of the Ia afferent terminals. However, we have not found supporting evidence from examinations of resin sections.

After the electrophysiological recordings on day four after surgery, the animal was perfused and fixed for histological examinations. Figure 3.16 (a) shows the spinal cord with the left dorsal roots cut, and Figure 3.16 (b) is a magnified picture of the dorsal column. Wallerian degeneration was observed within the left side of the dorsal column, which may explain why the amplitude of SAM had been reduced. Unilateral degeneration was obvious as shown in Figure 3.16 (c) and (d), where almost every axon in the left dorsal root was degenerated.

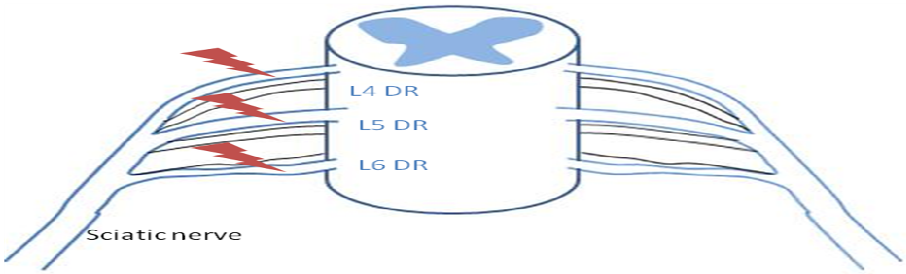

Figure 3.13. Diagram showing dorsal root cuts

The L4, L5 and L6 dorsal roots were severed in order to examine the contribution of 'H reflex-like responses' to the recordings of synaptic activation of motor neurons (SAM).

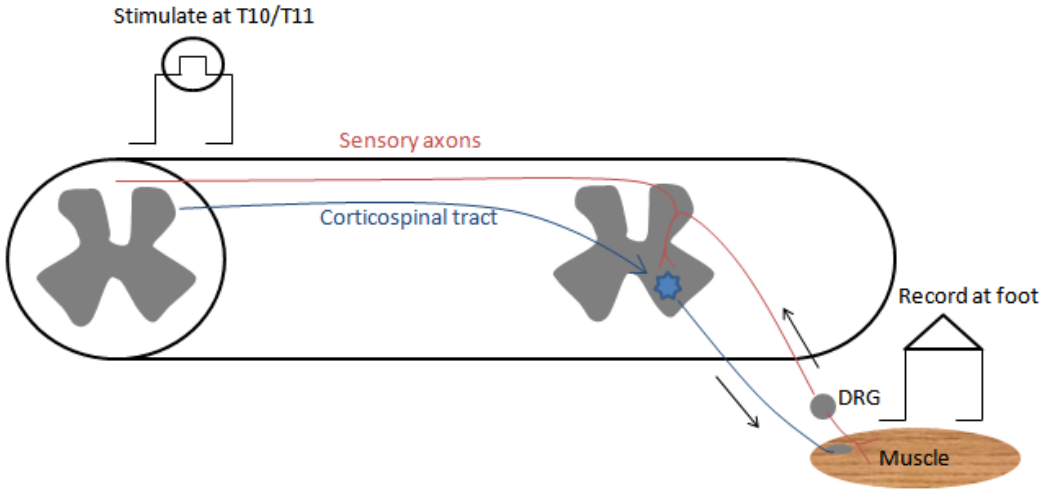

Figure 3.14. Proposed pathway of stimulating and recording 'synaptic activation of motor neurons (SAM)'

This diagram illustrates the stimulation and recording site for recording SAM. Stimulation and recording electrodes were placed at the vertebral junction of T10/T11 and foot dorsum respectively. When the vertebral junction of T10/T11 is stimulated, both the sensory axons and corticospinal tract are activated. Activation of both of these pathways triggers the motor neurons in the ventral horn by synaptic transmission, therefore activating the foot muscles.

(a) Left side 'waterfall' SAM

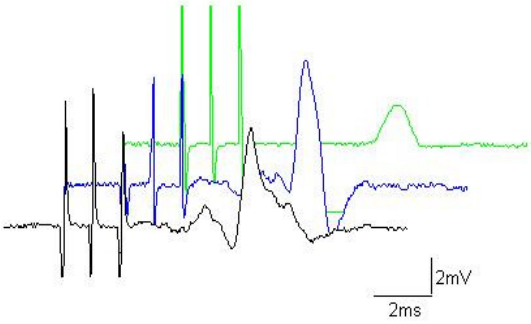

(b) Right side 'waterfall' SAM

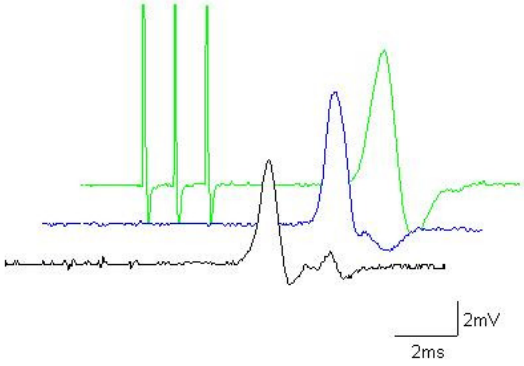

(c) Left side 'waterfall' H reflex

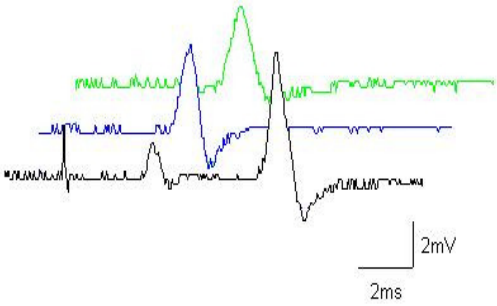

(d) Right side 'waterfall' H reflex

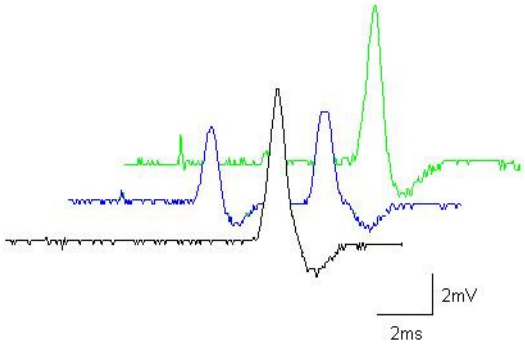

(e) Left side 'waterfall' F wave

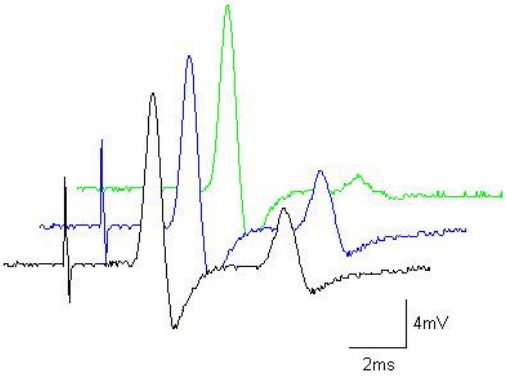

(f) Right side 'waterfall' F wave

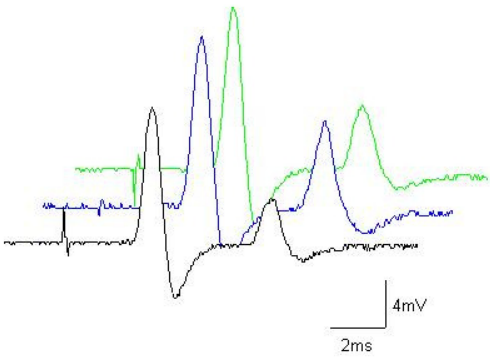

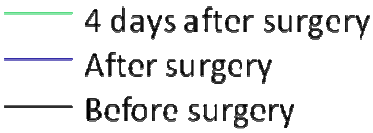

Figure 3.15. EMG recordings showing synaptic activation of motor neurons (SAM), H reflex, and F waves

Synaptic activation of motor neurons (SAM), H reflex and F wave recordings were examined in an animal before and after the left L4, L5 and L6 dorsal roots were cut, and also at four days post surgery. The recordings performed at the right side were similar on each recording occasions ((b), (d), (f)), while the left side recordings were affected. A waterfall plot of H reflex (c) shows that the H reflex was completely absent after the dorsal root cut. However, (a) shows that the SAM had decreased when examined four days after surgery. This indicates that the SAM may be composed of both the 'H reflex-like response' and the corticospinal tract response. Here, the reduction is likely to be due to axonal degeneration occurring in the left side of the dorsal column (shown in Figure 3.16). (e) shows a waterfall plot of F waves. At day four post-surgery, the F wave was decreased, which could be due to inflammation around the motor neurons resulting from the degeneration of the terminals of the Ia afferent axons.

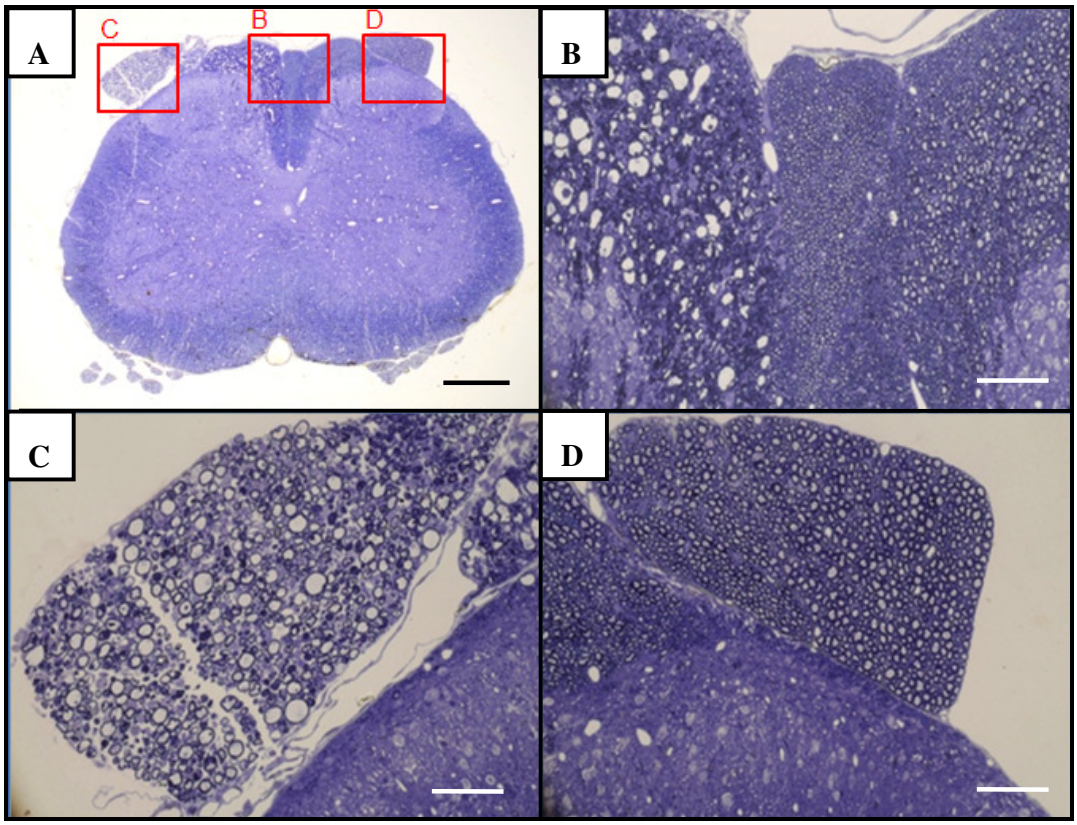

Figure 3.16. Histological examination of the spinal cord and dorsal roots

This figure shows the unilateral axonal degeneration (left side of the cord) four days post-surgery. The animal was perfused with glutaraldehyde after electrophysiological examinations. (a) shows the transverse section of the whole spinal cord, and the highlighted red boxes indicate the magnified areas shown as (b), (c), and (d). (b) shows the dorsal part of the dorsal column, which shows a clear distinction between the degenerated axons on the left, and the intact axons on the right side. The axons in the left side of the dorsal column show Wallerian degeneration. (c) shows at high magnification of the left damaged root, which also shows that the axons are degenerated, whilst the right dorsal root is intact (d).
(Black scale bar=1000µm , white scale bar=250µm)

3.4. Conclusion

This chapter shows that optimising the examining conditions is essential in obtaining reliable *in vivo* electrophysiological recordings. Anaesthetic agents should be carefully selected depending on the type of recordings made, and stimulation frequency and temperature of the animal must be taken into account when interpreting the recordings. Here, I showed that motor neuronal excitability (H reflexes and F waves) were better evoked under ketamine/xylazine, than under isoflurane, and at the lowest frequency of stimulation (0.1 Hz). Also, the negative correlation between latency and temperature finding can be informative when examining animals with different limb temperatures. These data can be particulary useful in understanding the increased latency of animals with EAE described in the next chapter, since these animals showed hypothermia.

All the *in vivo* electrophysiological methods described so far have been applied in the animals with EAE described in the following chapter, in order to understand the mechanisms responsible for the transient peak, recovery and relapse present within the disease course.

Chapter 4

Neurological, histological and electrophysiological assessment of DA rats induced with rMOG-EAE

Chapter 4. Neurological, histological and electrophysiological assessment of DA rats induced with rMOG-EAE

4.1. Introduction and aims

Relapsing- remitting multiple sclerosis (RR-MS) is the most common form of multiple sclerosis affecting around 80% of the patients. However, the mechanisms underlying the different phases are still not completely understood.

In this chapter, I aimed to explore the possible mechanisms by using a rat model of EAE that closely resembles the symptoms and pathology of MS. Dark Agouti (DA) rats were induced with EAE using recombinant myelin oligodendrocyte glycoprotein (rMOG), and five key stages along their disease course were characterised using neurological examinations. These stages are 'preinduction (PI)', 'predisease (PreD)', 'peak disease (PD)', 'remission (REM)' and 'relapse (REL)'. At these five stages, electrophysiological tests that were described in the previous chapter were employed to examine any dysfunction of axonal conduction, motor neuronal excitability, synaptic transmission and synaptic activation of motor neurons within the central nervous system. Furthermore, histological analysis of these animals at equal stages was performed in order to examine the degree of inflammation, demyelination and axonal degeneration occurring in the spinal cord. The pathology of the dorsal column was also investigated in order to explore the correlation with axonal conduction measured from the dorsal column axons.

4.2. Methods

4.2.1. Animals and anaesthesia

The methods have been previously described in Chapter 3, Methods 3.2.1 and 3.2.2. Animals that reached a neurological score of more than five were provided with mashed food in water on the floor of the cage.

4.2.2. Rectal temperature monitoring in non-anaesthetised animals

Rectal temperature was measured by inserting a rectal temperature probe into the rectum of a rat without anaesthesia. The temperature was recorded when the reading was stable for at least five seconds.

4.2.3. Induction of experimental autoimmune encephalomyelitis (EAE) with recombinant myelin oligodendrocyte glycoprotein (rMOG)

Recombinant myelin oligodendrocyte glycoprotein (rMOG) was kindly provided by Professor Chris Linington (University of Glasgow). A total volume of 200µl emulsion was made by adding 0.1mg of rMOG and incomplete Freunds adjuvant (IFA) using glass Hamilton syringes. For induction of EAE, the animals were shaved at the dorsal base of the tail under 2% isoflurane, and the emulsion was injected subcutaneously. For control animals, 200µl of IFA was injected.

4.2.4. Neurological assessments

Rats with EAE were weighed and scored for the magnitude of any neurological deficits, and this was performed at a designated time each day to minimise any circadian variability. Neurological assessment was performed by giving a daily 'neurological score' to every animal induced with EAE using a ten point scale system (Table 4.1.).

Table 4.1. Ten point scale system for neurological scoring

Score	Signs
1	Reduction of muscle tone of tail tip
2	Reduction of muscle tone of the whole tail
3	Tail paralysis
4	Inability to spread toes
5	Unsteady gait
6	Hind limb paresis (one side)
7	Hind limb paresis (other side)
8	Hind limb paralysis (one side)
9	Hind limb paralysis (other side)
10	Moribund/dead

For the study described in this chapter, five key stages along the disease course of EAE were selected for electrophysiological and histological analyses. These stages were 'preinduction (PI)', 'predisease (PreD)', 'peak disease (PD)', 'remission (REM)' and 'relapse (REL)'. Selection criteria for these stages are described in Table 4.2 below.

Table 4.2. Selection criteria of five key stages along the disease course of EAE

Stages	Criteria
Preinduction (PI)	Before induction of EAE (naïve).
Predisease (PreD)	5 days after the induction of EAE, prior to the onset of neurological deficit.
Peak disease (PD)	First peak of the disease, where neurological score is between seven and nine.
Remission (REM)	Recovery from the first peak of disease, the rats remain as a score of three to five for at least two days.
Relapse (REL)	Second peak of disease, after experiencing both peak disease (PD) and relapse (REL). The neurological score is between seven and nine.

4.2.5. Behavioural assessments by inclined plane measurements

The inclined plane is a tool designed for quantitative measurement of limb motor function. A ball screw is used to adjust the angle of the plane (Chang et al. 2008). The inclined plane used in this study was designed by Dr Andrew Davies from our laboratory. Behavioural assessments were performed by measuring the maximum angle of an inclined plane, at which the animal could stay on the plane without sliding down the plane for 10 seconds. Sandpaper was used to cover the plane, and was changed regularly to reproduce similar friction for each experiment.

4.2.6. Histological assessments

4.2.6.1. Perfusion and fixation

The animals were anaesthetised under 2% isoflurane, and fixed by transcardial perfusion using rinse buffer and 4% paraformaldehyde (4% in 0.15M phosphate buffer). The spinal cord of the rat was removed following laminectomy, and a 0.5mm transverse section was cut at L1/L2 vertebral junction for processing into resin blocks which were re-fixed in 4% glutaraldehyde (4% in 0.15M phosphate buffer). The remaining spinal cord was kept in 4% paraformaldehyde for processing into frozen sections for immunohistochemical analysis.

4.2.6.2. Resin section processing and quantification of pathology

The details of the resin section procedures have been described previously in Chapter 3, Methods section 3.2.4.2.

Quantification of pathology in resin sections of the spinal cord was achieved using Image J software (Rasband, W.S., ImageJ, U. S. National Institutes of Health, Bethesda, Maryland, USA, http://rsb.info.nih.gov/ij/, 1997-2009). The images of the spinal cord that were viewed and taken using the light microscope and camera were converted into a grayscale 8-bit file to measure the pathological areas.

In this study, pathological areas of both 'white matter' and 'dorsal column' were estimated by drawing around the area of interest. To obtain the 'percentage area of pathology in the white matter', the 'total area of axonal degeneration and demyelination' was divided by the 'area of white matter' and the answer x100. Likewise, the 'percentage area of pathology in the dorsal column' was calculated by dividing the 'total area of axonal degeneration and demyelination in the dorsal column' by the 'area of dorsal column' x100. In addition, within the dorsal columns, the 'area of axonal degeneration' and the 'area of demyelination' were measured separately, and these values were divided by the 'area of dorsal column' to assess the ratio of the two pathological features.

4.2.6.3. Frozen section processing for immunohistochemistry

Spinal cord which was fixed and kept in 4% paraformaldehyde overnight was moved into 30% sucrose for 3 days. A one centimetre block centred at the L1/L2 vertebral junction was embedded in a mould made with foil filled up with OCT (Bright, Huntingdon, UK). These blocks were then frozen in liquid nitrogen and kept at -20 ˚C before cryosectioning. Spinal cords were sectioned in 12 μm sections using a freezing crytostat (CM 1950, Leica, Milton Keynes, UK). The tissue sections were carefully collected on a glass slide and kept at -20 ˚C until immunohistochemical labelling.

4.2.6.4. Immunohistochemistry and quantification

Sections for immunohistochemical analysis were air-dried on slides for at least an hour and then washed with phosphate buffered saline (PBS) for 5 minutes. After the wash, the slides were pre-treated with hydrogen peroxide (H_2O_2) to eliminate endogenous peroxidase activity, and blocked with appropriate non-immune serum. The detailed protocol for pre-treatment is described in Table 4.3. After blocking, tissue sections were washed with PBST (0.05% Tween 20 dissolved in PBS) and incubated in appropriate primary antibodies overnight at either room temperature or 4 °C. Negative control slides were incubated with PBS without antibodies for the same length of time. Table 4.4. describes appropriate concentrations, time and temperature of treatment for each antibody used in this study.

After treatment with the primary antibody, the slides were washed with PBS 3x5 minutes to remove excess antibodies, and then incubated with appropriate biotinylated secondary antibody (Goat anti rabbit (BA1000) or horse anti mouse (BA2001), Vector labs, Peterborough, UK) for 45 minutes at room temperature. Secondary antibodies were selected depending on the species in which the primary antibody was produced.

Table 4.3. Pre-treatment information for different antibodies

Antibody	H_2O_2 treatment	Blocker treatment
ED1	30% H_2O_2 in methanol for 20 minutes at room temperature	10% normal horse serum for 1 hour at room temperature
iNOS	30% H_2O_2 in PBST (0.05% Tween 20 dissolved in PBS) for 20 minutes at room temperature, followed by 70% cold methanol for 20 minutes at room temperature	10% normal horse serum for 1 hour at room temperature

Table 4.4. Properties of primary antibodies used in this study

Antibody	Source	Dilution	Time/temperature of treatment	Company	Cat no.	Lot/batch
ED1	Mouse	1:200	Overnight at room temperature	Serotec	MCA341R	060509
iNOS	Rabbit	1:200	Overnight at room temperature	BD Biosciences	610333	54151

To remove excess secondary antibodies, the slides were washed with PBS 3x5 minutes. Following the washes, the sections were incubated in an Avidin Biotin Complex (ABC Elite kit, Vector labs, Peterborough, UK) for 45 minutes at room temperature. After another three washes with PBS, the chromogen diaminobenzidine (DAB) tetrahydrochloride (Vector labs, Peterborough, UK) was used to visualize the antibody binding. Incubation time was optimized depending on the specific protein under study and sections were checked under the microscope regularly until the optimum colour with the least background was achieved. The sections were then dehydrated by passing them through increasing concentrations of ethanol (70% for 5 minutes, 90% for 5 minutes, 95 % for 5 minutes, 100% for 2 minutes x 2, xylene for 5 minutes x 2). A coverslip was then applied with DPX mounting medium (Fluka Chemie, Buchs, Switzerland) and slides were left to air-dry overnight.

The quantification of immunohistochemical labeling was achieved by using the Image J software (Rasband, W.S., ImageJ, U. S. National Institutes of Health, Bethesda, Maryland, USA, http://rsb.info.nih.gov/ij/, 1997-2009). Images of the spinal cord that were viewed and taken using the light microscope and camera were converted into a grayscale 8-bit file. Whilst keeping the 'contrast/brightness' consistent in all images, the immunohistochemical labelling was converted into dark particles. The darkness and circularity of these particles were thresholded and defined to detect immunohistochemical labelling. The total area of the dark particles was measured and divided by the 'area of spinal cord' to obtain the 'percentage area of labelling'.

4.2.7. Electrophysiological assessment

Animals induced with EAE were examined at different stages of the disease using the electrophysiological tests introduced in Chapter 3. Detailed methods of these electrophysiological examinations have been described previously (Chapter 3, Methods section 3.2.3).

4.2.8. Statistics

Data were expressed with means and standard deviations, and plotted using GraphPad Prism version 4.00 for Windows (GraphPad Software, San Diego, USA). One-way ANOVA with Newman-Keuls post test was performed to compare the means in three or more groups, Spearman's rank correlation test was used for correlation analysis. 'Statistical significance' was determined by the p value obtained from these tests. ($p<0.05$ (*), $p<0.01$ (**), $p<0.001$ (***))

4.2.9. Plan of experiment

Figure 4.1 describes the disease course of EAE and the types of examinations performed along the disease course. The horizontal axis and vertical axis indicate the 'time course of EAE' and 'severity of the disease' respectively. The disease course shown in a black line is characterised by five key stages, which is composed of two peaks, namely the 'peak disease (PD)' and 'relapse (REL)' with a remission phase 'remission (REM)' in between. 'preinduction (PI)' indicates a time period before inducing EAE and 'predisease (PreD)' indicates a time taken at 5 days after induction

when there are no neurological signs observed in these animals. Neurological examinations including neurological scoring, weight measurements, inclined plane tests, and rectal temperature measurements were performed every day after the induction, until the end of the study. However, electrophysiological and histological examinations were performed selectively at the five key stages.

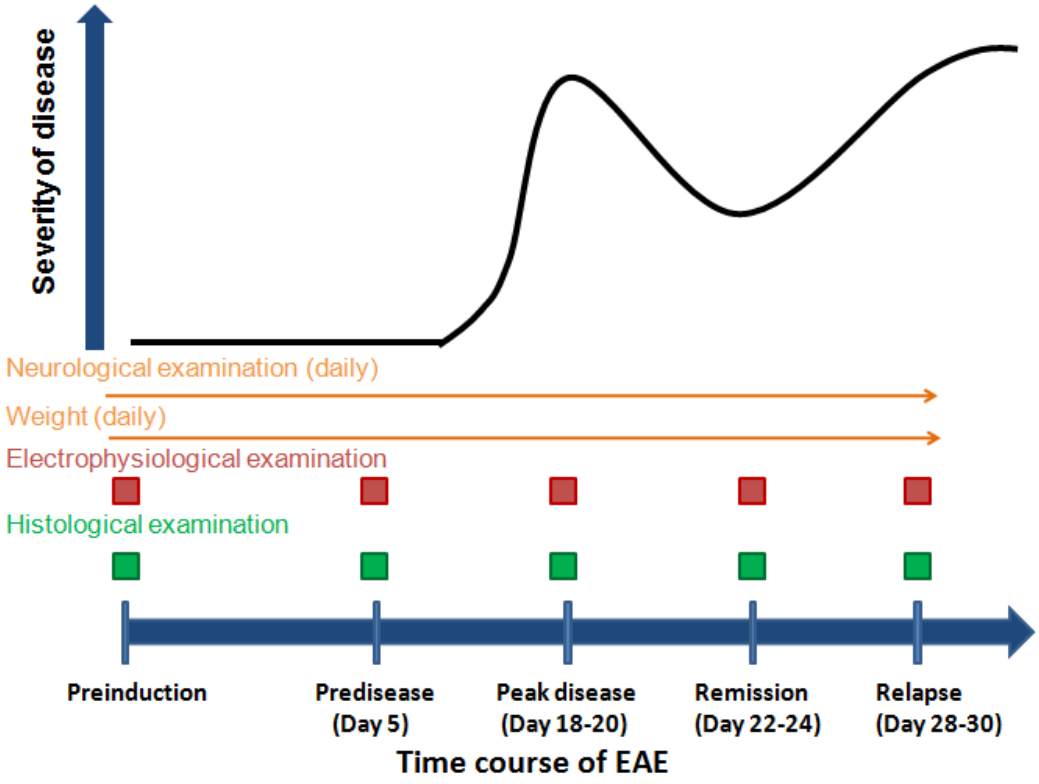

Figure 4.1. Diagram of experimental plans for this study

Neurological examination was performed daily after induction of the disease, whereas electrophysiological and histological assessments were made at five key stages along the disease course. These stages are 'preinduction (PI)', 'predisease (PreD)', 'peak disease (PD)', 'remission (REM)', and 'relapse (REL)'. Animals were scored using a ten point scale and were appointed to the key stages using the selection criteria described previously (Table 4.2).

4.3. Results

4.3.1. Neurological assessment

4.3.1.1. Neurological scoring and weight measurements

Initially 15 rats were induced with EAE for neurological scoring and ten of these were included in the analysis illustrated in Figure 4.2. One rat did not present any neurological signs, 2 died at their first peak of disease, and the other 2 were culled according to the Animals Act 1986 when they were found as moribund. After induction of EAE, ten rats gradually gained neurological signs such as tail weakness and paralysis, and reached the peak of disease showing hindlimb paralysis, around day 18-20 post induction. The animals recovered from some of these signs around day 22-24 post induction, and relapse occurred showing severe characteristics of the disease, around day 28-30 post induction. Figure 4.2 (a) shows the daily averaged neurological score of ten animals, and (b) shows the average of neurological scores collected from these animals at the five stages of EAE ('preinduction (PI)', 'predisease (PreD)', 'peak disease (PD)', 'remission (REM)', 'relapse (REL)'), selected according to the selection criteria described in Table 4.2. At these stages the mean neurological scores of animals were 0, 0, 8, 3.25, 8.08 respectively. The mean neurological scores at the 'peak disease (PD)' and 'relapse (REL)' were significantly higher than 'preinduction (PI)' ($P < 0.001$). Also, the mean difference was significant between 'peak disease (PD)' and 'remission (REM)' ($P < 0.001$), and between 'remission (REM)' and 'relapse (REL)' ($P < 0.001$).

A

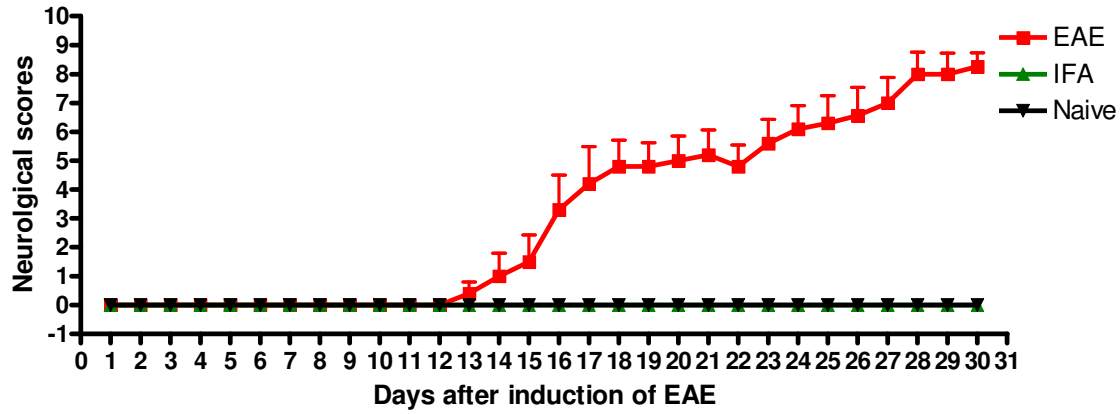
Neurolgical scores
10
9
8
7
6
5
4
3
2
1
0
-1
0 1 2 3 4 5 6 7 8 9 10 11 12 13 14 15 16 17 18 19 20 21 22 23 24 25 26 27 28 29 30 31
Days after induction of EAE
EAE
IFA
Naive

B

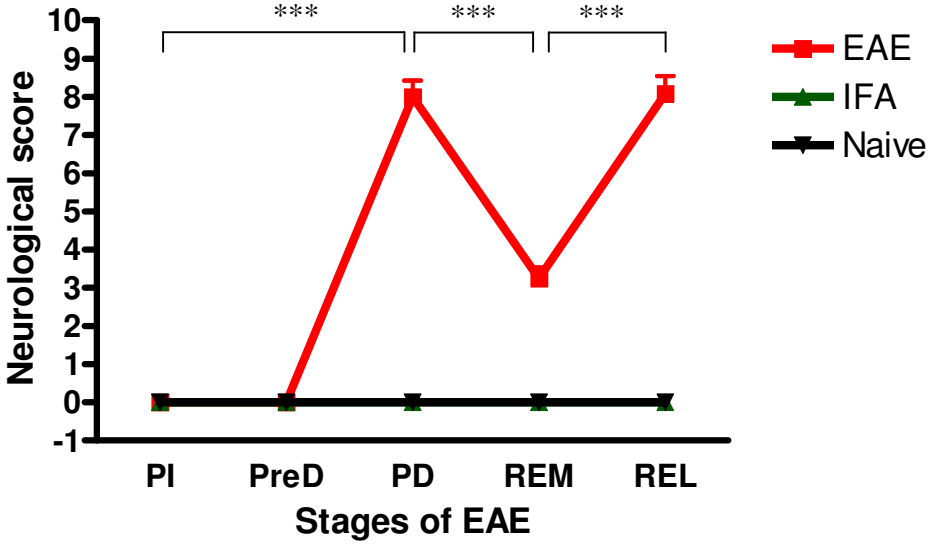
***
***
***
Neurological score
10
9
8
7
6
5
4
3
2
1
0
-1
PI
PreD
PD
REM
REL
Stages of EAE
EAE
IFA
Naive

Figure 4.2. 'Neurological score' plotted against time, and at the five key stages of EAE

Neurological scores were assessed daily in animals induced with EAE after the induction of disease. (a) The first peak of the disease occurred around day 18-20, and was followed by remission around day 22-24. The animals slowly gained neurological signs after the remission, and reached their relapse (around day 28-30) (N=10 in each group, red; EAE, green; IFA control, black; naïve control). (b) The mean neurological scores were 0, 0, 8.5, 3.3, 8.6 at 'preinduction (PI)', 'predisease (PreD)', 'peak disease (PD)', 'remission (REM)', 'relapse (REL)'. The mean neurological score at the 'peak disease (PD)' and 'relapse (REL)' were significantly higher than 'preinduction (PI)' ($P < 0.001$). Also, the difference was significant between 'peak disease (PD)' and 'remission (REM)' ($P < 0.001$), and between 'remission (REM)' and 'relapse (REL)' ($P < 0.001$) (N=10 in each group). (P value was obtained by One way ANOVA, Newman-Keuls post test).

The weight of these animals was also monitored daily, and it was found that animals with a more severe disease course lost more weight than the ones with milder courses. Hence, the weights of the severe animals and mild animals were compared. Animals that were selected for severe and mild disease course showed a neurological score of more than six (at least paresis on one side was observed), and not more than five (no paresis), respectively, at both their 'peak disease (PD)' and 'relapse (REL)'. Figure 4.3 shows that animals with severe neurological scores showed significant weight loss at the 'peak disease (PD)' ($p<0.01$ to 'preinduction (PI)') and 'relapse (REL)' ($p<0.01$ to 'preinduction (PI)'). However, mild animals did not show any decrease of weight along the entire disease course.

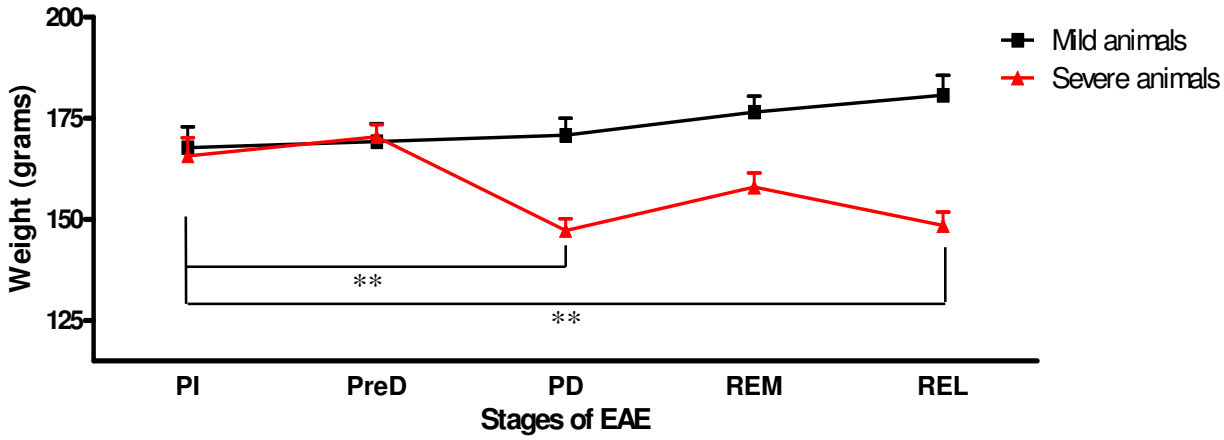

Figure 4.3. Comparison of the weight between animals with a mild and severe disease course at the five key stages of disease

Animals with EAE were weighed every day, and the mean weights were plotted at five time points along the time course of EAE. The mild animals (black boxes, N=6) which did not reach a score of more than five did not show loss of weight throughout the disease course. However, the severe animals (red triangles, N=8) lost weight significantly at the 'peak disease (PD)' compared to 'preinduction (PI)' ($P < 0.01$), followed by an increase at 'remission (REM)'. At 'relapse (REL)', these animals lost significant amount of weight compared with 'preinduction (PI)' ($P < 0.01$). (P value was obtained by One way ANOVA, Newman-Keuls post test).

4.3.1.2. Behavioural tests using inclined plane

An inclined plane test was used as a quantitative measure of motor function. Firstly, in order to test reproducibility of the measurements, five naïve rats were examined every half an hour for two hours, and daily up to five days. The angle of the inclined plane that these animals could stay on was between 49°-52° (Figure 4.4). Therefore, this range of angles was used to determine the normal motor function of the limb in the following experiments using rats with EAE.

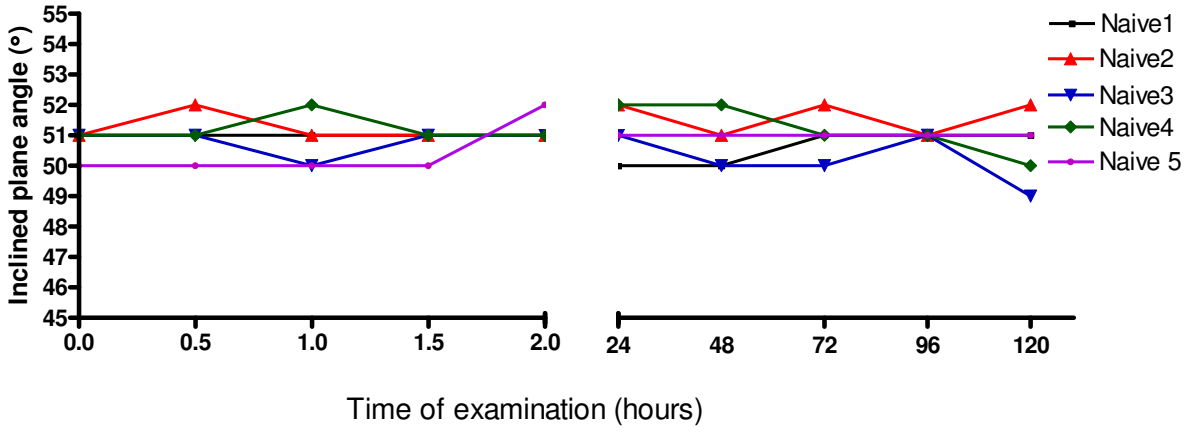

Figure 4.4. Reproducibility of inclined plane measurements in naïve animals

The inclined plane measurements were performed in five naïve animals over five days. It shows that the range of angles that the rats could stay on without sliding down the plane for 10 seconds were between 49° and 52°.

Following the reproducibility test in naïve animals, the inclined plane measurement was performed in EAE animals and controls (IFA and naïve) at the five key stages of disease. As expected, in animals with EAE, motor function of the limbs was significantly decreased at the 'peak disease (PD)', and 'relapse (REL)' compared with 'preinduction (PI)' ($p<0.001$). However at 'remission (REM)', the angle significantly increased in association with recovery from the hindlimb paralysis at the 'peak disease (PD)' ($P<0.001$).

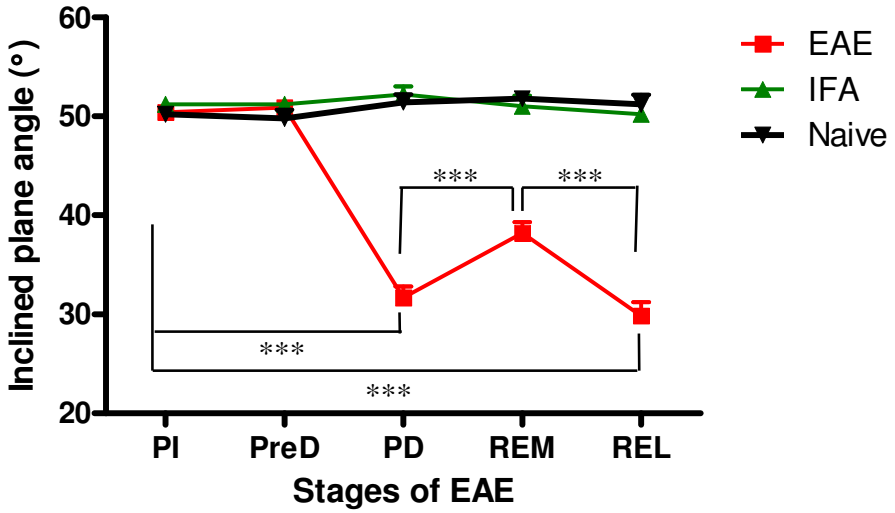

Figure 4.5. Inclined plane measurements along the course of EAE

Inclined plane measurement was performed in animals with EAE (N=17), controls (IFA (N=5) and naïves (N=5)). Control animals showed normal motor function of the limb and the measurements were within the normal range (49-52°). However, animals with EAE showed a significant decrease at the 'peak disease (PD)' compared with both 'preinduction (PI)'($P < 0.001$) and 'predisease (PreD)'($P < 0.001$). The ability to stay on the plane was significantly increased at 'remission (REM)' in contrast to 'peak disease (PD)' ($P<0.001$), but decreased again at 'relapse (REL)' ($P<0.001$). (P value was obtained by One way ANOVA, Newman-Keuls post test).

To explore whether the inclined plane measurements correlate with the neurological scores, a dot plot was used to compare the two values (Figure 4.6). There was a significant negative correlation between the 'inclined plane angle' and 'neurological score' (the Spearman r value was -0.86, and P<0.0001). These results show that the inclined plane test can be used in conjunction with neurological scoring in order to assess neurological deficits in animals with EAE.

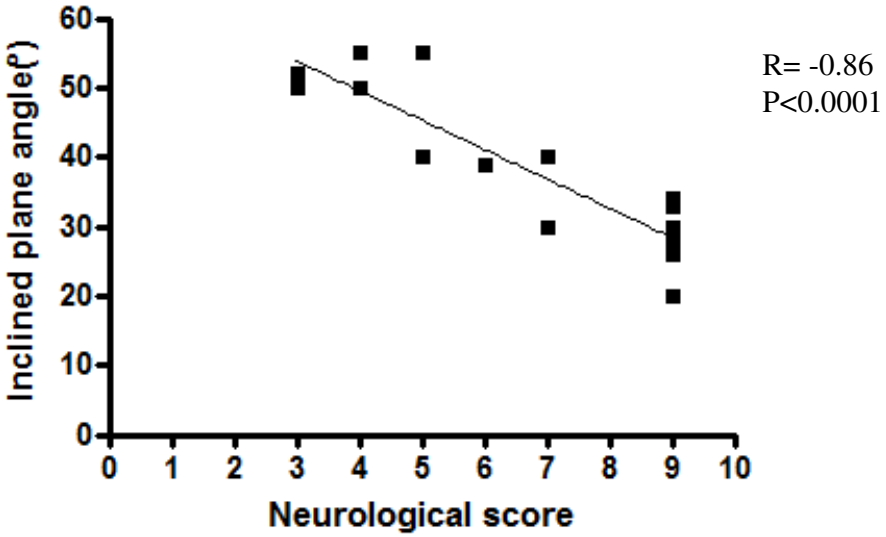

Figure 4.6. Correlation between the inclined plane measurements and neurological scores in animals with EAE

Inclined plane measurement was performed in EAE animals with various neurological scores (N=17). The graph shows that there was a significant negative correlation between the 'inclined plane angles' and 'neurological scores' in these animals. The Spearman r value was -0.86, and P<0.0001 (Spearman's rank correlation test).

4.3.1.3. Rectal temperature measurements

It is good practice to monitor the rectal temperature of the animals during electrophysiological recordings or surgery under anaesthesia. However, while handling non-anaesthetised EAE animals, it was noticed that they had lower temperature at the 'peak disease (PD)' than naïves. Based on this observation, I measured the core temperature in animals with EAE using a rectal probe. Interestingly, the animals showed hypothermia at the 'peak disease (PD)' and 'relapse (REL)', and the temperature was 34°C and 34.3°C respectively (Figure 4.7), which was both significantly different from the temperature measured at 'preinduction (PI)' (36.5°C, $P<0.001$). At 'remission (REM)', the temperature increased in these animals to a normal level (36.1°C, $P<0.05$, compared with 'peak disease (PD)'). In addition, when the rectal temperature was plotted against the neurological score, there was a significant negative correlation (Spearman r value= -0.84, $P<0.0001$) as shown in Figure 4.8.

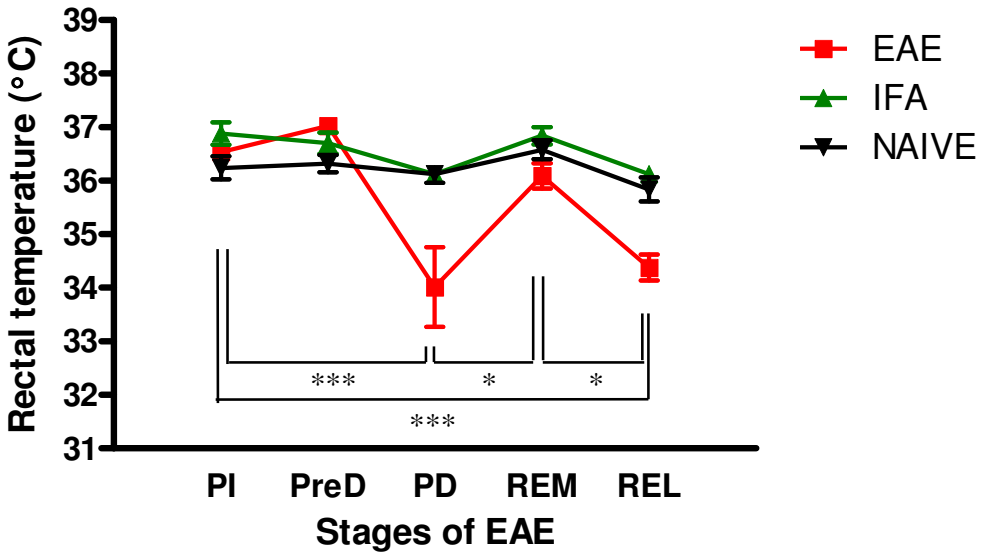

Figure 4.7. Rectal temperature along the time course of EAE

Rectal temperature was measured in non-anaesthetised animals at five time points along the disease course of EAE (EAE (N=23), IFA (N=5), naïve (N=5)). The animals showed a significant decrease of temperature at the 'peak disease (PD)' and 'relapse (REL)' compared with 'preinduction (PI)' ($P < 0.001$). The temperature at remission '(REM)'was significantly higher ($p<0.05$) than both 'peak disease (PD)' and 'relapse (REL)' (P value was obtained by One way ANOVA, Newman-Keuls post test).

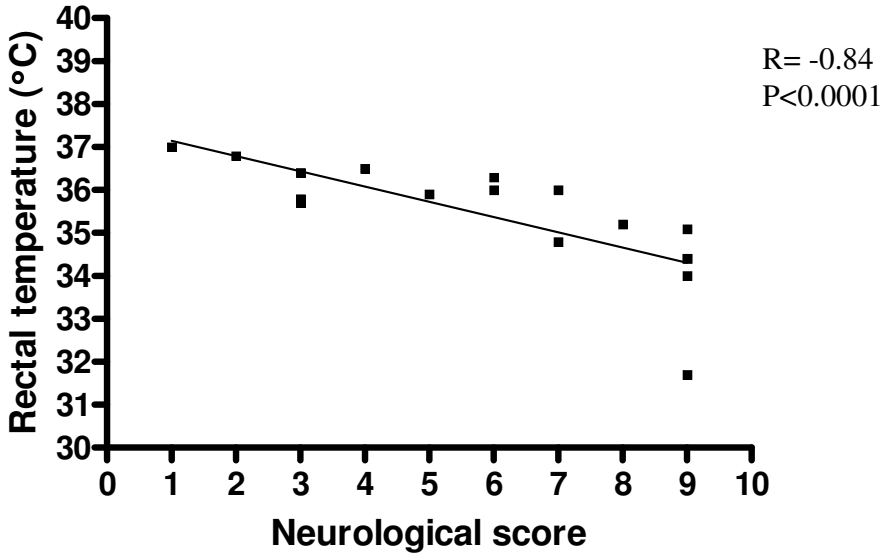

Figure 4.8. Correlation between rectal temperature and neurological scores in animals with EAE

Rectal temperature was measured in non-anaesthetised animals (N=17) with EAE. A significant negative correlation was found between the rectal temperatures and neurological scores in these animals. The Spearman r value was -0.84, and P<0.0001 (Spearman's rank correlation test).

4.3.2. Electrophysiological assessment

For electrophysiological examinations, only animals that had gone through all the five key stages of EAE described in Table 4.2. were included for the final analysis. Thirty animals were induced with EAE for the measurement of axonal conduction, motor neuronal excitability, and synaptic transmission, and among the induced animals, only 21 rats matched the criteria for the final analysis (3 did not present neurological signs, 4 died at the first peak of disease, 2 did not relapse after remission). However, another new batch of 13 animals was induced with EAE separately for the analysis of synaptic activation of motor neurons, due to the time required for development of the technique. Among these animals, nine were included for analysis of the electrophysiological recordings (one had no signs, 2 died at the first peak, 1 died after remission).

4.3.2.1. Sensory compound action potential (SCAP)

The antidromic sensory compound action potential (SCAP) was measured in animals with EAE at five stages along the disease course. Using Excel software, the peak amplitude was measured in each recording, and a mean value was calculated per group. As shown in Figure 4.9 (a), the mean peak amplitude of EAE animals shown in red decreased significantly at 'peak disease (PD)' compared with 'preinduction (PI)', and it remained decreased until 'relapse (REL)' ($P<0.001$). The mean peak response amplitude was 153.7μV, 142.9μV, 58.48μV, 34.9μV, 24.6μV at 'preinduction (PI)', 'predisease (PreD)', 'peak disease (PD)', 'remission (REM)', 'relapse (REL)' respectively. The representative recordings of SCAP at the five key stages are shown in Figure 4.9 (b), where the graphs are plotted from front to back chronologically (from 'preinduction (PI)' to 'relapse (REL)').

A

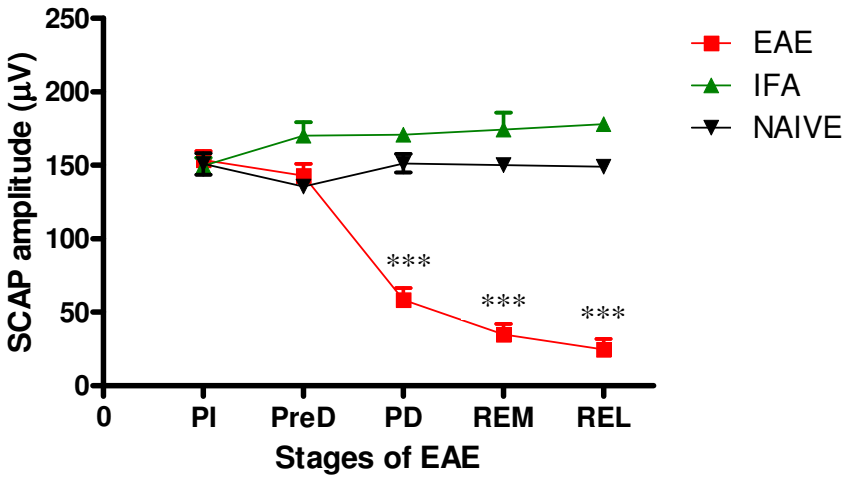
250
200
150
100
50
0
SCAP amplitude (µV)
0
PI
PreD
PD
REM
REL
Stages of EAE
***
***
***
EAE
IFA
NAIVE

B

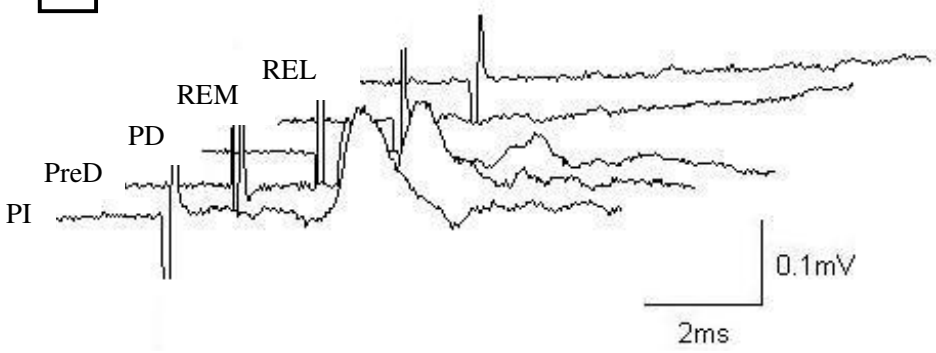
REL
REM
PD
PreD
PI
0.1mV
2ms

Figure 4.9. Sensory compound action potentials (SCAP) measured in animals with EAE and controls (IFA, naïve)

Sensory compound action potentials (SCAP) were measured at five stages along the disease course of animals with EAE (N=21) and controls (IFA, naïve, N=5 each).
(a) The mean (±SE) SCAP amplitude was significantly reduced at the 'peak disease (PD)' and remained decreased until 'relapse (REL)' compared with 'preinduction (PI)' ($P<0.001$, One way ANOVA, Newman-Keuls post test).
(b) Shows a representative waterfall plot of SCAP recorded at five stages of the disease course. Recordings are aligned from front to back chronologically ('preinduction' to 'relapse')

4.3.2.2. H reflex, M response and F wave

H reflexes, which are the result of a monosynaptic reflex, were measured at different stages along the disease course in animals with EAE. The mean peak response amplitudes were measured using Excel software and plotted in Figure 4.10 (a). The mean response amplitude of H reflex at 'preinduction (PI)' was 7.1mV and it decreased significantly only at 'relapse (REL)' ($P<0.001$) to 2.42mV. Figure 4.10 (b) shows representative waterfall recordings of H reflexes taken at different stages, starting from 'preinduction (PI)' to 'relapse (REL)' aligned from front to back. It shows that at the 'relapse (REL)', the H reflex was significantly reduced.

When the stimulation was increased to a supramaximal level, the M responses and F waves were recorded. The mean peak response amplitudes of M responses and F waves were plotted at five different stages in Figure 4.10 (c) and (d) respectively. Similar to the H reflexes, F waves were only significantly reduced at 'relapse (REL)' at a mean value of 1.84mV. However, the M response was decreased significantly, earlier than H reflex or F waves during 'remission (REM)' to 'relapse (REL)' ($P<0.001$). The representative recordings of M responses and F waves taken at each of the five key time points along the disease course are aligned as a waterfall plot in Figure 4.10 (e).

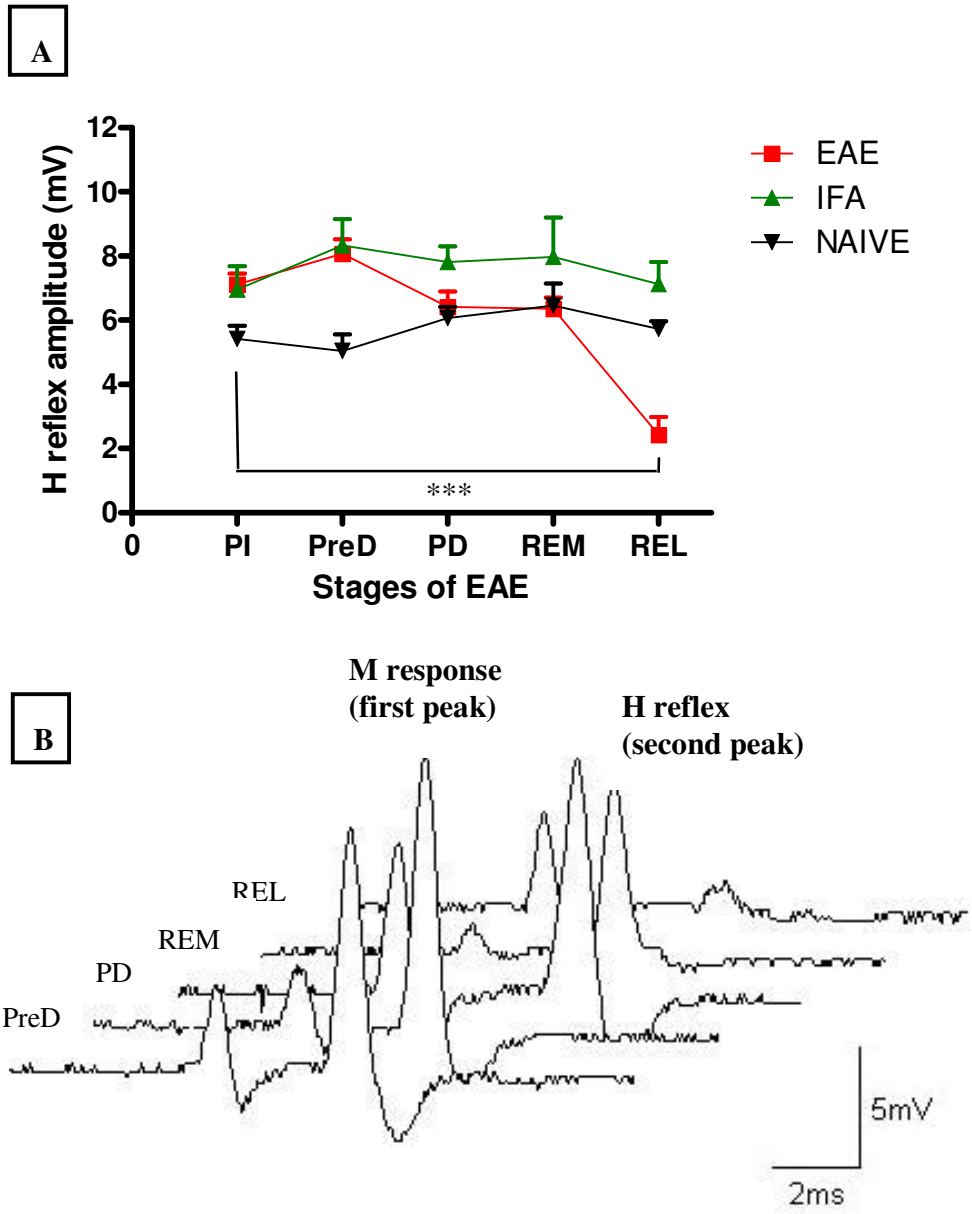
A
H reflex amplitude (mV)
12
10
8
6
4
2
0
0
PI
PreD
PD
REM
REL
Stages of EAE
***
EAE
IFA
NAIVE
B
M response
(first peak)
H reflex
(second peak)
REL
REM
PD
PreD
PI
5mV
2ms

C

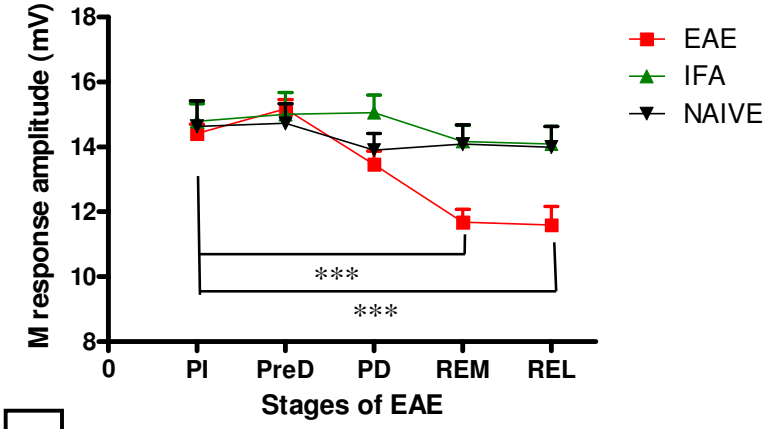
M response amplitude (mV)
18
16
14
12
10
8
0
PI
PreD
PD
REM
REL
Stages of EAE
***
***
EAE
IFA
NAIVE

D

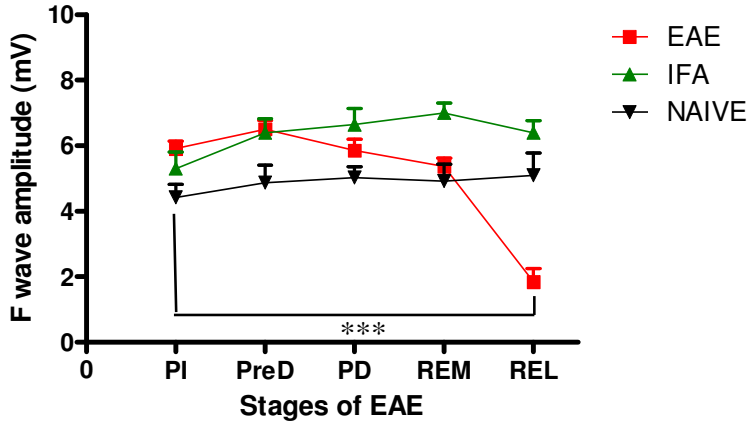
F wave amplitude (mV)
10
8
6
4
2
0
0
PI
PreD
PD
REM
REL
Stages of EAE
***
EAE
IFA
NAIVE

E

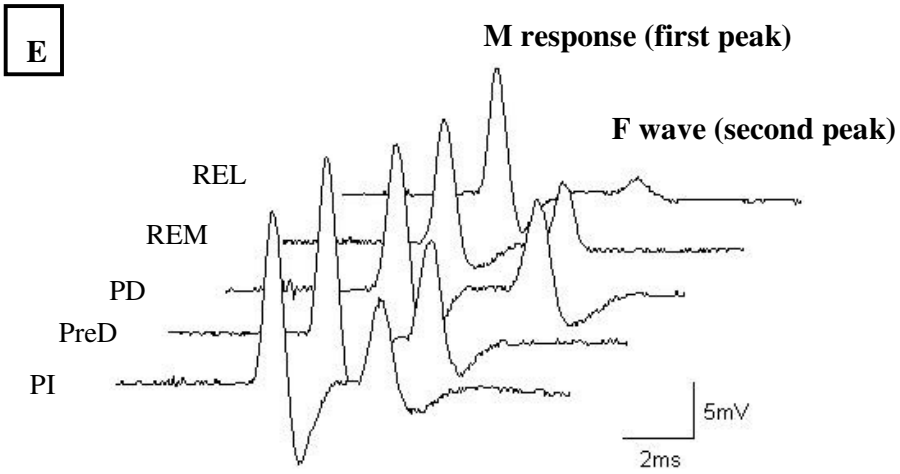
M response (first peak)
F wave (second peak)
REL
REM
PD
PreD
PI
5mV
2ms

Figure 4.10. H reflex, M response and F wave measured in animals with EAE and controls (IFA, naïve)

The H reflex, M response and F wave were measured at the five key stages of disease of animals with EAE (N=21) and controls (IFA, naïve, N=5 each).
(a) H reflex was measured in animals at five different stages, and the means (±SE) were plotted. A significant reduction of the response amplitude was only seen at 'relapse (REL)' compared with 'preinduction (PI)' (P<0.001, One way ANOVA, Newman-Keuls post test).
(b) A representative waterfall plot of M response and H reflex recordings at different stages of EAE are illustrated in a chronological order from front to back ('preinduction' to 'relapse').
(c) ,(d) Means (±SE) of M responses and F waves are plotted respectively. The F waves were reduced significantly only at 'relapse (REL)' (P<0.001), whereas the M response was reduced from 'remission (REM)' until 'relapse (REL)' (P<0.001). P value obtained by One way ANOVA, Newman-Keuls post test.
(e) A representative waterfall plot of M responses and F waves recorded at the key stages along the disease course of EAE is shown sequentially, aligned in chronological order.

4.3.2.3. Cord dorsum potential (CDP)

Cord dorsum potentials (CDP) were measured in animals with EAE and the peak response amplitudes of these dorsal horn synaptic responses were plotted as line graphs, shown in Figure 4.11 (a). At 'preinduction (PI)', the mean dorsal horn synaptic response was 74.89μV, and this response was significantly reduced at the 'peak disease (PD)' (58.98μV, $P<0.01$), 'remission (REM)' (57.98μV, $P<0.01$) and also at 'relapse (REL)' (45.78μV, $P<0.001$). Figure 4.11(b) illustrates each recording taken at five time stages, aligned sequentially from front to back.

4.3.2.4. Synaptic activation of motor neurons (SAM)

The response amplitude of the synaptic activation of motor neurons (SAM) was measured and plotted in line graphs as shown in Figure 4.12 (a). There was a noticeable significant decrease of SAM at 'peak disease (PD)', where the response amplitude was 2.16mV compared to 9.92mV at 'preinduction (PI)' ($P<0.001$). Although there was a slight increase of SAM at 'remission (REM)', the difference was not significant. At 'relapse (REL)', the SAM was almost absent, and the mean value was 0.09mV (significantly decreased, $P<0.001$). Figure 4.12 (b) illustrates representative recordings of SAM at five different stages sequentially, in chronological order from front to back.

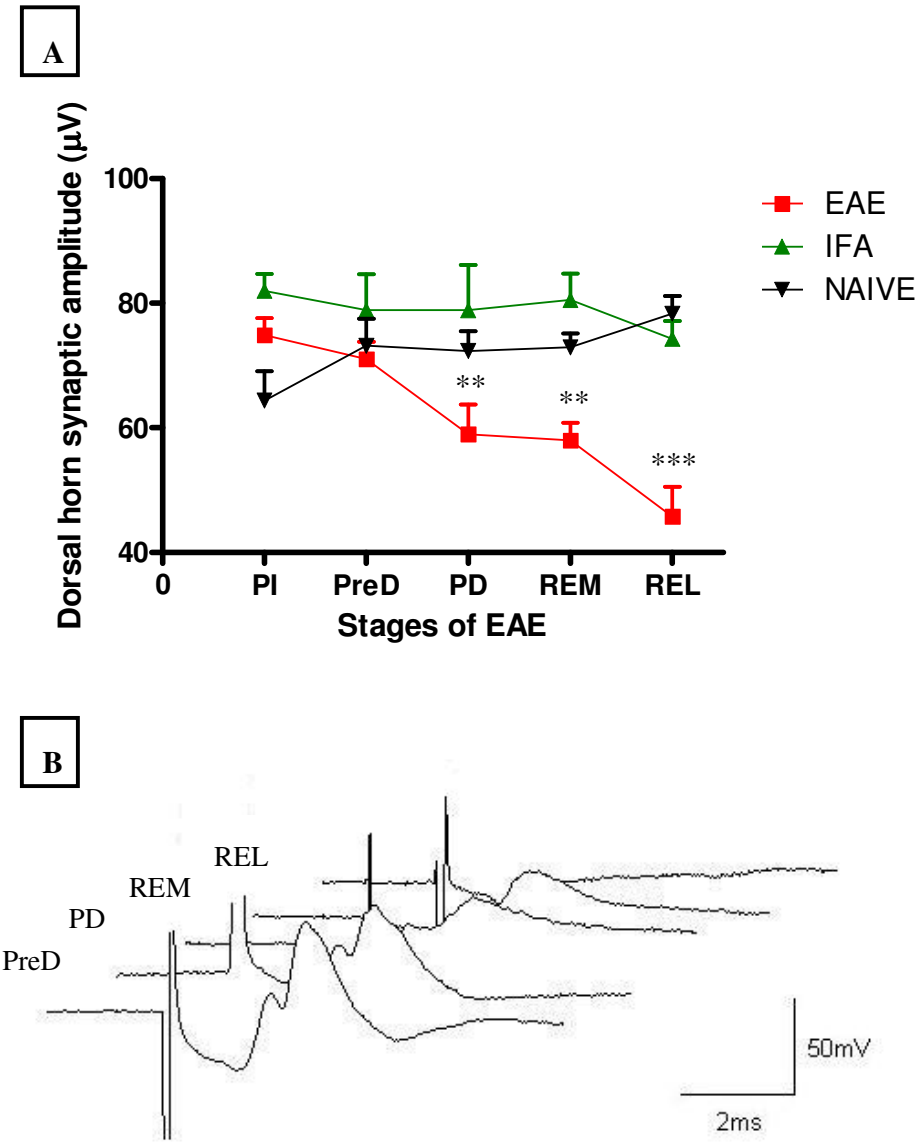
A
Dorsal horn synaptic amplitude (µV)
100
80
60
40
0
PI
PreD
PD
REM
REL
Stages of EAE
**
**
***
EAE
IFA
NAIVE
B
REL
REM
PD
PreD
PI
50mV
2ms

Figure 4.11. Cord dorsum potentials (CDP) measured in animals with EAE and controls (IFA, naïve)

The CDPs were recorded at the five key stages along the disease course of animals with EAE (N=21) and controls (IFA, naïve, N=5 each).
(a) The means (±SE) of the dorsal horn synaptic response amplitudes were plotted and show that a significant reduction of the response amplitude was observed at 'peak disease (PD)' (P<0.01), 'remission (REM)' (P<0.01), and at 'relapse (REL)' (P<0.001) compared with 'preinduction (PI)'(P value obtained by One way ANOVA, Newman-Keuls post test).
(b) Representative waterfall plot of CDP taken at each of the five key stages of EAE, aligned sequentially in chronological order from front to back ('preinduction' to 'relapse').

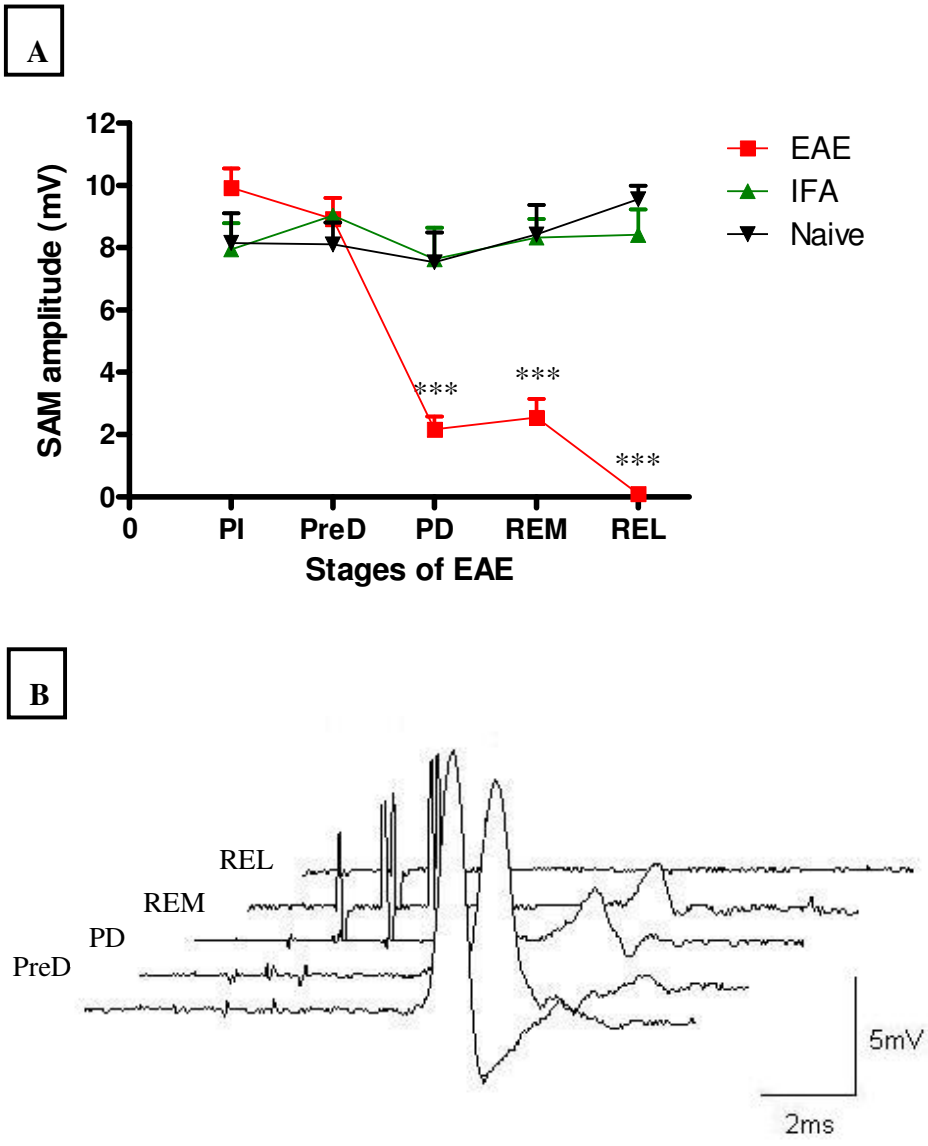
A
SAM amplitude (mV)
12
10
8
6
4
2
0
0
PI
PreD
PD
REM
REL
Stages of EAE
***
***
***
EAE
IFA
Naive
B
REL
REM
PD
PreD
PI
5mV
2ms

Figure 4.12. Synaptic activation of motor neuron (SAM) measured in animals with EAE and controls (IFA, naïve)

SAM was measured at the five key stages along the disease course of animals with EAE (N=9) and controls (IFA, naïve, N=5 each).
(a) The means (±SE) of SAM were plotted and show that a significant reduction of the response amplitude was observed from 'peak disease (PD)' to 'relapse (REL)' (P<0.001, One way ANOVA, Newman-Keuls post test) compared with 'preinduction (PI)'.
(b) Representative waterfall plot of SAM taken at five different stages is aligned sequentially in chronological order from front to back ('preinduction' to 'relapse').

4.3.2.5. Summary of the electrophysiological changes in the disease course of EAE

Table 4.5 below summarises the electrophysiological changes at the five key stages of EAE. At the 'peak disease (PD)', axonal conduction (SCAP), synaptic transmission (CDP) and synaptic activation of motor neurons (SAM) were all significantly reduced. These measures remained reduced during 'remission (REM)' and 'relapse (REL)', at which time motor neuronal excitability (H reflex, M response, and F wave) was also significantly decreased. Surprisingly, none of the measures showed an increase upon remission from the deficits.

Table 4.5. Table summarising electrophysiological changes along five different stages of EAE

	Preinduction (PI)	Predisease (PreD)	Peak Disease (PD)	Remission (REM)	Relapse (REL)
SCAP	–	–	***	***	***
M response	–	–	–	***	***
H reflex	–	–	–	–	***
F wave	–	–	–	–	***
CDP	–	–	**	**	***
SAM	–	–	***	***	***

Note: symbols are used to indicate * P<0.05, ** P<0.01, ***P<0.001, - no significant change

4.3.3. Histological assessment

Histological changes in the spinal cord at different stages along the disease course of EAE were explored (three animals at each stage). A total of twelve animals were induced with EAE, and the neurological scores of these animals are plotted in Figure 4.13, where the five groups are colour coded ('preinduction (PI)' in black, 'predisease (PreD)' in orange, 'peak disease (PD)' in red,' remission (REM)' in green, 'relapse (REL)' in blue). This graph shows that animals for 'preinduction (PI)' were culled before induction of the disease, and animals for 'predisease (PreD)' were culled at day five post induction. Animals for 'peak disease (PD)', were culled at day 9,10 and 11 post induction, and all of these animals showed paralysis of both limbs (i.e. a neurological score of nine). The animals that were used for 'remission (REM)' reached a neurological score of nine at their 'peak disease (PD)', and recovered eventually to a score of three. Also, animals for 'relapse (REL)' had reached their second peak between day 15 and 17 post induction. The selection procedure of these animals for histology fulfilled the criteria listed in Table 4.2. For control tissue, IFA animals were culled at the same time points with the EAE animals (N=3 in each group).

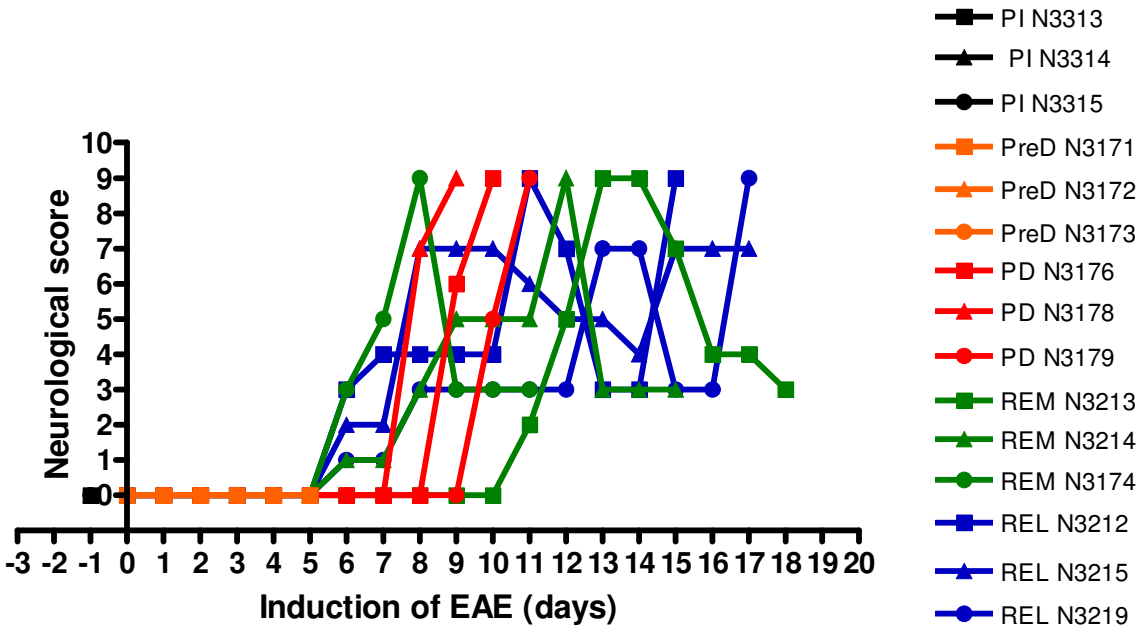

Figure 4.13. Neurological scores of animals for histological analysis

Neurological scores of animals used for histological assessments are plotted against time in days following the 'induction of EAE' (N=3 in each group). These groups are colour-coded as follows; 'preinduction (PI); black', 'predisease (PreD); orange', 'peak disease (PD); red', 'remission (REM); green', and 'relapse (REL); blue'. The animals were selected according to the criteria described in Table 4.2 and cullled for histological analyses.

4.3.3.1. Microglial/macrophage activation (ED1 labelling)

Immunoreactivity for ED1 was assessed quantitatively by calculating the percentage area of labelling in transverse sections of the spinal cord of animals at the key stages of EAE. No ED1 expression was observed at 'preinduction (PI)' and 'predisease (PreD)', (Figure 4.14). However, ED1 expression was significantly increased at 'peak disease (PD)' to 6% ($P<0.05$), and at 'relapse (REL)' to 5.87% ($P<0.05$), compared with 'preinduction (PI)'. Figure 4.15 (e) shows the cord labelled with ED1 at the 'peak disease (PD)', where clustered ED1 positive cells were mostly found in the subpial and perivascular regions. At 'remission (REM)', the degree of labelling was decreased to 2.41%, and the pattern of labelled cells was similar to 'peak disease (PD)' (Figure 4.15 (g)). At 'relapse (REL)' the degree of labelling was increased to a mean of 5.87%, but ED1 positive cells were mostly accumulated in the white matter rather than the grey (Figure 4.11 (i)). None of the control animals showed immunoreactivity for ED1.

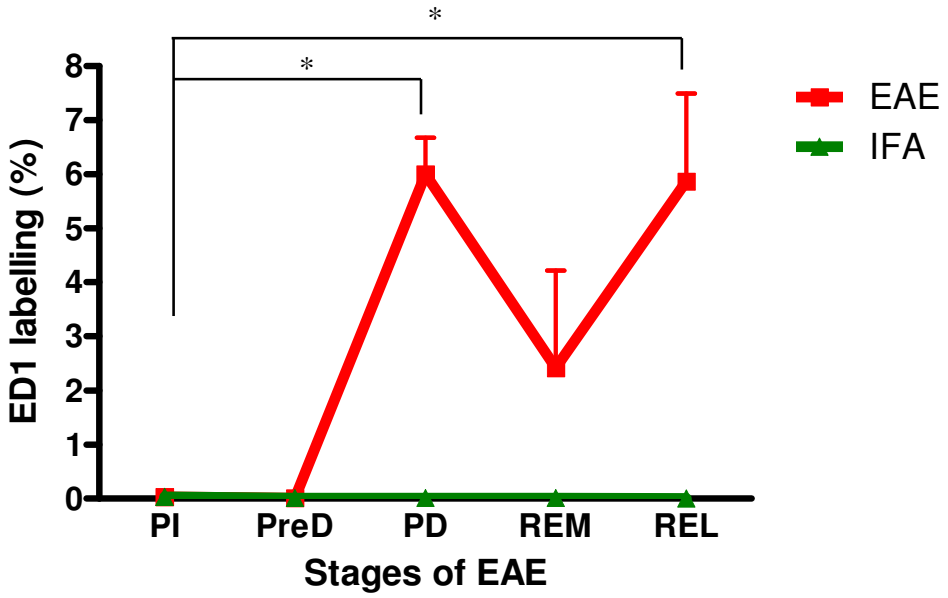

Figure 4.14. ED1 expression in percentages at different stages of EAE

ED1 immunoreactivity was quantified by calculating the percentage area of labelling in the spinal cords of animals with EAE and controls (IFA) (N=3 in each stage). ED1 expression was significantly increased at 'peak disease (PD)' and 'relapse (REL)' compared with 'preinduction (PI)' (P<0.05, One way ANOVA, Newman-Keuls post test).

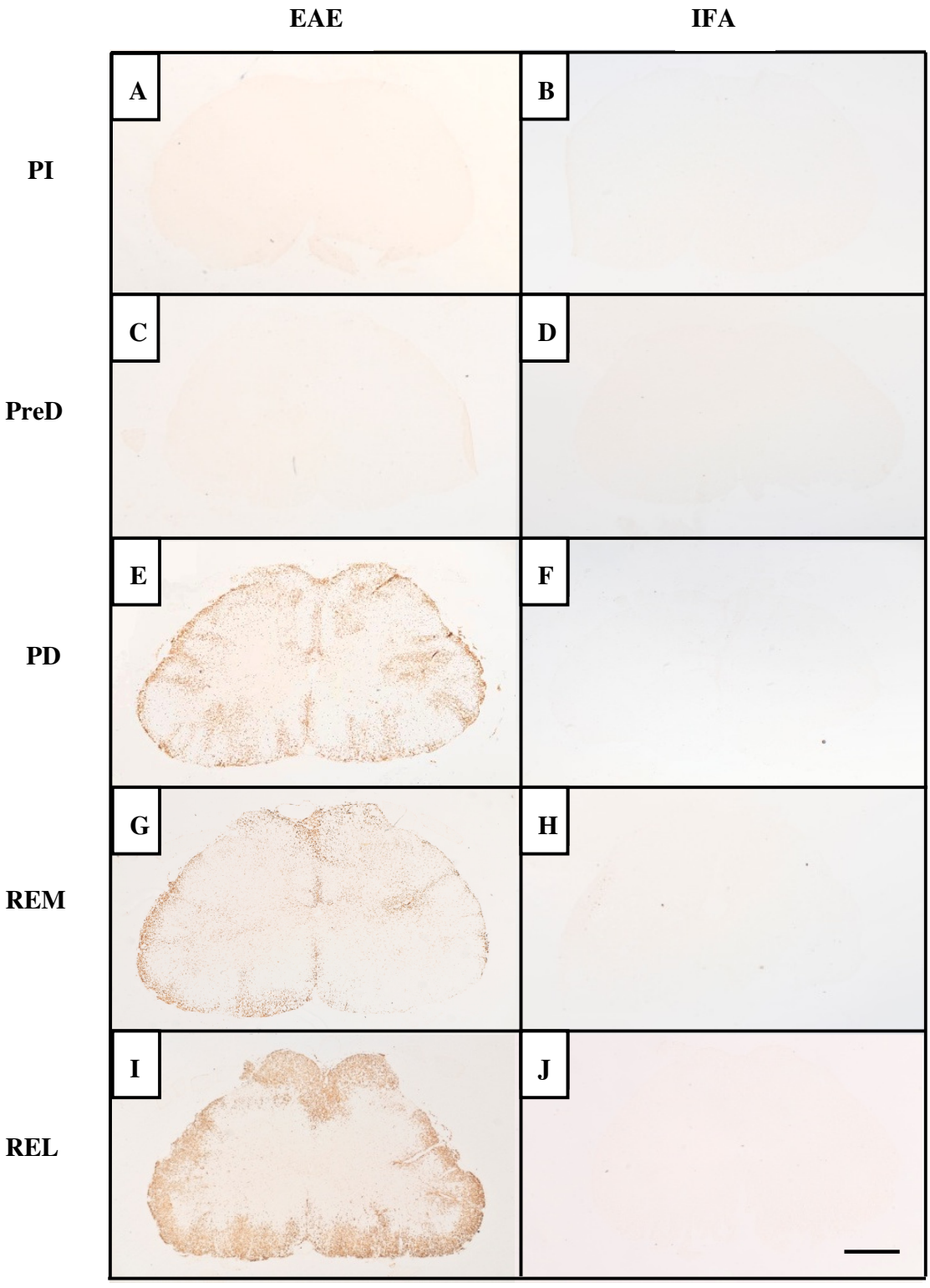
EAE
IFA
PI
PreD
PD
REM
REL
A
B
C
D
E
F
G
H
I
J

Figure 4.15. ED1 labelling of spinal cord sections at different stages of EAE

Transverse sections of the spinal cords were taken from animals at the key stages of EAE, and were labelled immunohistochemically for the presence of ED1. The sections in the left and right columns are taken from EAE and control (IFA) respectively.
(a) and (b) are spinal cords at 'preinduction (PI)', (c) and (d) are at 'predisease (PreD)', (e) and (f) are at 'peak disease (PD)', (g) and (h) are at 'remission (REM)', (i) and (j) are at 'relapse (REL)'. In animals with EAE, ED1 immunoreactivity was significantly increased at 'peak disease (PD)' especially around subpial and perivascular regions of the spinal cord. At 'remission (REM)', the level of ED1 staining was decreased compared with 'peak disease (PD)'. However at 'relapse (REL)', the degree of labelling was increased showing concentrated immunoreactivity in the white matter compared to the grey. (Scale bar=1000μm)

As it was observed that the immunoreactivity of ED1 was positive mainly during the period when the animals showed neurological signs (i.e. at 'peak disease (PD)', 'remission (REM)' and 'relapse (REL)'), the correlation between 'ED1 labelling' and 'neurological scores' was analysed. Figure 4.16 shows that there was a significant correlation ($p<0.0001$, $R^2=0.81$) between the two values.

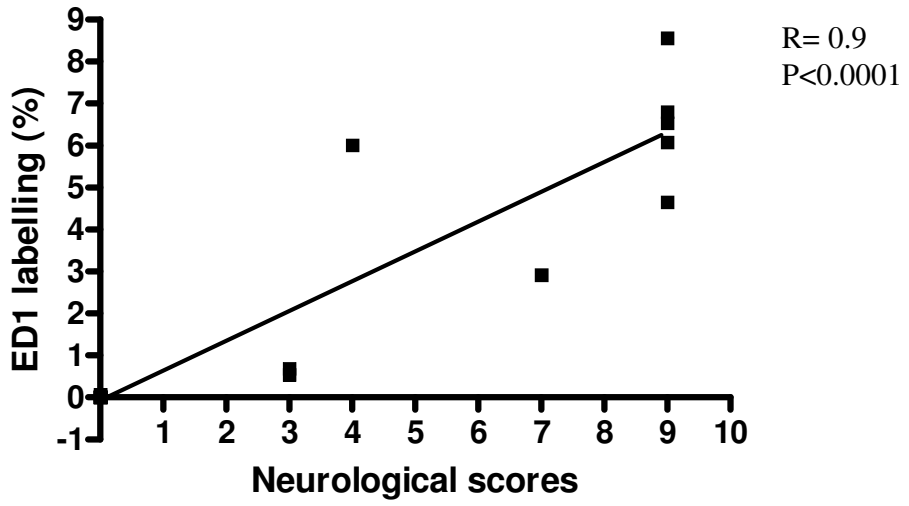

Figure 4.16. Correlation of ED1 labelling and neurological scores

ED1 labelling (%) and neurological scores of animals with EAE show significant positive correlation (N=15). The Spearman r value was 0.9, and P<0.0001 (Spearman's rank correlation test).

4.3.3.2. iNOS labelling

Immunoreactivity for iNOS was assessed quantitatively by measuring the percentage area of labelling in transverse spinal cord sections of animals at different stages of EAE. The results are plotted in Figure 4.17. The expression of iNOS was exclusively detected at the 'peak disease (PD)' stage of EAE, and it showed a mean of 1.2% of spinal cord area. The pattern of expression was similar to the expression of ED1 observed at the same stage, as iNOS labelling was found mostly around subpial and perivascular regions (Figure 4.18 (e)). No animals at other stages of the disease, or controls showed, iNOS positivity.

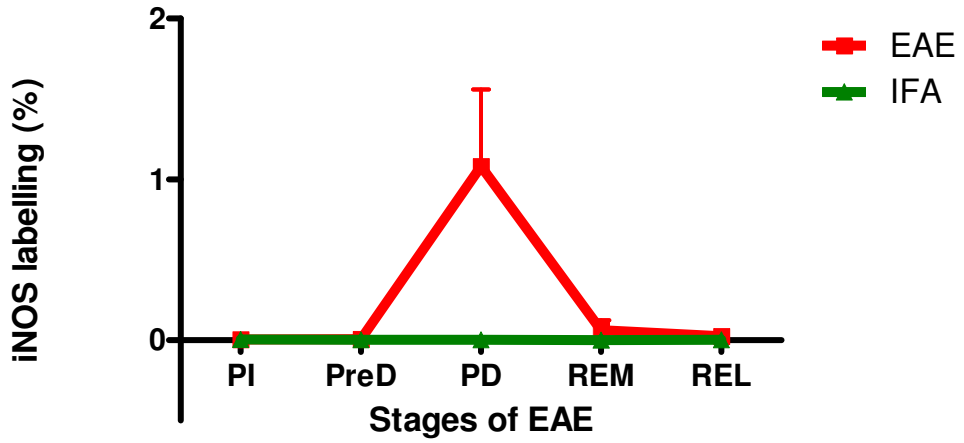

Figure 4.17. iNOS labelling of spinal cord sections at different stages of EAE

iNOS expression was quantitatively analysed using animals at different stages of EAE (N=3 in each stage). The expression was exclusive at 'peak disease (PD)', where labelling was a mean of 1.2% of the whole spinal cord area.

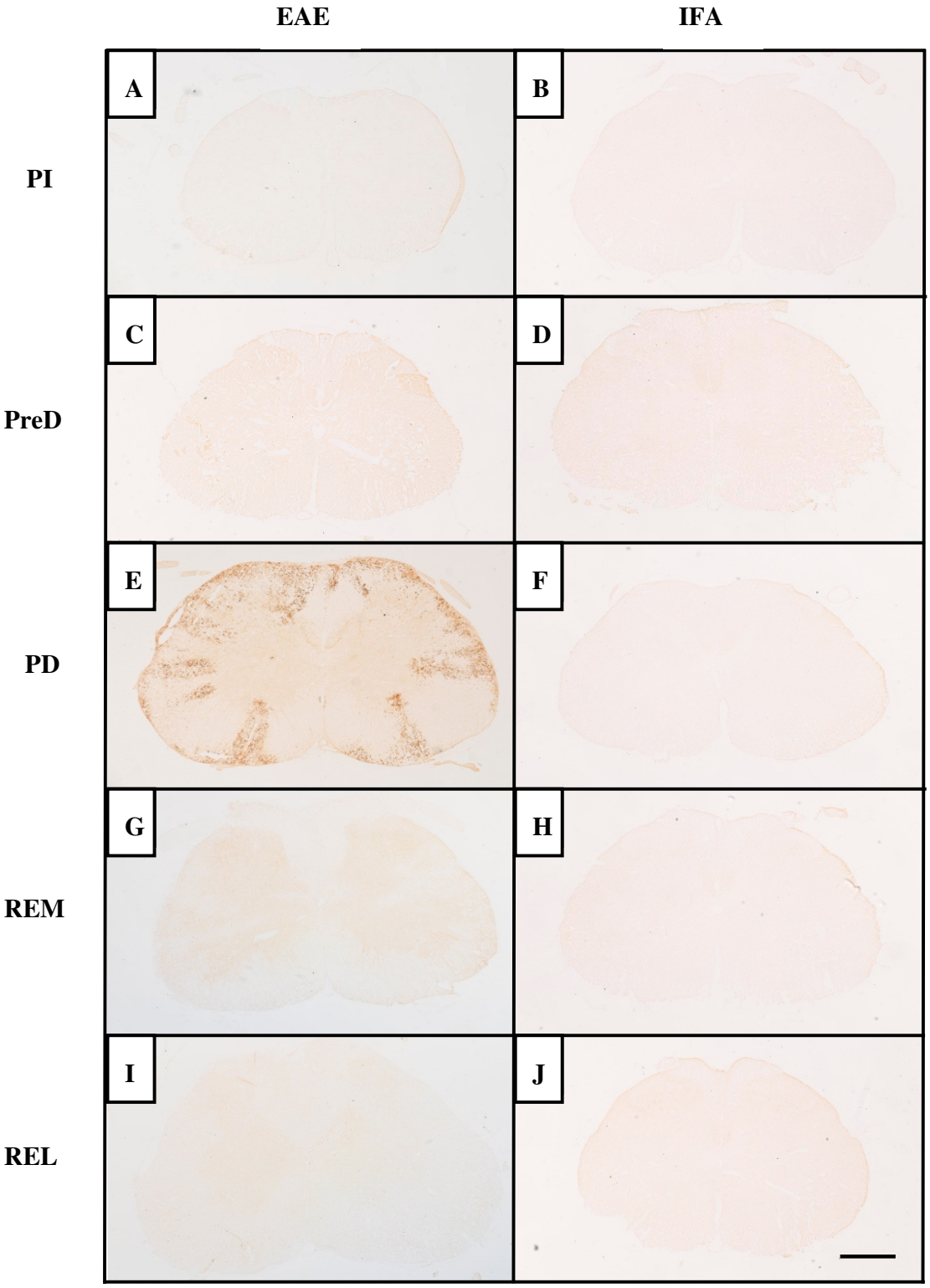
EAE
IFA
A
B
PI
C
D
PreD
E
F
PD
G
H
REM
I
J
REL

Figure 4.18. iNOS labelling of spinal cord sections at different stages of EAE

Transverse sections of the spinal cords were taken from animals at the key stages of EAE, and were labelled immunohistochemically for the presence of iNOS. The sections in the left and right columns are taken from EAE and control (IFA) respectively.
(a) and (b) are spinal cords taken at 'preinduction (PI)', (c) and (d) are at 'predisease (PreD)', (e) and (f) are at 'peak disease (PD)', (g) and (h) are at 'remission (REM)', (i) and (j) are at 'relapse (REL)'. In EAE tissue, iNOS immunoreactivity was exclusively expressed at 'peak disease (PD)', and the labelling occurred in the subpial and perivascular regions. (Scale bar=1000μm)

4.3.2.3. Degeneration and demyelination

Pathology of the white matter was quantified in animals with EAE at different stages, using resin sections of the same animals used for immunohistochemistry. The pathology included areas of both axonal degeneration and demyelination. At 'preinduction (PI)' and 'predisease (PreD)', no pathology was observed in any of the tissues (Figure 4.19 and Figure 4.20 (a), (c)). However, a mean area of 16.5% of the white matter was affected at 'peak disease (PD)' ($P<0.001$ compared with PI), and the pathology was mostly present around the rim of the spinal cord, perivascular regions and the dorsal column (Figure 4.20 (e)). At 'remission (REM)', less pathology was found than at 'peak disease (PD)' where the mean value was 6.4%, occurring in the similar areas (Figure 4.20 (g)). The pathology at 'relapse (REL)' was widespread ($P<0.001$ compared with PI), covering more than half of the white matter (mean was 58.9%, Figure 4.20 (i)). None of the animals injected with IFA showed pathological changes.

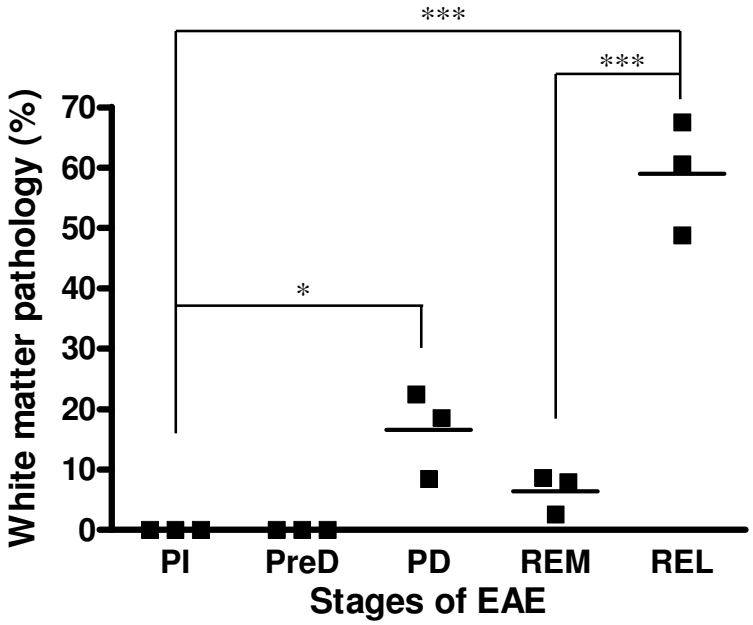

Figure 4.19. Percentage of pathology in white matter at different stages of EAE

Pathological area of the white matter of the spinal cord was measured in animals with EAE, at different stages (N=3 in each stage). No pathology was observed at 'preinduction (PI)' and 'predisease (PreD)', but a significant amount of pathology was found at the 'peak disease (PD)' (16.5%, P<0.05) compared with 'preinduction (PI)'. At 'relapse (REL)' the percentage area of pathology significantly increased to 58.9% (compared with 'preinduction (PI)' and 'remission (REM)' (P<0.001). (P value was obtained by One way ANOVA, Newman-Keuls post test).

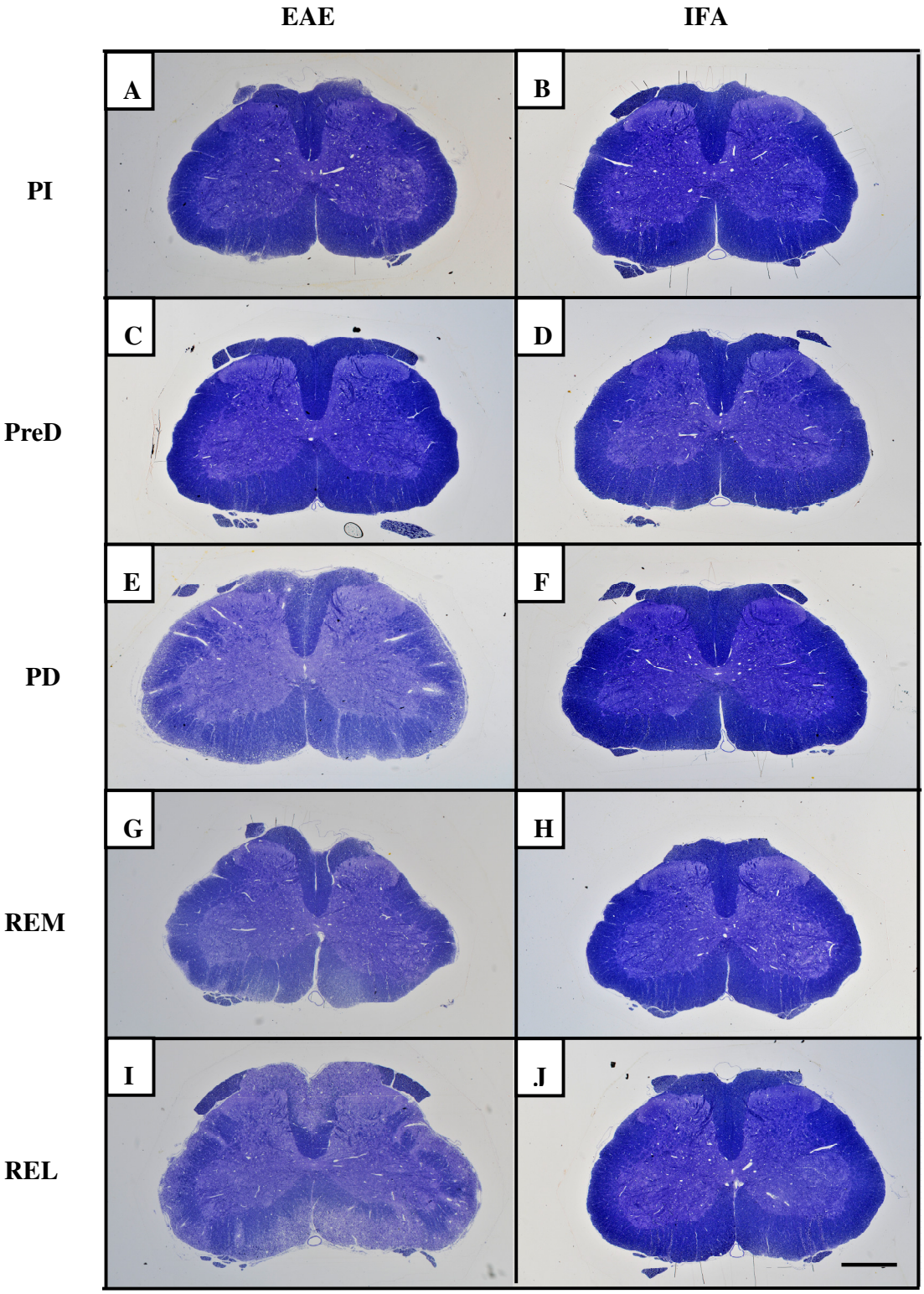
EAE
IFA
PI
PreD
PD
REM
REL
A
B
C
D
E
F
G
H
I
J

Figure 4.20. Resin sections of spinal cord at different stages of EAE

Transverse sections of the spinal cord were taken from animals at the five key stages of EAE, and were processed into resin sections. The sections in the left and right columns are taken from EAE and control (IFA) respectively.
(a) and (b) are spinal cords taken at 'preinduction (PI)', (c) and (d) are at 'predisease (PreD)', (e) and (f) are at 'peak disease (PD)', (g) and (h) are at 'remission (REM)', (i) and (j) are at 'relapse (REL)'. In EAE animals, a significant increase in pathology was observed at 'peak disease (PD)' compared with 'preinduction (PI)' ($P<0.05$), including both axonal degeneration and demyelination which were found at the rim of the spinal cord, perivascular regions and dorsal column. Animals at 'remission (REM)' also showed pathology in the same regions, but the amount of pathology was reduced. At 'relapse (REL)', the pathology was more widespread, affecting more than half of the white matter. (Scale bar=1000μm)

Further investigations of the pathological changes in the dorsal column of the spinal cords were performed, in order to study the correlation with axonal conduction measured from the dorsal column axons. The pathology was quantified by adding the areas of both demyelination and axonal degeneration. Figure 4.21 (a) shows that there was no pathology observed at either 'preinduction (PI)' or 'predisease (PreD)'. However, at the remaining stages of the disease, the percentage of pathology showed a biphasic pattern. At the 'peak disease (PD)', the mean percentage was 83.33%, which was significantly higher than at 'preinduction (PI)' ($P<0.001$). At 'remission (REM)', the percentage decreased to a mean of 36.4%, and at 'relapse (REL)' the mean percentage increased to 96.67% ($P<0.001$). In these tissues, the composition of the pathology (ratio of degeneration and demyelination) was different as shown in Figure 4.21 (b). Axonal degeneration was more prominent than demyelination in tissues collected at 'peak disease (PD)' (a photomicrograph is presented in Figure 4.22 (e)), but demyelination became dominant at 'remission (REM)' (Figure 4.22 (g)). However, at 'relapse (REL)', the pathology showed a similar amount of each of these two factors (Figure 4.22 (i)).

Using the area of pathology of the dorsal columns, the correlation between the pathology and axonal conduction was explored. Axonal conduction was measured by recording the SCAP, and the response amplitudes of SCAP at different stages are plotted in Figure 4.23 (a). The SCAP was significantly decreased at 'peak disease (PD)' ($P<0.001$) and remained decreased until 'relapse (REL)' ($P<0.001$), which was reminiscent of the SCAP recordings shown previously with a larger number of rats (Figure 4.9). However, the dot plot in Figure 4.23 (b) illustrates that there was no significant correlation between the axonal conduction and area of pathology in the dorsal columns.

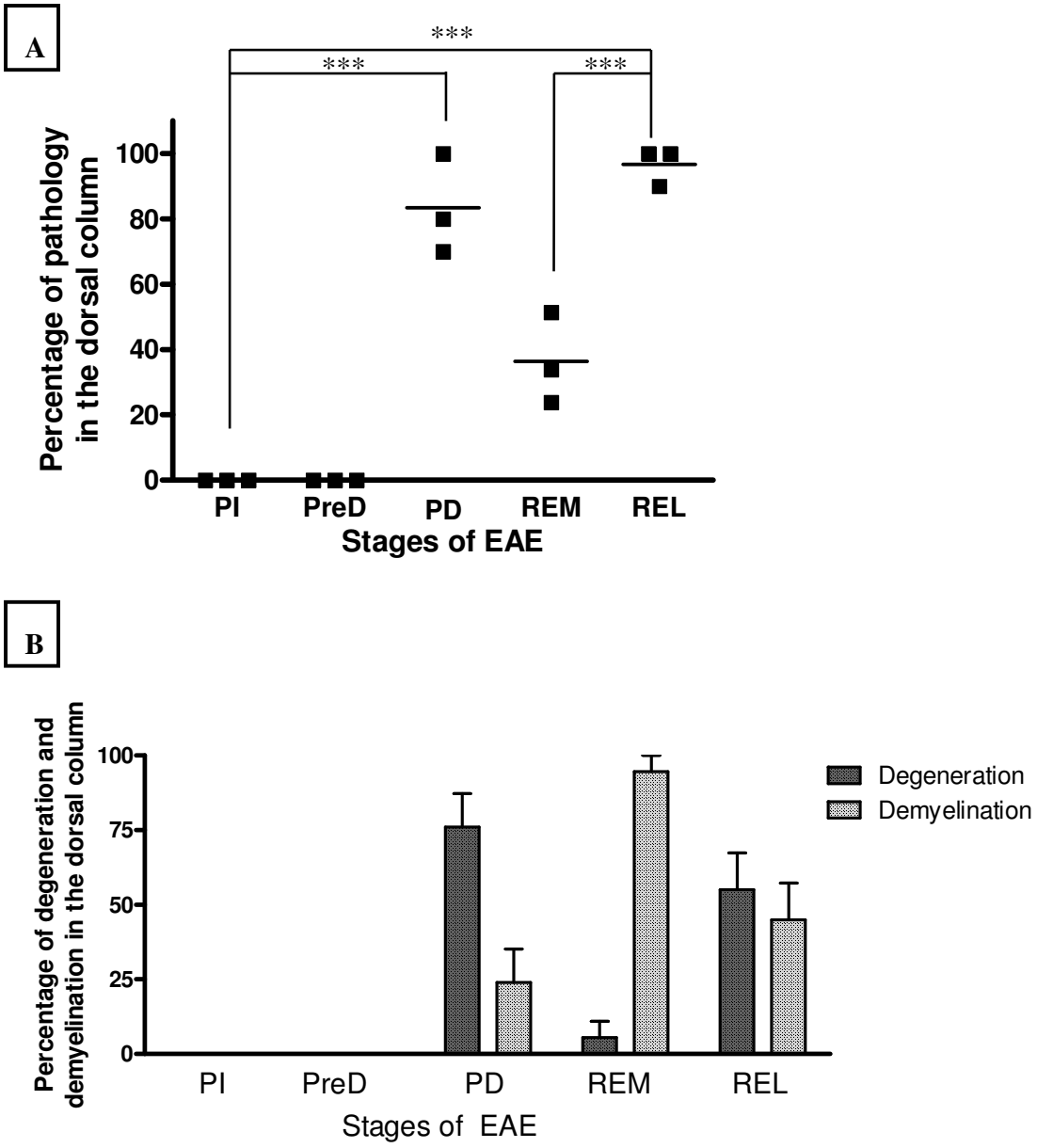
A
***
***
***
Percentage of pathology in the dorsal column
100
80
60
40
20
0
PI
PreD
PD
REM
REL
Stages of EAE
B
Percentage of degeneration and demyelination in the dorsal column
100
75
50
25
0
Degeneration
Demyelination
PI
PreD
PD
REM
REL
Stages of EAE

Figure 4.21. Pathology in the dorsal columns at different stages of EAE

(a) The percentage of total pathology in the dorsal columns was measured and plotted at the five key stages of the disease (N=3 in each stage). No pathology was found at 'preinduction (PI)' and 'predisease (PreD)'. However, significant amount of pathology was found at 'peak disease (PD)' and 'relapse (REL)' (P<0.001, One way ANOVA, Newman-Keuls post test). The mean percentage of pathology at each stage was 83.33%, 36.4%, and 96.67% at 'peak disease (PD)', 'remission (REM)' and 'relapse (REL)' respectively.
(b) The areas of axonal degeneration and demyelination were measured and plotted as percentages at each stage of the disease (N=3 in each stage). Degeneration was dominant at 'peak disease (PD)', but demyelination was dominant at 'remission (REM)'. At 'relapse (REL)', these two factors were more balanced.

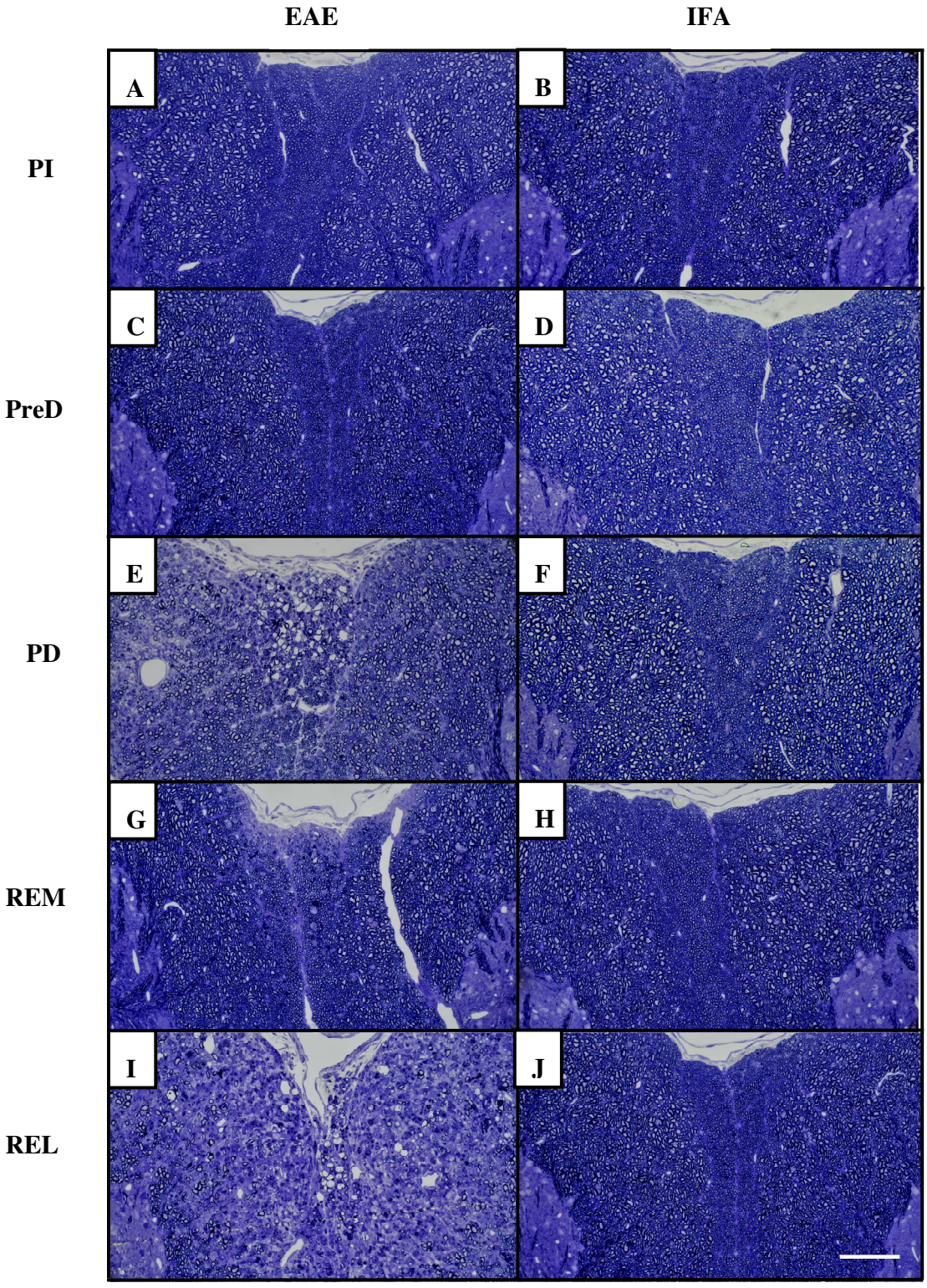
EAE
IFA
PI
PreD
PD
REM
REL
A
B
C
D
E
F
G
H
I
J

Figure 4.22. Dorsal columns at different stages of EAE

Transverse sections of the dorsal columns were taken from animals at the five key stages along the disease course of EAE. The sections in the left and right columns are taken from EAE and control (IFA) respectively.
(a) and (b) are spinal cords taken at 'preinduction (PI)', (c) and (d) at 'predisease (PreD)', (e) and (f) are at 'peak disease (PD)', (g) and (h) are at 'remission (REM)', (i) and (j) are at 'relapse (REL)'. In EAE tissues, a significant increase of pathology was observed at 'peak disease (PD)', where axonal degeneration was more prominent than demyelination. However, the amount of degeneration decreased at 'remission (REM)' and the pathology was mostly composed of demyelination. At 'relapse (REL)', the amount of both degeneration and demyelination were similar in the dorsal column. (Scale bar=250μm)

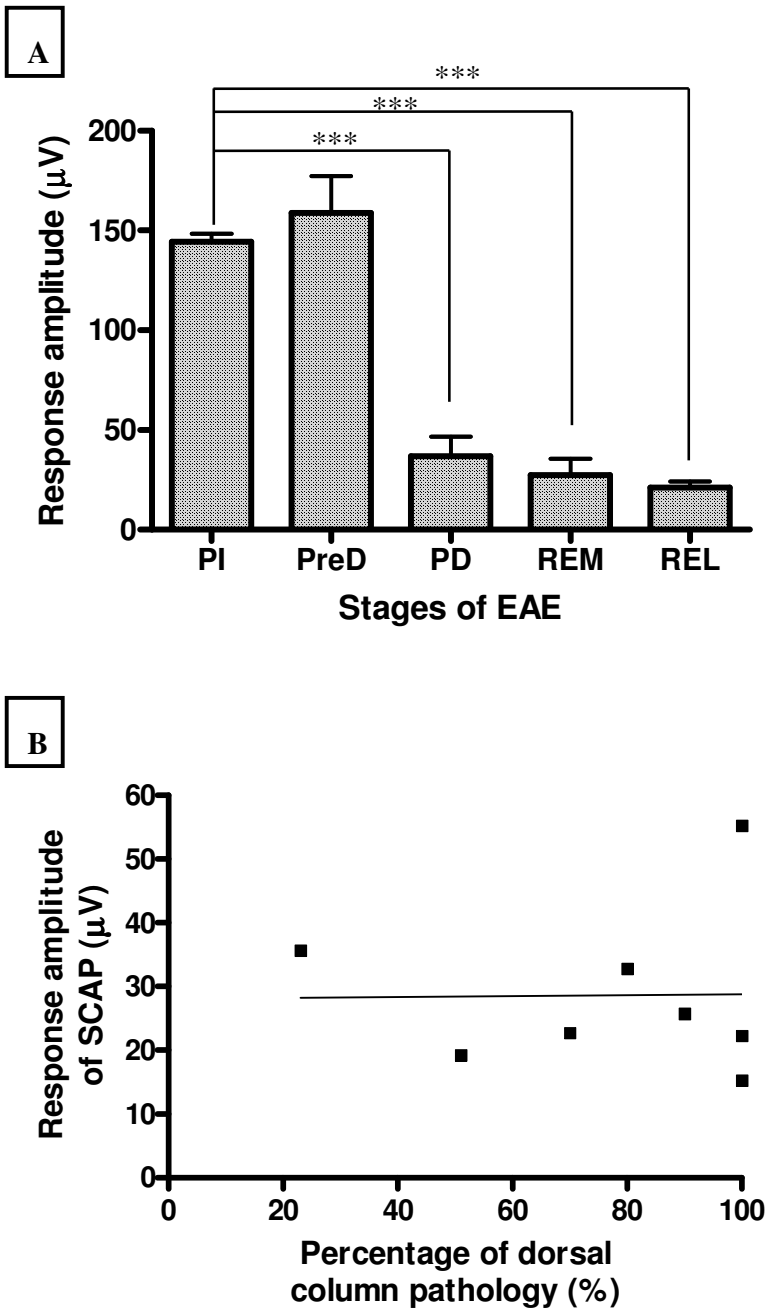
A
***
***
***
200
150
100
50
0
Response amplitude (μV)
PI
PreD
PD
REM
REL
Stages of EAE
B
60
50
40
30
20
10
0
Response amplitude of SCAP (μV)
0
20
40
60
80
100
Percentage of dorsal column pathology (%)

Figure 4.23. Sensory compound action potentials (SCAP) measured in animals used for histology, and their correlation with dorsal column pathology

(a) Sensory compound action potentials (SCAP) were measured at the key stages of EAE in the same animals that were used for histology (N=3 in each stage). The amplitude of the SCAP was significantly decreased from 'peak disease (PD)' until 'relapse (REL)' (P<0.001, compared with 'preinduction (PI)', One way ANOVA, Newman-Keuls post test).
(b) There was no significant correlation between the 'response amplitude of SCAP' and 'percentage of dorsal column pathology' (N=8) in animals with EAE. (Spearman r value was 0.01, and P =0.96 by Spearman's rank correlation test)

4.4. Conclusion

The neurological, electrophysiological and histological analyses were performed to understand the mechanisms underlying relapses and remissions, in animals with EAE. In these animals, hypothermia was found in association with worsening of the neurological signs and limb function at 'peak disease' and 'relapse', and further investigation is required to understand the cause.

Electrophysiological analysis showed that axonal conduction and synaptic transmission were impaired from the 'peak disease' until 'relapse', and motor neuronal excitability was also impaired at 'relapse'. It is surprising that none of the measures recovered at 'remission', which implies that there could be other factors responsible for the deficits in these animals. Also, histological methods were used to identify any inflammatory factors which may correlate with the neurological deficits, such as activation of macrophages/microglia or iNOS expression. Significantly increased ED1 expression was found at both 'peak disease' and 'relapse', but iNOS was specifically expressed at the 'peak disease'. Pathological changes were also quantified using resin sections, but no correlation was found between the axonal conduction and pathology in the dorsal columns.

The specific expression of iNOS observed during the first peak of disease lead us to focus on nitric oxide (NO), which has been implicated in MS and EAE by our and other laboratories. Thus, I planned to administer a selective iNOS inhibitor (1400W) in these animals to explore whether it inhibited the expression of neurological deficits. The results are described in the following chapter five.

Chapter 5
Understanding mechanisms underlying relapses and remissions by modulation of inflammatory factors

Chapter 5. Understanding mechanisms underlying relapses and remissions by modulation of inflammatory factors

5.1. Introduction and aims

It has become clear that neurological deficits in multiple sclerosis (MS), such as paralysis, blindness and numbness, can arise not only from the demyelination that is characteristic of the disease, but also from the accompanying inflammation, even in the absence of demyelination. However, the mechanisms responsible remain unclear.

The aim of this chapter was to investigate whether modulating inflammatory factors could affect the disease course of EAE. Firstly I explored whether inducing systemic inflammation by administering lipopolysaccharide (LPS) systemically in animals with EAE in their 'remission (REM)' stage, exacerbates the disease causing relapse. Since LPS is a bacterial endotoxin which elicits strong innate immune response within the injected animals (Marshall 2005), we hypothesised that this pro-inflammatory agent may induce an inflammatory exacerbation in the animals with EAE, therefore providing us with a model for studying the possible mechanisms underlying the relapse by using neurological, and electrophysiological techniques. An exacerbation of EAE caused by LPS has been described by Hugh Perry's group (public communication), but according to our Pubmed search, it appears that the method has not been published in the years since its description.
Secondly, a selective iNOS inhibitor 1400W was administered to animals with EAE at their onset of disease expression to examine whether iNOS inhibition ameliorates neurological signs and protects axonal function. This experiment is based on the finding previously described in Results Chapter 4, where iNOS immunoreactivity was expressed exclusively at the 'peak disease (PD)'. Neurological, electrophysiological

and histological assessments were used in this study and any differences between the drug treated group and controls were noted.

5.2. Methods

5.2.1. Animals and anaesthesia

The methods have been previously described in Chapter 3, Methods 3.2.1 and 3.2.2. Animals that reached a neurological score of more than five, were provided with mashed food.

5.2.2. Systemic injection of lipopolysaccharide (LPS) in animals with EAE

EAE was induced in DA rats as described in Chapter 4, Methods 4.2.3. When these animals reached 'remission (REM)' (selection criteria described in Table 4.2.), the animals were given an injection of lipopolysaccharide (LPS, Sigma Aldrich, St Louis, USA, 1mg/kg dissolved in saline) into their saphenous vein using a 0.5 mL insulin syringe (Terumo, MD21921, USA).

5.2.3. Administration of 1400W in animals with EAE

Animals induced with EAE that reached a score of two or three (around day eight to eleven post immunisation) were paired for similarity of deficit, and either a selective iNOS inhibitor 1400W (Enzo Life Sciences (UK) Ltd., Exeter, UK, 10mg/kg/day,

dissolved in saline) or vehicle (saline) was administered intraperitoneally, for seven days. The animals were monitored daily by neurological assessment, and were culled at the last day of administration for electrophysiological and histological examinations.

5.2.4. Rectal temperature monitoring, and neurological assessment

The rectal temperature was monitored by a temperature probe as described in Chapter 4, Methods 4.2.2. Neurological assessment was performed according to the ten point scale introduced in Methods 4.2.4.

5.2.5. Behavioural assessment by inclined plane measurements

Behavioural assessments were performed by measuring the maximum angle that the animal could sustain on an inclined plane, as described in Chapter 4, Methods 4.2.5.

5.2.6. Electrophysiological assessment

Sensory compound action potential (SCAP), H reflex, F wave, M response, and cord dorsum potentials (CDP) were examined in animals injected with LPS. The sensory compound action potential (SCAP) was examined in animals that were used for the iNOS inhibition experiment. Methods for these electrophysiological examinations are described in Chapter 3, Methods section 3.2.3.

5.2.7. Histological assessment

Cardiac perfusion (Methods 3.2.4.1.) with fixative (paraformaldehyde) was performed in animals treated with 1400W/vehicle (saline) on the last day of administration. A laminectomy was performed and the spinal cords were removed and processed for resin sections (Method 3.2.4.2.). Image J software (Rasband, W.S., ImageJ, U. S. National Institutes of Health, Bethesda, Maryland, USA, http://rsb.info.nih.gov/ij/, 1997-2009) was used to draw around, and measure, the area of pathology in images of the spinal cord taken using light microscopy.

5.2.8. Statistics

Data were expressed with means and standard deviations, and plotted using GraphPad Prism version 4.00 for Windows (GraphPad Software, San Diego, USA). One-way ANOVA with Newman-Keuls post test was performed to compare the means in three or more groups, and Paired T test was performed to compare the means of two groups. 'Statistical significance' was determined by the p value obtained from these tests. ($P<0.05$ (*), $P<0.01$ (**), $P<0.001$ (***))

5.3. Results

5.3.1. Induction of systemic inflammation by LPS injection

5.3.1.1. Neurological and behavioural assessments

Animals which received an intravenous injection of LPS at 'remission (REM)' stage showed significantly increased neurological scores (+2.5, $P<0.05$), which peaked at 3.5 hours post injection (Figure 5.1(a)). This exacerbation had ameliorated by 30 hours post injection. Also, the inclined plane test showed that there was a significant decrease in motor function ($P<0.01$) at the time when the neurological score peaked in these animals (Figure 5.1(b)). Surprisingly, hypothermia was associated with the exacerbation, showing a 1.4 °C decrease at 3.5 hours post injection ($P<0.01$), which was recovered to normal with the amelioration in neurological deficit (Figure 5.1(c)). These results are reminiscent of data shown in Figure 4.7. in chapter four, where rectal temperature was significantly low at 'peak disease (PD)' and 'relapse (REL)', when the neurological scores were significantly low.

5.3.1.2. Electrophysiological assessments

Electrophysiological examination was performed in order to examine the possible mechanism underlying the exacerbation of the disease in EAE animals receiving LPS. Sensory compound action potentials (SCAP), H reflex, F wave and cord dorsum potential (CDP) were recorded at 'remission (REM)', 'peak of exacerbation after injection of LPS (at 3.5 hours post injection, LPS)' and 'recovery from the peak (at 30 hours post injection, REC)'. However, none of the electrophysiological properties

showed any significant changes (Figure 5.2), and thus none could explain the mechanism of exacerbation responsible for the LPS-induced relapse.

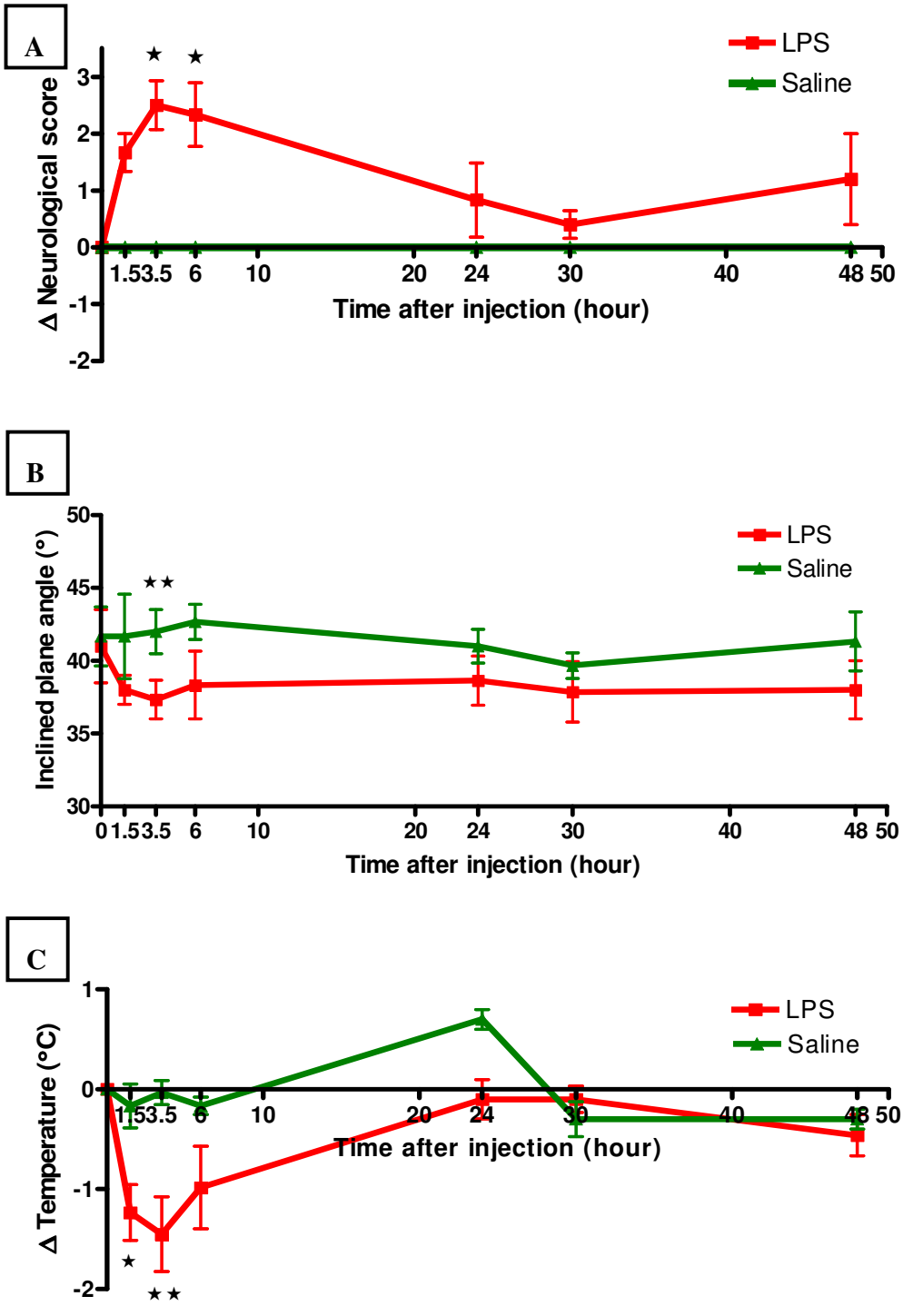
A
LPS
Saline
Δ Neurological score
3
2
1
0
-1
-2
★
★
1.5
3.5
6
10
20
24
30
40
48
50
Time after injection (hour)
B
LPS
Saline
Inclined plane angle (°)
50
45
40
35
30
★★
0
1.5
3.5
6
10
20
24
30
40
48
50
Time after injection (hour)
C
LPS
Saline
Δ Temperature (°C)
1
0
-1
-2
1.5
3.5
6
10
20
24
30
40
48
50
Time after injection (hour)
★
★★

Figure 5.1. Examination of neurological score, inclined plane measurements, and rectal temperature after injection of LPS in animals with EAE at 'remission (REM)'

(a) Exacerbation of disease was observed in animals after the injection of LPS, which peaked at 3.5 hours post injection (N=6 in each group). Neurological score was significantly increased by 2.5 (P<0.05, One-way ANOVA and Newman-Keuls post test) at this time point.

(b) Inclined plane angle measurement was also decreased significantly at the peak of exacerbation (P<0.01, One-way ANOVA and Newman-Keuls post test).

(c) Rectal temperature also decreased in association with the exacerbation (P<0.01, One-way ANOVA and Newman-Keuls post test). All of these measures recovered by 30 hours post injection.

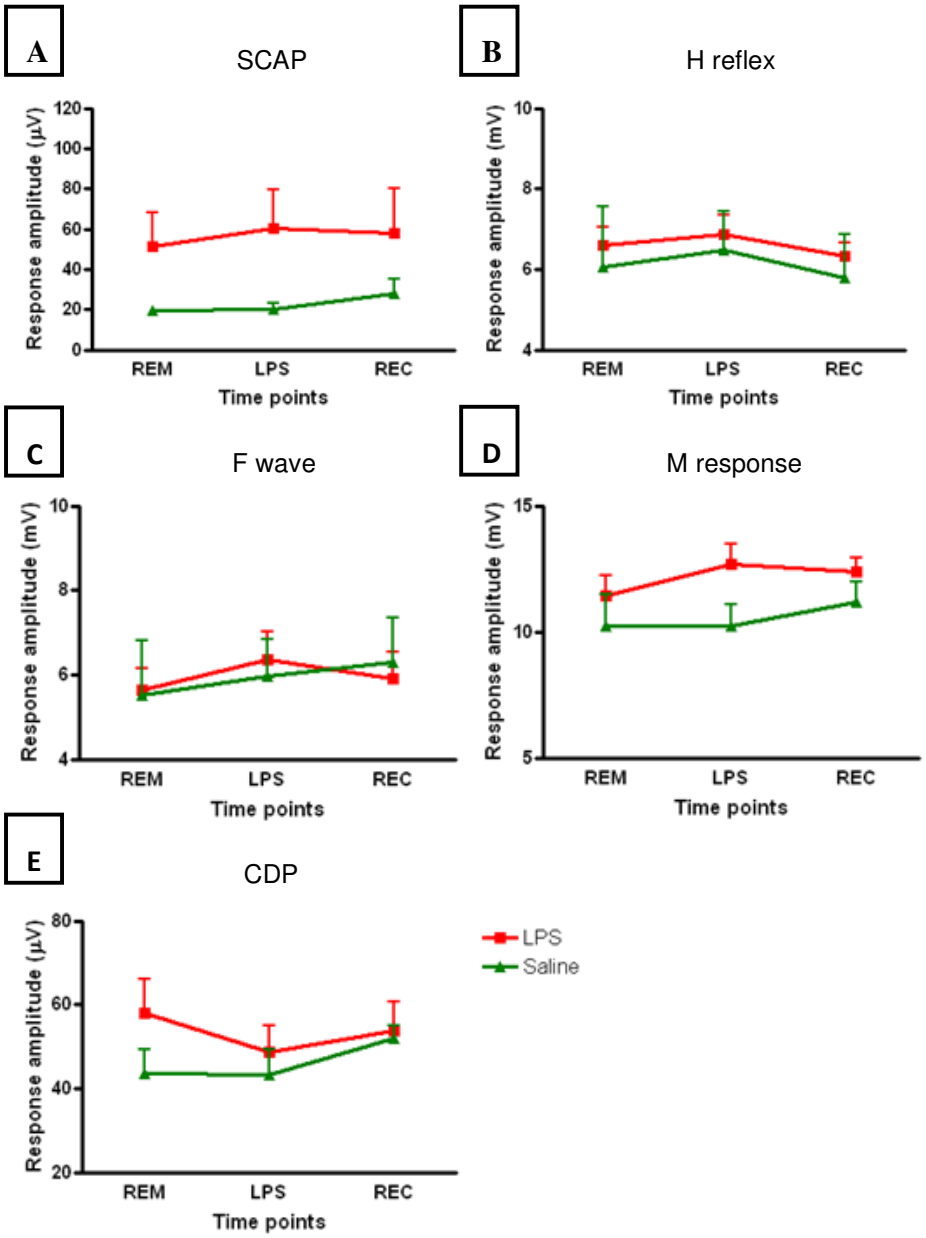

Figure 5.2. Electrophysiological changes in animals injected with LPS

Electrophysiological examination was performed in animals with EAE at 'remission (REM)', 'peak of exacerbation after injection of LPS (at 3.5 hours post injection, LPS)' and 'recovery from the peak (at 30 hours post injection, REC)', (N=5 in EAE, N=3 in control (saline)). There were no significant changes observed in the response amplitude measured in (a) sensory compound action potential (SCAP), (b) H reflex, (c) F wave, (d) M response, and (e) cord dorsum potential (CDP).

5.3.2. Inhibition of iNOS by a selective iNOS inhibitor 1400W

5.3.2.1. Neurological assessment

The iNOS inhibitor 1400W or vehicle (saline) were administered at the onset of disease in 8 pairs of animals paired for their similarity of neurological deficit induced with EAE, when they reached a score of two to three (i.e. reduction of muscle tone, or paralysis of the tail, which occurred around day 8 to 11 post immunisation). On the first day of administration, the animals were monitored every hour for six hours, but did not show any improvement or worsening of the neurological signs (data not shown). However, a day afterwards, a significant difference ($P<0.05$) was present between the neurological scores of the two groups, and on day two post administration, the animals showed the biggest difference between the neurological scores ($P<0.001$) (Figure 5.3). At this time point, most of the animals treated with vehicle (seven out of eight) reached a peak score of nine, with paralysed hindlimbs (mean score was 9), whilst only one out of eight animals receiving 1400W reached a score of nine (mean score 6.37, apart from one animal, the rest did not get paralysed). In addition, the vehicle-treated animals reached their peak scores at two days after administration, however, the drug-treated animals reached their peak a day later. The animals in both groups showed a recovery after reaching their peaks, and they showed similar neurological scores at day five post administration. On day six post administration, sensory compound action potentials (SCAP) were recorded from all of the animals, followed by perfusion for histological analysis. To assess the effectiveness of the drug, the neurological score inhibited at the peak and at termination were averaged and compared between the two treatment groups (Figure 5.4(a),(b)). Although there was no difference at termination, the peak neurological score showed a significant difference ($P<0.01$), where the mean scores of drug-treated animals and vehicle-treated animals were seven and nine respectively.

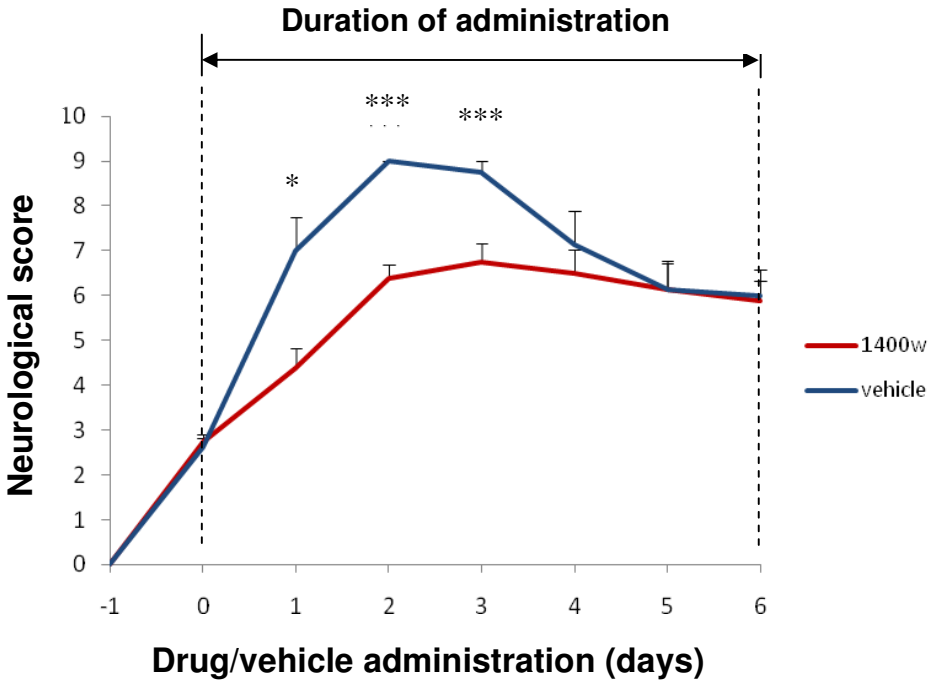

Figure 5.3. Neurological scores of the animals with EAE administered with 1400W/vehicle (saline)

The animals were paired for expression of neurological deficit at the onset of the disease of EAE, when they reached a neurological score of two to three, and were administered with either drug (1400W) or vehicle (saline) for seven days (N=8 in each group). The animals were assessed by neurological scoring daily. Vehicle- and drug- treated animals showed the peak of disease at day 2 and day 3 post administration respectively. The neurological scores between the two groups were significantly different from day one ($P<0.05$) to three ($P<0.001$) post administration (Paired T test).

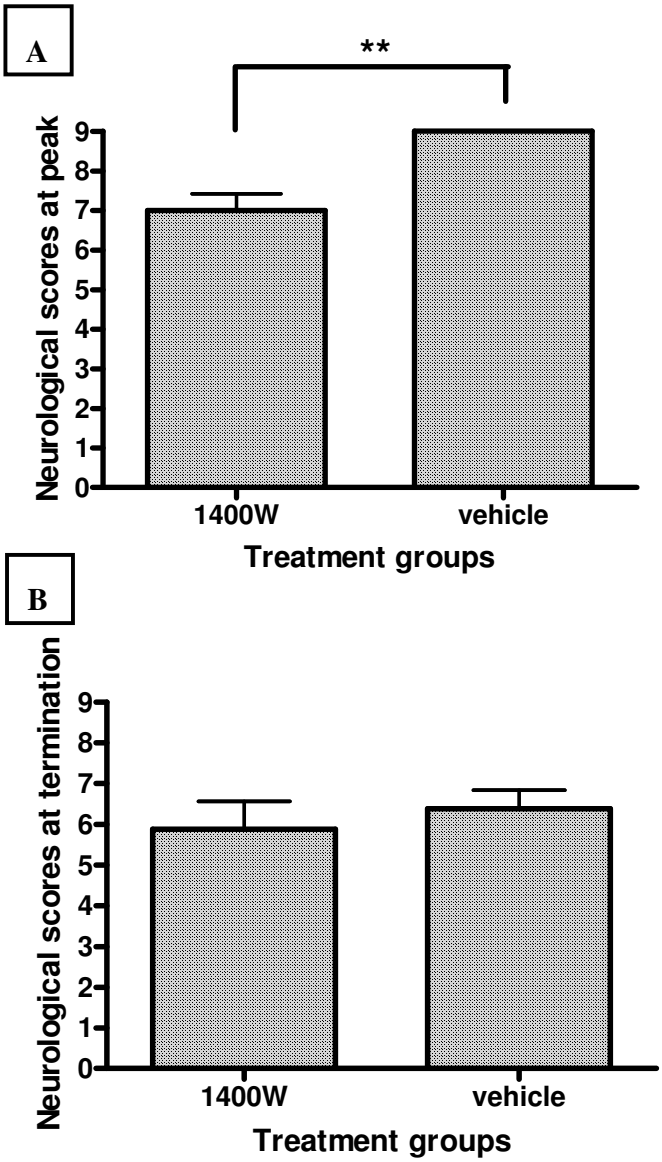

Figure 5.4. Neurological scores at peak of disease, and at termination, in animals with EAE treated with 1400W and vehicle (saline)

(a) The means (±SE) of neurological scores at the peak of disease in drug- and vehicle- treated animals are shown as bar graphs (N=8 in each group). The mean neurological scores of drug- and vehicle- treated animals were 7 and 9 respectively, which were significantly different (P<0.01, paired T test). (b) shows means (±SE) of neurological scores of each group at the day of termination. The mean score was similar between the two groups, being 5.87 and 6.37 in drug- and vehicle- treated animals respectively.

5.3.2.2. Electrophysiological assessment

The sensory compound action potential (SCAP) was recorded at the day of termination (day six post administration) under ketamine/xylazine anaesthesia. The peak SCAP amplitude was measured to assess the number of conducting axons in these animals. No SCAP was detectable in any of the animals treated with vehicle, whereas animals that received 1400W showed a mean response amplitude of 24.39μV (Figure 5.5 shows the representative recordings).

5.3.2.3. Histological assessment

Following electrophysiological examination, the animals were perfused for histological analysis. The percentage of white matter pathology was calculated in a section from each animal using computer software (Image J), and the means of the two groups were compared. The mean percentage of pathology measured in the white matter was similar in each group (26.7% and 23.5% in 1400W- and vehicle- treated animals respectively) as shown in Figure 5.6. Representative images of each group are shown in Figure 5.8. ((a) 1400W treated, (c) vehicle treated), and they exhibit a similar amount of pathology in their white matter. However, when the percentage of axonal degeneration and demyelination were compared within the measured pathological area of dorsal columns, the animals treated with 1400W showed significantly lower percentage of axonal degeneration ($P<0.05$) and higher demyelination ($P<0.05$) compared with the controls (Figure 5.7).

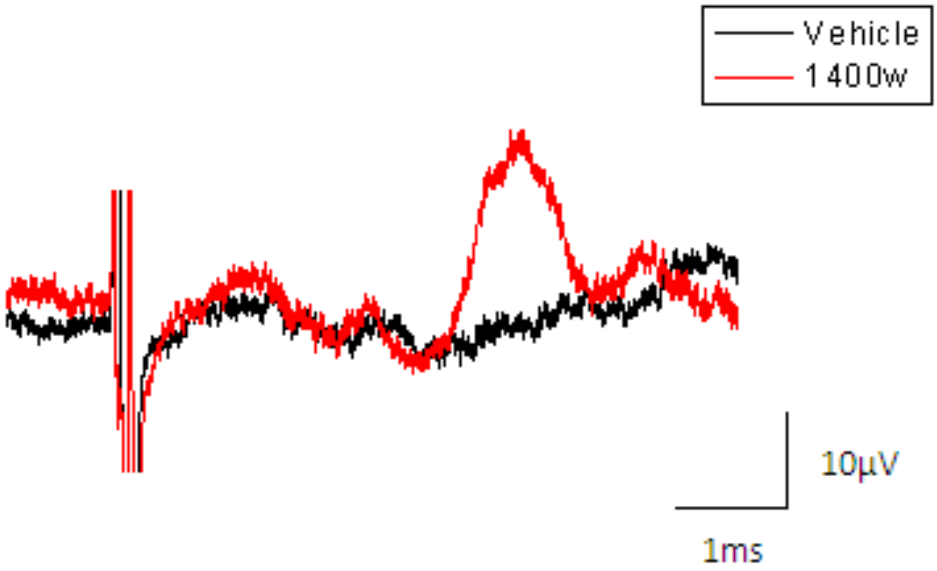

Figure 5.5. Sensory compound action potential (SCAP) in animals with EAE treated with 1400W and vehicle (saline)

On day six post administration of agents, the animals were anaesthetised for examination of axonal conduction by measuring the peak response amplitude of SCAP (N=8 in each group). Black and red recordings are averages of all the SCAP recordings of animals with EAE treated with vehicle and drug respectively. The mean response amplitude of SCAP in vehicle- and drug- treated animals was 0 µV and 24.39 µV respectively.

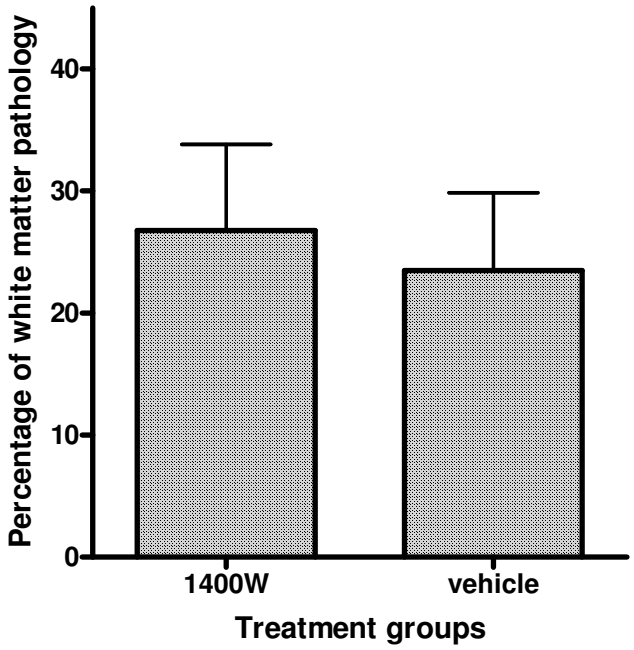

Figure 5.6. Percentage of white matter pathology in animals treated with 1400W and vehicle (saline)

The mean percentage area of pathology in the white matter was similar in the two groups : 26.7% and 23.5% in 1400W- and vehicle- treated animals respectively (N=8 in each group).

When the area of axonal degeneration, and of demyelination were separately measured in the dorsal column of these animals, a noticeable difference was observed. Animals with 1400W treatment showed significantly less axonal degeneration, and more demyelination (both show $P<0.05$ by Paired T test), compared with vehicle- treated animals, as shown in Figure 5.7. The representative images of the dorsal columns are presented in Figure 5.8 ((b) 1400W- treated, (d) vehicle- treated).

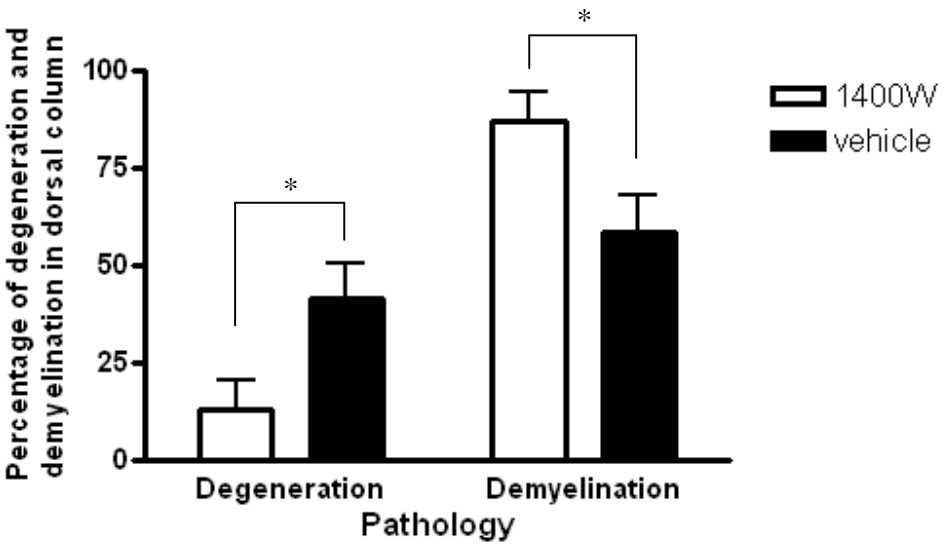

Figure 5.7. Comparison of degeneration vs demyelination in the dorsal columns of animals treated with 1400W and vehicle (saline)

The percentages of axonal degeneration and demyelination in the dorsal columns were measured in animals treated with 1400W or vehicle (saline) (N=8 in each group). A significantly lower percentage of axonal degeneration, and a higher percentage of demyelination were observed in 1400W- treated animals compared with vehicle- treated ($P<0.05$, Paired T test).

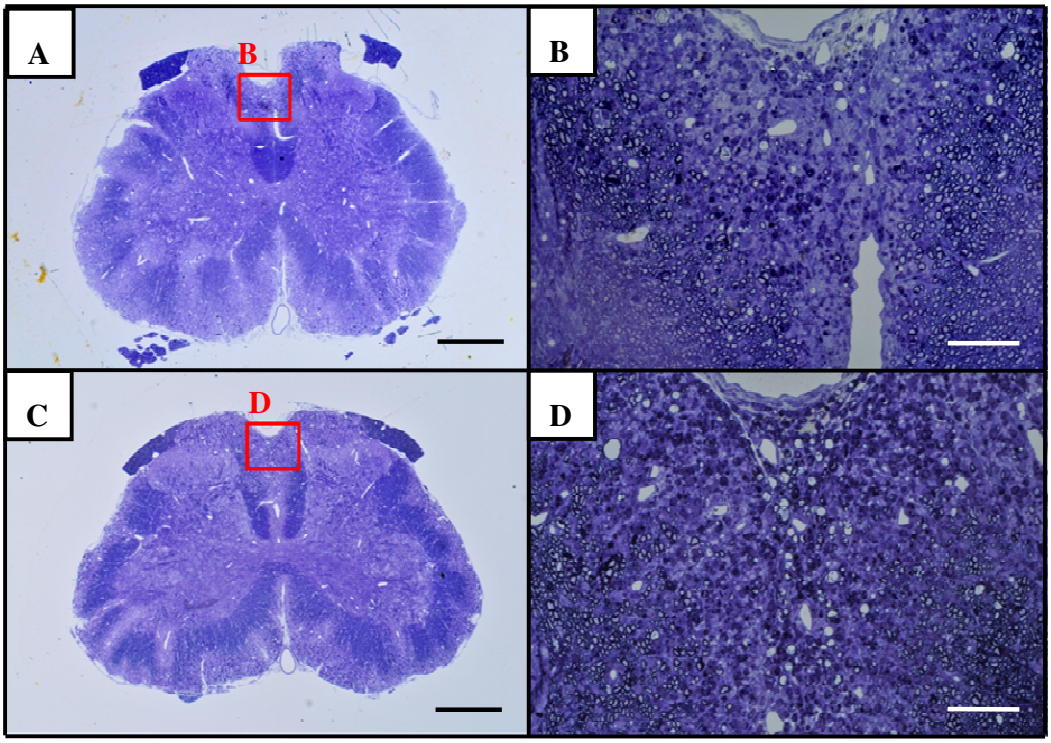

Figure 5.8. Representative images of spinal cords, and corresponding dorsal columns, of animals treated with 1400W and vehicle (saline)

(a) and (b) show transverse sections of spinal cord of animals treated with 1400W or vehicle (saline) respectively, and they exhibit similar amounts of white matter pathology. However, the dorsal column of these spinal cords showed a different composition of pathology (shown in (b) and (d) (magnified images of the red inset shown in (a) and (b) respectively)). The dorsal columns of the animals treated with vehicle (d) showed more axonal degeneration than demyelination compared with animals treated with 1400W (b).
(Black scale bar=1000µm, white scale bar=250µm)

5.4. Conclusion

The results described in this chapter show that the systemic administration of the pro-inflammatory agent LPS in animals with EAE at their 'remission', causes an acute relapse that peaks 3.5 hours post injection. This exacerbation was associated with impaired motor function and hypothermia. The hypothermia was reminiscent of that exhibited in EAE animals at the 'peak disease', and at 'relapse'. It is surprising that none of the electrophysiological changes observed could easily explain the mechanisms responsible for these deficits. In addition, animals that were administered with a selective iNOS inhibitor 1400W showed significantly decreased neurological scores at their peak, and the peak appeared a day later than in control animals. Also, the number of functional axons measured by recording the sensory compound action potentials (SCAP) in these animals was enhanced compared with controls. Moreover, although the percentage area of pathology in the white matter measured in the two groups was similar, axonal degeneration was significantly less prominent in 1400W-treated animals, which implies that 1400W may protect axons from degeneration, but not necessarily from demyelination.

Collectively the results show that inflammation may play an important role in the development of neurological signs in EAE, and that iNOS inhibition could be used as a potential therapy for MS.

Chapter 6
Discussion

Chapter 6. Discussion

6.1. Optimisation of electrophysiological techniques

Together with MRI techniques, electrophysiological examinations have been used for diagnosing and evaluating the clinical disease course in patients with MS (Fuhr and Kappos 2001;Kallmann et al. 2006). It has been reported from Waxman *et al* that a combination of visual evoked potentials (VEPs), somatic sensory evoked potentials (SEPs) and brain stem auditory evoked potentials detected subclinical lesions in patients, which later were confirmed to have a diagnosis of MS (Waxman 1988). Also, patients showing evoked potential (EP) abnormalities had a 71% higher risk of clinical deterioration compared with others having normal EPs (Hume and Waxman 1988). As implied in these studies, electrophysiological assessments can be useful in the diagnosis of the disease in MS patients, and indeed a correlation of EP data with scores on the expanded disability status scale (EDSS) was described in several studies (Salle et al. 1992;O'Connor et al. 1998;Fuhr et al. 2001;Kallmann et al. 2006). In particular, Kallmann *et al* reported that EPs recorded within two years after the disease onset of MS correlated with EDSS scores after five and ten years, suggesting that EPs may assist predicting future disabilities of the patients and decisions in introducing treatments (Kallmann et al. 2006).

Based on the advantages of electrophysiological examinations in patients, it would be reasonable also to examine animal models of MS electrophysiologically, not only in order to understand the mechanisms of neurological deficits, but also to apply this knowledge in therapeutic studies. However, little has been done in this direction, and therefore this study is valuable as it aims to present electrophysiological features of the key stages (‘preinduction’, ‘predisease’, ‘peak disease’, ‘remission’ and ‘relapse’) of EAE induced in DA rats. For this purpose, electrophysiological techniques were

optimised in naïve animals prior to application in animals with EAE. Factors including the anaesthetic agent, stimulation frequency during recordings, temperature of the animal and placement of electrodes were optimised, as these elements affect the reliability and reproducibility of the recordings

Anaesthetic agents affect the central nervous system characterised by analgesia and suppression of reflexes. These agents act by depressing postsynaptic excitation, prolonging pre- or post-synaptic inhibition, and by blockade of ion channels (Dodd and Capranica 1992;Antkowiak 2001;Kopp et al. 2009). Therefore it is anticipated that the configuration of recordings obtained under anaesthesia will be different from those taken without anaesthesia (i.e. under normal physiological conditions). Also, the type of anaesthesia would be expected to influence the recordings depending on its mechanism of action. Here in this study two different anaesthetic agents were used to test the excitability of motor neurons, as measured by the H reflex and F wave, and both recordings were better elicited under ketamine/xylazine than isoflurane (Figure 3.6). These findings accord well with the results reported from studies which demonstrated that volatile anaesthetics depress and/or abolish evoked potentials, while ketamine alone or in combination with xylazine had little or no influence on evoked potentials (Goss-Sampson and Kriss 1991;Chiba et al. 1998;Zandieh et al. 2003). In addition, Zhou *et al* reported a suppression of spinal cord motor neuronal excitability using isoflurane anaesthesia in human (Zhou et al. 1997;Zhou et al. 1998) by measuring both H reflexes and F waves. Similarly in animals, the amplitude of the F wave was also decreased in animals under isoflurane (Antognini and Carstens 1999). Studying the exact mechanism of depression under isoflurane is beyond the scope of this thesis, but this effect is unlikely to be due to effects at the neuromuscular junction or muscle, as the M responses were not influenced by the type of anaesthesia. Therefore, these findings suggest that ketamine/xylazine is a more appropriate agent for measuring motor neuronal excitability by monitoring H reflexes and F waves, compared with isoflurane. Importantly, an appropriate stimulation frequency under anaesthesia should also be determined in order to obtain reproducible H reflexes and F

waves, as reflex attenuation occurs from post-activation depression (in this case the lowest frequency of 0.1Hz was used, Figure 3.6).

The temperature at the site of recording (usually peripheral limbs) also affects electrophysiological recordings, and therefore in clinical settings, electrodiagnostic consultants generally aim to maintain the lower extremities of the patients between 32 °C and 34°C during examinations. In order to explore the effect of temperature on recordings of H reflexes and F waves, the hindlimbs were cooled down using ice bags. As a result, it was found that the latency, duration and amplitudes of both H reflexes and F waves increased as the temperature decreased (Figure 3.7, Figure 3.8). This change of the action potential may occur due to the slowed opening and closing of the Na^+ channel at low temperatures, as reported by Hodgkin *et al* (HODGKIN and KATZ 1949). Slow depolarisation of the axon results in reduced conduction velocity, and the combination of slow depolarisation and repolarisation causes longer channel opening time, therefore producing longer duration responses. Also, larger response amplitude is as a result of more Na^+ moving into the axon during prolonged opening of its channel, due to a larger depolarisation of the axon (Rutkove 2001).

Placement of electrodes is also important in achieving reproducible data, as has been illustrated in Figure 3.12. It shows that the response amplitude can be markedly increased or decreased by a movement of only 1mm of the recording electrode. This implies that the proximity between the recording electrode and the nerve may affect the response amplitude, and therefore careful placing of the electrode is required in repeated consecutive analyses.

In conclusion, these findings indicate the importance of optimising electrophysiological skills in naïve animals for achieving reliable data. Based on these data, the developed techniques have been applied to the animals induced with EAE in order to interpret the recordings accurately.

6.2. Characterisation of DA rats with rMOG-EAE to understand possible mechanisms underlying the relapses and remissions

The aim of this study was to characterise DA rats induced with rMOG-EAE by using neurological, electrophysiological and histological techniques, at five key stages along the disease course, with the hope that these observations may indicate possible mechanisms responsible for the neurological deficits. Neurological assessments were made by neurological scoring and examination of motor function of the limbs. The weight and core temperature of these animals were also monitored in addition to record physiological changes. Also, electrophysiological and histological assessments were performed in order to identify correlations between these factors and the severity of disease indicated by neurological scoring.

6.2.1. Neurological characterisation

The results show that the neurological scores (Figure 4.2) and motor function of the limbs (Figure 4.5) was significantly decreased in animals with severe disease. The examination of the motor function of the limbs which was measured by the inclined plane test, proved to be a reliable assessment as it was highly reproducible in naïve animals (Figure 4.4) and strongly correlated with the neurological scores in animals with EAE (Figure 4.6). In addition, significant weight loss was also observed in animals present with severe neurological signs (Figure 4.3). Weight loss in animals with EAE is a common feature of the disease, and some reports have suggested that the loss may be due to side effects from inflammatory mediators, suppression of appetite and ability to hydrate (Tracey et al. 1988;Strassmann et al. 1992;Encinas et al. 2001).

Surprisingly, a significant negative correlation between the rectal temperature and neurological score of the animals with EAE was discovered (Figure 4.8). The average core temperature of the animals at 'peak disease (PD)' and 'relapse (REL)' were both below 35 °C, which indicates a hypothermic state (hypothermia is defined as a reduction of the core body temperature below 35°C (Fischbeck and Simon 1981). This result is in line with the data from both rabbits and Lewis rats with EAE, where these animals also showed hypothermia correlating with severity of the disease (Pender and Sears 1984;Hansen and Pender 1989). The authors claimed that hypothalamic lesion-induced impairment of thermoregulation, and interruption of shivering pathways caused by demyelination/axonal degeneration could be the cause of hypothermia. Indeed cases of hypothermia have also been documented from MS patients with core temperatures ranging from 30°C to 35° (White et al. 1996;Linker et al. 2006;Weiss et al. 2009;Davis et al. 2010). Most patients showing hypothermia typically had a long history of MS with severe clinical symptoms, and hypothermia was presented as acute, relapsing or even chronic. A post-mortem pathological analysis (Linker et al. 2006) and MRI studies (White et al. 1996) revealed lesions around the hypothalamic area in these patients, but the exact relationship between thermo-dysregulation and neurological impairment is not yet clearly understood. Therefore, further research on thermoeffector functions in animal models of MS may be required, such as by focusing on the functioning of shivering, sweating and heat dissipation. In addition, studies on energy metabolism and distribution in these animals may also be valuable, and mitochondrial research in this regard could be helpful as it is recognised as a major source of heat production (Gambert and Ricquier 2007). Indeed, mitochondrial dysfunction has been reported in MS lesions (Mahad et al. 2008;Witte et al. 2010), although the relationship between energy metabolism and temperature in patients is unknown.

6.2.2. Electrophysiological and histological characterisation

Previous electrophysiological studies on EAE concluded that demyelination occurring in both the CNS and PNS is the main cause of neurological deficits (described in Introduction section 1.3). However, this explanation is less convincing to be applied in animals presenting transient neurological deficits, especially in the model used in this study which shows a transient first peak (named as 'peak disease (PD)', Figure 4.2). In this model, 'peak disease (PD)' occurred around day 18-20 post induction presenting severe neurological deficits, with recovery from some of the deficits around day 22-24 post induction (Figure 4.2). This fast recovery is unlikely to be attributed to demyelination, as remyelination would take longer to occur (Smith et al. 1979). In order to further understand the mechanisms responsible for the transient peak, recovery and relapse, longitudinal assessments were made at five key stages of EAE induced in DA rats to characterise the difference between each stage. Several types of electrophysiological tests were used to examine neurological function within the CNS, and histological assessments were used to detect inflammation, axonal degeneration and demyelination. In particular, the key role of inflammation in causing the deficits has been reported from clinical studies (Youl et al. 1991;Moreau et al. 1996;Bitsch et al. 2000), and indeed a marked role has also been confirmed in this study, by investigating the effect of systemic inflammation and iNOS inhibition in animals with EAE, which is further discussed in section 6.3.2.

6.2.2.1. Electrophysiological characteristics of the key stages of EAE

Electrophysiological assessments were made in order to examine axonal conduction, motor neuronal excitability, synaptic transmission and synaptic activation of motor neurons within the central nervous system. At the 'peak disease (PD)', axonal conduction (measured by SCAP, Figure 4.9.), synaptic transmission (CDP, Figure

4.11) and synaptic activation of motor neurons (SAM, Figure 4.12) were all significantly reduced, and these measures remained reduced during 'remission (REM)' and 'relapse (REL)'.

Conduction block is a well known cause of the deficits in EAE, shown by previous electrophysiological studies. The impairment of axonal conduction has been classically attributed to the demyelination process (Waxman 1989;Smith and Hall 2001;Wolswijk and Balesar 2003) or inflammatory mediators such as nitric oxide (NO) (Redford et al. 1997). Indeed both demyelination and inflammatory factors were examined histologically and were detected in animals with EAE during the period presenting neurological deficits (Histopathological characteristics of EAE are further discussed in 6.2.2.2).

The impairment of synaptic transmission in the grey matter has also been reported to be affected by inflammation in animals with EAE. For example, a report from Centonze *et al* showed that synaptic degeneration and dendritic spine loss in animals with EAE were promoted by enhanced glutamate transmission under inflammatory conditions (Centonze et al. 2009). In addition, an electrophysiological examination performed in animals with EAE *in vitro,* showed that AMPA-mediated spinal cord transmission deficits occurred from the onset of disease, which was sustained for two weeks (Hanak et al. 2004). Within these two weeks, the animals underwent neurological remission, yet this recovery was not mirrored in the electrophysiological data, similar to the results described in this study. Furthermore, synaptic changes of the motor neurons were also found in EAE, where dendritic abnormalities of distal motor neurons (Zhu et al. 2003) and lumbosacral motor neurons (Bannerman et al. 2005) were observed. Also, Marques *et al* described synaptic retraction and reapposition of the motor neurons in EAE using ultrastructural techniques, and suggested that these changes could account for the paralysis observed during the peak of the disease (Marques et al. 2006).

However, motor neuronal excitability measured by the H reflex and F wave only showed a significant decrease at 'relapse (REL)' (Figure 4.10). The reduction in amplitude of H reflex has also been reported in Lewis rats with MBP-EAE (Pender 1989;Stanley and Pender 1991), and the reduction was attributed to demyelination in the PNS, especially in the dorsal and ventral roots and their entry/exit zones. However, no pathology in the PNS was detected in animals induced with rMOG-EAE in this study, and the exact mechanism of the decreased excitability is not understood. It is plausible that this decrease is due to the loss of motor neurons, as has been found in both actively and passively induced EAE (Vogt et al. 2009). The authors claimed that a reduction of 47% to 74% of α-motor neurons was observed in animals with EAE compared to controls, and this could be due to neuronal damage caused by activated T cells and microglia. Indeed activated microglia under inflammatory conditions have been reported to secrete inflammatory mediators such as TNFα, inducing motor neuron death (He et al. 2002;Sedel et al. 2004). However, whether motor neuron loss occurs in animals with EAE from this study is not known.

As described above, electrophysiological dysfunction which may contribute to the neurological deficits observed at 'peak disease (PD)' and 'relapse (REL)' was detected, but it was surprising that none of the measures showed an improvement upon 'remission (REM)' from the neurological deficits. This disassociation between electrophysiological finding and neurological presentation has also been documented in studies from MS patients, and these observations have lead some authors to suggest that evoked potentials may not be suitable for monitoring the course of MS (Matthews and Small 1979;Aminoff et al. 1984;Anderson et al. 1987). In particular, Matthews *et al* found that abnormal somatosensory evoked potentials measured in patients with MS did not return to normal at remission, similar to the finding of this study. This imbalance may occur if electrophysiological recordings at remission detected the progression of underlying disease. It could also be influenced by unstable conduction properties of demyelinated axons with reduced safety factors, which are easily affected by subtle environmental changes such as temperature (Davis 1970;Davis et al.

2010). Indeed various physiological properties including temperature (Lenhardt 2010), heart rate, respiration, oxygen saturation and blood pressure are affected by anaesthetic agents (Karwacki et al. 2001), and any changes in these factors may influence the electrophysiological outcome. Moreover, the effect of anesthetic agents on the nervous system *per se* should not be neglected, as these depress postsynaptic excitation or block ion channels, creating a totally different environment in contrast to the properties when awake. Although it seems to be a difficult task, efforts to avoid the use of general anaesthesia in laboratory animals during recordings may become essential for the improvement in electrophysiological studies. Although the electrophysiological mechanisms of remission in EAE have not been revealed from this study, inflammatory factors have been studied using histological techniques, and these have shed light on our understanding, as discussed below.

6.2.2.2. Histopathological characteristics of the key stages of EAE

EAE has been the subject of several histological studies, but in this thesis the pathological hallmarks of MS, inflammation, demyelination and axonal degeneration, have been characterised and quantified at the five key stages of disease in DA rats induced with rMOG-EAE.

A role for inflammation in causing neurological deficits has been suggested from clinical studies (Youl et al. 1991;Moreau et al. 1996;Bitsch et al. 2000), although the exact mechanisms remain unknown. However, it has been described that inflammatory cells and their mediators may play a role in the pathogenesis of MS and its animal model EAE (Ford et al. 1995;Bruck et al. 1995;Raivich and Banati 2004). In particular, brain- resident microglia and hematogenous macrophages are representative inflammatory cells which are involved in the pathology, by presenting antigen to T lymphocytes after being recruited to sites of inflammation, and

synthesising molecules such as cytokines, chemokines and reactive oxygen radicals which could exert damaging effects on the surrounding tissue (Raivich and Banati 2004). Indeed, the role of macrophages and microglia has been implicated in a number of earlier studies using various models of EAE, where these cells were detected in accordance with the expression of disease (Berger et al. 1997;Brown and Sawchenko 2007;Rasmussen et al. 2007). Accordingly, it was found in this study that the activity of macrophages/microglia shown by ED1 labeling was significantly increased at the 'peak disease (PD)' and 'relapse (REL)' in animals with EAE (Figure 4.14), and a positive correlation between the ED1 labeling and neurological severity was shown (Figure 4.16). The increased labeling at the two peaks could be due to the proliferation of resident microglia or recruitment of blood borne macrophages, as has also been suggested from a study by Bauer *et al* using Lewis rats induced with chronic relapsing EAE (Bauer et al. 1994). Noticeably, these authors reported that the pattern of ED1 labeling in the brain of the animals was different between the first peak and relapse. They described that at the first peak, ED1 labeling was confined in or around the lesions, but at relapse, the labeling affected a larger area including fields further away from the lesions, suggesting that newly recruited positive macrophages may have infiltrated the brain. A difference in the pattern of ED1 labeling between the two peaks was also found in this study (Figure 4.15), where the cells were confined in subpial and perivascular regions at 'peak disease (PD)' but were concentrated in the white matter at 'relapse (REL)'. These findings suggest that the phagocytic cells may behave differently at the two peaks, and may contribute to pathology via different mechanisms. However, so far the proportion of these cells within the ED1 positive population and their interaction is not known from this study, nor from any others. Therefore, further investigation is required to find out the composition of these cells and also to understand their role in the pathogenesis of EAE.

This study has especially explored a potential role for another important inflammatory factor, inducible nitric oxide synthase (iNOS), which can be expressed by

macrophages, microglia or neutrophils under inflammatory conditions. iNOS is known to produce large amounts of NO, and it was found to be exclusively expressed at the 'peak disease (PD)' of EAE (Figure 4.17 and Figure 4.18) in this study. The presence of iNOS produced by macrophages has been demonstrated in other studies using EAE animals, and the iNOS expression was found to correlate with the disease activity (Van Dam et al. 1995;Cross et al. 1996;Zhao et al. 1996;Brenner et al. 1997). In both the published and current study, iNOS expression was mostly perivascular, and it has been suggested that the perivascular iNOS positive cells may contribute to damage of the blood-brain barrier, and other CNS tissues. The current findings suggest that ED1 positive and iNOS positive macrophages or microglia may be responsible for the neurological deficits at the 'peak disease (PD)'. The possible role of NO was specifically explored in this thesis by administrating an iNOS inhibitor (1400W) in the animals with EAE to block the production of NO and its detrimental effect. The results are discussed in section 6.3.2.

The amount of demyelination and axonal degeneration was quantified in the spinal cords of animals at each stage of EAE. The pathology of the white matter affected by either demyelination or degeneration was initially detected at the first peak of disease (PD, 16.5%) and it further increased at 'relapse (REL)' to 58.9% (Figure 4.19, Figure 4.20). Increasing white matter pathology has also been documented in relapsing-remitting EAE models induced in Biozzi ABH mice with spinal cord homogenate (Hampton et al. 2008;Jackson et al. 2009), and in DA rats with rMOG (Papadopoulos et al. 2006) as the disease progressed. However, in this thesis, the dorsal columns of the same animals were separately assessed, in order to find out whether there was a correlation with axonal conduction measured by sensory compound action potentials (SCAP). Results show that the proportion of axonal degeneration in the dorsal column was more than 50% at both 'peak disease (PD)' and 'relapse (REL)' (Figure 4.21 (b)), but only approximately 6% was present at 'remission (REM)'. This unexpectedly small area of axonal degeneration found at 'remission (REM)' is an unexplained observation in the current study, as it is implausible that the observed animals at 'peak

disease (PD)' would lose any evidence of the pathology suspected to have caused the severe deficits observed earlier in these particular animals. The findings need further study in a larger cohort of animals, but this is beyond the scope of this thesis. A contributing factor might be the fact that the lesions of EAE are widespread within the CNS, so there is a chance of overlooking the pathology that may be present at other locations, hence an investigation exploring the cord longitudinally may provide the explanation.

6.2.3. Possible mechanisms underlying the first peak and relapse in rMOG-EAE induced in DA rats

In the present study the main differences in electrophysiological and histological features were found between the first peak ('peak disease') and the relapse in animals with EAE. At the first peak, axonal conduction, synaptic transmission, and synaptic activation of motor neurons were significantly impaired. However, motor neuronal excitability was not affected at this stage but showed significant decrease measured by the H reflex and F wave at relapse. The exact mechanisms of how these electrophysiological changes occur in pathological animals is not clear from this study, but several studies have reported that pathological events such as demyelination or inflammation can be the cause of conduction block (Waxman 1989;Redford et al. 1997;Smith and Hall 2001;Wolswijk and Balesar 2003) and synaptic dysfunction (Hanak et al. 2004;Centonze et al. 2009). Roles for NO for contributing to neurological deficits seem especially likely from the present results, and this agent is known to be a potent cause of conduction block, especially in demyelinated axons (Redford et al. 1997). The presence of actively phagocytic ED1 positive cells and demyelination were also found in the present study within the spinal cord of animals, which may also have contributed to the presentation of neurological deficits. However, it was also noted that the localisation of ED1 expressing cells within the spinal cord

was different between the two stages, and the expression of iNOS was exclusively at the first peak and not at relapse.

These findings suggest that different pathological events arising through different mechanisms could be responsible for the neurological deficits present at the two peaks, although the expression of neurological deficits was similar. More importantly, present data are valuable for understanding the characteristics of the two peaks and applying these findings for developing therapies for MS. For example, in the current study, the administration time of iNOS inhibitor (1400W) was selected depending on the exclusive expression of iNOS at the first peak of EAE, therefore increasing the efficacy of the treatment (further discussed in later section 6.3.2.). In addition, it has been described for the first time from this study that the significant reduction of motor neuronal excitability (determined using electrophysiological techniques) occurs only at relapse. Although motor neuronal loss has been reported in MS (Vogt et al. 2009), it is not yet known whether there is a tendency for increased motor neuronal pathology in patients with progressive phase of MS than in patients during their acute phases, as seen in our model of MS. As it is difficult to obtain tissues from acute patients for histological comparison with patients with progressive disease, the value of research on relapsing remitting EAE exploring the acute and progressive phase is clear. Indeed a study on rMOG-EAE induced in DA rats focusing on the immunobiology of the disease revealed that the first peak may be driven by CD4+ Th1 lymphocyte-induced inflammation, but relapse may be due to demyelination caused by MOG-specific antibodies (Schubart A 2001). Clinical data also support this interpretation by reporting increased serum levels of anti MOG antibodies in patients at their relapse (Angelucci et al. 2005). On the basis of these observations, it would be reasonable to try to develop a therapy to eliminate circulating MOG antibodies. In conclusion, further electrophysiological and histological profiling of animals with EAE will be required not only to understand the mechanisms of deficits occurring at both the acute and relapse phase, but also to develop an effective treatment.

6.3. Modulation of inflammatory factors affects the disease course of EAE

6.3.1. LPS injection exacerbates the disease course

In this study, systemic inflammation was induced in the animals with EAE during remission by intravenous injection of a bacterial endotoxin, lipopolysaccharide (LPS), in order to explore whether and how LPS injection exacerbates the disease, using neurological and electrophysiological techniques. Indeed there has been clear evidence in patients with MS that infection-derived inflammation may cause relapses (Edwards et al. 1998;Confavreux 2002;Buljevac et al. 2002), and sequence similarity between microbial and self antigens has been suggested to induce autoimmunity which may explain these relapses. However, so far no specific pathogen has been identified, and the exact mechanisms are poorly understood.

In the present study, the neurological scores of animals which were injected with LPS had significantly increased after 3.5 hours post injection in association with decreased motor function of the limbs (Figure 5.1 (a), (b)). These findings bear similarities to a study from Nogai *et al*, where the authors observed relapses in SJL mice induced with MBP-EAE after systemic injection of LPS during remission (Nogai et al. 2005). The mean neurological score of these mice at their relapse was 2.5 scores higher than the first episode of EAE. This exacerbation was attributed to antigen-independent 'bystander activation' of T cells, supported by *in vitro* observations of activated Th lymphocytes in the absence of TCR mediated signals. Also another study demonstrated that a systemic inflammatory challenge by LPS injection reactivated the quiescent lesions in the brain of Lewis rats induced with MOG-EAE, using multimodal MRI techniques and histology (Serres et al. 2009). Noticeably, the authors described that there was an increase in the number of newly recruited lymphocytes and macrophages/microglia at the lesion sites, following the inflammatory insult. LPS-

induced activation of peripheral macrophages was also described earlier in Australian albino rats, and these macrophages were suggested to cause neurological impairment evidenced by experiments using macrophage inhibitors (Brown et al. 1999). Thus, exploring whether active macrophages/microglia also reappear in animals during LPS-induced exacerbation following the first appearance at 'peak disease (PD)' (Figure 4.14), may be helpful in understanding the pathological role of these cells in causing relapse.

Surprisingly, no significant change of electrophysiological measure was detected at the peak of LPS-induced transient exacerbations (Figure 5.2). This finding is in contrast to an electrophysiological study performed by Brown *et al*, using Australian albino Wistar rats injected with LPS, both intraperitoneally and intravenously (Brown et al. 1999). These rats also exhibited a transient neurological dysfunction after the injection, but electrophysiological analysis revealed that the impairment was associated with a transient conduction block in the sciatic nerve, or impaired function of the neuromuscular junction. As discussed earlier, the reason for the disassociation between the neurological presentation and electrophysiological data found in the current study is not fully understood, but it may be due to unstable conduction properties in axons with reduced safety factors, or the side effects from anaesthesia *per se* during electrophysiological recordings.

So far from the results described in this study, the exact mechanisms underlying the LPS-induced relapse in animals with EAE remain unknown. However, a study from Moreau *et al* provided good evidence supporting the role for cytokines in causing transient worsening of symptoms in patients with MS using CAMPATH-1H, a drug which depletes lymphocytes and some monocytes (Moreau et al. 1996). In most of the patients, symptoms appeared in accordance with the administration of CAMPATH-1H associated with an increase in the level of cytokines. The exacerbation did not occur in patients treated with an anti-inflammatory drug, which blocked the surge of cytokines. The authors suggested that cytokines such as TNF-α and IFN-γ may contribute to

production of symptoms in these patients, by affecting conduction. It is plausible that the exacerbation reported in this thesis may have also occurred through a similar mechanism, as reports have shown that systemic injection of LPS in animals also induces production of cytokines such as TNF-α and IFN- γ (Varma et al. 2002;Qin et al. 2007).

It is not yet known why cytokines might cause relapses, but hypoxia in spinal cords of animals with EAE has been investigated as a potential cause of neurological dysfunction in our laboratory, evidenced by histological data and oxygen electrode recordings (unpublished data). In this regard, it is plausible that the spinal cord may have also become hypoxic in response to systemic inflammation by LPS injection, due to hyper-metabolism and limitation in the amount of oxygen the blood can supply to the tissue. It is therefore possible that anaesthesia-induced suppression of physiological activity, coupled with non-physiological stimulation frequencies (no greater than 1Hz) used in the current study during recordings under anaesthesia, hence providing reduced electrical activity, may alleviate hypoxia in animals with EAE, by reducing the demand for ATP. If so, the alleviation of hypoxia may have relieved conduction deficits due to this cause, meaning that no conduction deficits were present at the time of recording. However, whether hypoxia is induced by systemic LPS injections needs to be determined.

It is also noticeable that a decrease of core temperature was observed at the peak of exacerbation in association with neurological impairment, in rats which received LPS (Figure 5.1 (c)). This decrease of temperature was reminiscent of hypothermia observed at the 'peak disease (PD)' in animals with EAE (Figure 4.7), and whether a common mechanism causing the temperature decrease applies to both cases is possible. It has been reported that hypothermia was induced in a dose dependent, monophasic manner, which was maximised at 2 hours post intravenous injection of LPS in mice (Greer and Rietschel 1978). In this report the mice lost a maximum of 2°C when they were injected with the highest dose of LPS (100μg per mice). Also, Arkarsu *et al*

reported hypothermia in Wistar albino rats injected with LPS (250μg/kg) measured by a temperature transmitter implanted into the peritoneal cavity (Akarsu and Mamuk 2007). The authors described that the loss of temperature in these animals was in association with the increased serum level of TNF-α, suggesting that antipyretic cytokines may be involved in the generation of hypothermia. Whether the level of cytokines such as TNF-α is elevated after the injection of LPS in animals used in this study remains to be determined.

In conclusion, these results show that systemic inflammation can cause transient neurological deficits in animals with EAE, and these animals may serve as a model of MS with brief relapses. For example, this model may be useful for studying the mechanisms of transient worsening of symptoms observed in the CAMPATH-1H trial (Moreau et al. 1996). Further efforts are required to identify potential factors contributing to the exacerbation, such as the involvement of inflammatory cells and their soluble mediators. Also, understanding the relationship between the neurological deficits and physiological properties of the animal such as body temperature and tissue oxygen concentration will be beneficial in revealing the exact mechanisms of relapse. Investigation to develop strategies for preventing or treating infectious diseases to prevent relapse in MS should also be pursued.

6.3.2. iNOS inhibition ameliorates the disease course and may be useful in therapy for MS

Together with evidence from several laboratories reporting a positive correlation between iNOS and disease activity in animals with EAE (Van Dam et al. 1995;Cross et al. 1996;Zhao et al. 1996;Brenner et al. 1997), the exclusive expression of iNOS at peak disease (PD) in animals in this study (Figure 4.17, Figure 4.18) supports a pathological role of NO in EAE. Based on these data, a highly selective iNOS inhibitor, 1400W, was administered to animals with EAE at the onset of disease, in order to determine whether iNOS inhibition ameliorates the disease, as assessed by neurological, electrophysiological and histological techniques. Animals treated with 1400W exhibited a significantly reduced severity of neurological deficit during the peak of disease (Figure 5.3), and the average of neurological scores at peak was also significantly lower than controls (Figure 5.4). Furthermore, electrophysiological examination showed that sensory compound action potentials (SCAP) obtained from animals treated with 1400W were significantly larger than in controls, indicating that many more functioning axons survived in treated animals (Figure 5.5). The larger SCAP in the treated group correlated with the histological findings of the dorsal columns, as there were more surviving, demyelinated axons in animals treated with 1400W than in controls. Altogether these findings suggest that NO produced by iNOS may contribute to the loss of function, and to axonal degeneration, and that judiciously timed iNOS inhibition may be beneficial in the therapy of MS.

These findings are in agreement with studies that suggest a role for NO in tissue damage. NO has been reported to be cytotoxic and destructive to tissues for many reasons such as the fact that it up-regulates the production of TNF-α in macrophages (Deakin et al. 1995). Also, NO, being a free reactive radical in its own right, has been demonstrated to damage oligodendrocytes in EAE (Merrill et al. 1993;Koprowski et al. 1993). NO also binds to superoxide anion ($O_2^{\bullet-}$) to generate peroxynitrite anion

($ONOO^-$), which is an even stronger oxidant than either NO or $O_2^{\bullet-}$ (Beckman et al. 1990). More importantly, several studies have shown that inhibition of NOS in animals with EAE ameliorated the severity of disease, re-affirming a deleterious role for NO (Cross et al. 1994;Zhao et al. 1996;Brenner et al. 1997). However, contradicting outcomes from studies using NOS inhibitors in EAE have also been reported, indicating that NO can have a protective role under some circumstances (Zielasek et al. 1995;Ruuls et al. 1996;Fenyk-Melody et al. 1998). Based on these varied results it has been suggested that different methods of EAE induction, type of inhibitors, different administration routes or dosing schedules of the inhibitors may influence the outcome. Different strains or genders of animals may also affect the data, as the amount of NO produced varies accordingly (Ding et al. 1997;Cowden et al. 1998). Taking these factors into consideration, it is worth comparing the present data with results from a study using a similar protocol. Thus Kahl *et al* used DA rats induced with rMOG-EAE which showed a relapsing disease form and administered a relatively selective iNOS inhibitor, aminoguanidine (AG) (Kahl et al. 2003). AG was administered at two time points in order to understand the role of NO during the induction and effector phases of EAE. The animals were found to have a more severe disease course when they received the treatment early during the induction phase (beginning on the day after induction), but no significant effect was observed when the administration started after the onset of disease. These results supported a protective role of NO in the pathogenesis of EAE (in contrast to the present study, which showed protection after disease onset) and also pointed to a complex role of NO in different phases of disease. There are two obvious differences between the study by Kahl *et al* and the present study, which may have caused the contradictory outcomes. Firstly, AG is not as specific for iNOS as is 1400W, and hence the use of this drug in animals may have caused an inhibition of the constitutively expressed endothelial NOS (eNOS) or neuronal NOS (nNOS) (Ou and Wolff 1993;Laszlo et al. 1995). In contrast, 1400W is a highly selective inhibitor of iNOS over the other forms of NOS (Garvey et al. 1997). Secondly, the route of administration was different which may have affected the pharmacokinetics of the drug, influencing its time of action. However, the exact

reasons which explain the contradictory results are not yet understood, and further studies should be designed not only to understand this difference, but also to understand the exact role of NO in the disease course of EAE.

Two important goals in assessing the role of NO in EAE by administrating NOS inhibitors are, firstly, to determine the type of NOS present within the tissue, and also how expression changes during the disease course. This information allows the most specific inhibitor to be administered at the most opportune time. The second goal is to achieve reliable methods to examine the efficacy of the drug, including neurological, electrophysiological, and histological methods. In the present study, the time frame of administering the iNOS inhibitor (1400W) was prescribed by the expression of iNOS exclusively at the peak disease (PD), which also defined our strategy of administration of the 1400W at the onset of disease expression. To assess the efficacy of the drug, all animals in the trial were examined not only by the functional analysis of the axons measured by sensory compound action potential (SCAP) recordings, but also by histological examinations of the corresponding axons in the dorsal column. These data combined have provided a more complete explanation for the amelioration of neurological deficits observed in animals administered with 1400W, by presenting both physiological and pathological information. So far, only one previous study has aimed to explore the electrophysiological outcome of NOS inhibition in animals with EAE and EAN (experimental autoimmune neuritis, an animal model of Guillain-Barré syndrome) in association with histological examinations (Zielasek et al. 1995). There were no significant clinical or electrophysiological changes found in the drug-treated animals with EAE, but the compound muscle action potentials measured from the sciatic nerve remained intact in EAN animals treated with NMMA which was attributed to the decreased numbers of cellular infiltrates in the sciatic nerve compared to controls. Therefore, electrophysiological examinations can be helpful in assessing the efficacy of the NOS inhibitors, although it has not been successful in revealing the cause of the transient peak, remission and relapse in animals with EAE in this study.

In conclusion, the data presented in the current study are supportive of a deleterious role of NO in DA rats with rMOG-EAE, in which NO impairs function, and promotes degeneration. It remains to be determined whether the current findings also apply in MS, and to which stages of lesion development. iNOS expression in MS does not only occur in the active inflammatory lesions, but it is also widely expressed throughout the CNS in progressive disease (Smith and Lassmann 2002;Alastair Compston et al. 2005) raising the intriguing possibility that NO may contribute to the 'slow burn' of axonal degeneration in progressive disease, as well as the substantial, synchronous degeneration that characterises acute relapses.

6.3.3. Conclusive remarks

The aim of this thesis was to explore the mechanisms of relapse and remission in EAE using neurological, electrophysiological, and histological techniques. The results have been unexpected in that, so far, none of the electrophysiological measures have correlated with the recovery from the neurological deficits of the animals, although some electrophysiological deficits were decreased at the first peak of deficit, and at relapse. To understand this unexplained finding, it is required to further explore the potential effects from some factors which may affect the physiology of the animals with EAE, such as anaesthetic agents or hypoxia. However, current data revealed that modulation of inflammatory factors significantly affected the severity and pathology of the disease course of EAE. Systemic inflammation activated by an injection of lipopolysaccharide (LPS) into animals with EAE at their remission, induced a transient exacerbation of disease. This finding suggests that inflammation may play a significant role in the pathology of MS, and that these animals may serve as a model of MS with brief relapses. Importantly, inhibition of an inducible nitric oxide synthase (iNOS) using a selective iNOS inhibitor, 1400W, at the onset of the disease in animals with EAE significantly ameliorated the neurological deficits. These animals were also present with improved axonal conduction measured by sensory compound action potential (SCAP) compared to controls, which may be due to the protection of axonal degeneration as shown by histological observations. These data suggest that duly timed inhibition of iNOS may be therapeutic for patients with MS. However, further accurately designed experiments are required to confirm this finding using other models of MS to understand the contradicting results reported from NOS inhibition in animals with EAE.

6.4. Future directions

The present work shows that inflammation may play a significant role in the neurological deficits associated with MS, and that the inhibition of iNOS can be beneficial in alleviating these deficits. However in order to apply iNOS inhibition as a therapy for the patients, a few points remain to be validated using the animal model.

Firstly, sampling error must be minimised which occurs inevitably when selecting animals for analysis at different stages along the disease course. Basically, most EAE studies are based on the assumption that all the animals in the study go through a similar disease course. However, during this study, it was noticed that some animals developed neurological deficits earlier than others (showing first sign of deficits earlier than day 11 post-induction), and that these were more likely to acquire a primary progressive disease course with more severe deficits (paralysed limbs). In contrast, the majority of the animals which showed the first sign of deficit around day 13 to 15 post-induction, was more likely to present a relapsing-remitting disease course as has been illustrated in Figure 4.1. In the present study, naturally, animals developing the disease earlier than others were selected for the analysis of 'peak disease', and therefore there is a possibility that these animals may have developed a primary progressive disease course, when other animals selected for 'remission' and 'relapse' developed a relapsing-remitting disease course. In this case, animals in different groups may have shown different pathology according to their disease progression, hence introducing sampling error in histological analysis. Therefore in the future studies, it is reasonable to minimise the sampling error by avoiding animals with an atypical disease course or expression of deficits. Also, it is important to take into account the heterogeneous characteristics when interpreting the data obtained from these animals.

Secondly, further research is required to understand the exact mechanisms of NO-

induced damage revealed by the present study. It was found that the iNOS inhibitor-treated animals showed significantly lower neurological scores compared to controls, and the difference in scores between the two groups was maximised by day 2 post-administration (Figure 5.3). Further histological analysis aimed at this time point measuring the levels of iNOS expression will confirm the mechanism of action and efficacy of the inhibitor. Also, in order to measure the degree of damage, measuring nitrotyrosine production, axonal degeneration or inflammatory mediators such as cytokines may be useful. In addition, observations at an extended time point after administrating the iNOS inhibitor may reveal the effect of drug on the overall disease course of EAE. In the present study, the effect of the drug on the progression of the disease was not determined due to the termination of study at day seven post-administration of drug. Exploring whether iNOS inhibition also prevents relapse in these animals and preserves axonal function in the later progressive stage of the disease would be valuable for understanding the therapeutic value of this drug in progressive inflammatory neurological diseases.

Furthermore, administering the iNOS inhibitor in another type of relapsing-remitting model of EAE may enhance our understanding of the exact role of NO in the disease, by comparing the results with the present study. Thus LEW.1AV1 rats induced with MOG-EAE can be used as a relapsing-remitting model as these animals express a clear first peak and relapse (Matsumoto et al. 2009). Importantly, the time frame of iNOS expression should be primarily determined within these animals to ensure the effective delivery of the drug.

In conclusion, although there are many hurdles which must be overcome for iNOS inhibition to be applied to the clinic, the potential seems to be great based on the findings from the present work and other studies supporting the damaging role of NO. It is particularly notable that iNOS inhibition could prove to be protective against axonal damage, as degeneration of axons is associated with permanent disability in patients with MS.

Reference List

Ahern GP, Hsu SF, Jackson MB. Direct actions of nitric oxide on rat neurohypophysial K+ channels. J Physiol 1999;520 Pt 1:165-176.

Ahern GP, Hsu SF, Klyachko VA, Jackson MB. Induction of persistent sodium current by exogenous and endogenous nitric oxide. J Biol Chem 2000;275:28810-28815.

Akarsu ES, Mamuk S. Escherichia coli lipopolysaccharides produce serotype-specific hypothermic response in biotelemetered rats. Am J Physiol Regul Integr Comp Physiol 2007;292:R1846-R1850.

Alastair Compston, Ian Mcdonald, John Noseworthy, Hans Lassmann, David Miller, Kenneth Smith, Hartmut Werkerle, Christian Confavreux. McAlpine's Multiple Sclerosis 2005.

Alderton WK, Cooper CE, Knowles RG. Nitric oxide synthases: structure, function and inhibition. Biochem J 2001;357:593-615.

Aminoff MJ, Davis SL, Panitch HS. Serial evoked potential studies in patients with definite multiple sclerosis. Clinical relevance. Arch Neurol 1984;41:1197-1202.

Amitai Y. Physiologic role for "inducible" nitric oxide synthase: a new form of astrocytic-neuronal interface. Glia 2010;58:1775-1781.

Anderson DC, Slater GE, Sherman R, Ettinger MG. Evoked potentials to test a treatment of chronic multiple sclerosis. Arch Neurol 1987;44:1232-1236.

Angelucci F, Mirabella M, Frisullo G, Caggiula M, Tonali PA, Batocchi AP. Serum levels of anti-myelin antibodies in relapsing-remitting multiple sclerosis patients during different phases of disease activity and immunomodulatory therapy. Dis Markers 2005;21:49-55.

Antkowiak B. How do general anaesthetics work? Naturwissenschaften 2001;88:201-213.

Antognini JF, Carstens E. Isoflurane blunts electroencephalographic and thalamic-reticular formation responses to noxious stimulation in goats. Anesthesiology 1999;91:1770-1779.

Artemiadis AK, Anagnostouli MC, Alexopoulos EC. Stress as a Risk Factor for Multiple Sclerosis Onset or Relapse: A Systematic Review. Neuroepidemiology 2011;36:109-120.

Bagasra O, Michaels FH, Zheng YM, Bobroski LE, Spitsin SV, Fu ZF, Tawadros R, Koprowski H. Activation of the inducible form of nitric oxide synthase in the brains of patients with multiple sclerosis. Proc Natl Acad Sci U S A 1995;92:12041-12045.

Bajada S, Mastaglia FL, Black JL, Collins DW. Effects of induced hyperthermia on visual evoked potentials and saccade parameters in normal subjects and multiple sclerosis patients. J Neurol Neurosurg Psychiatry 1980;43:849-852.

Bannerman PG, Hahn A, Ramirez S, Morley M, Bonnemann C, Yu S, Zhang GX, Rostami A, Pleasure D. Motor neuron pathology in experimental autoimmune encephalomyelitis: studies in THY1-YFP transgenic mice. Brain 2005;128:1877-1886.

Bauer J, Sminia T, Wouterlood FG, Dijkstra CD. Phagocytic activity of macrophages and microglial cells during the course of acute and chronic relapsing experimental autoimmune encephalomyelitis. J Neurosci Res 1994;38:365-375.

Beckman JS, Beckman TW, Chen J, Marshall PA, Freeman BA. Apparent hydroxyl radical production by peroxynitrite: implications for endothelial injury from nitric oxide and superoxide. Proc Natl Acad Sci U S A 1990;87:1620-1624.

Berger T, Weerth S, Kojima K, Linington C, Wekerle H, Lassmann H. Experimental autoimmune encephalomyelitis: the antigen specificity of T lymphocytes determines the topography of lesions in the central and peripheral nervous system. Lab Invest 1997;76:355-364.

Bitsch A, Schuchardt J, Bunkowski S, Kuhlmann T, Bruck W. Acute axonal injury in multiple sclerosis. Correlation with demyelination and inflammation. Brain 2000;123 (Pt 6):1174-1183.

Bjartmar C, Trapp BD. Axonal degeneration and progressive neurologic disability in multiple sclerosis. Neurotox Res 2003;5:157-164.

Black JA, Felts P, Smith KJ, Kocsis JD, Waxman SG. Distribution of sodium channels in chronically demyelinated spinal cord axons: immuno-ultrastructural localization and electrophysiological observations. Brain Res 1991;544:59-70.

Black JA, Newcombe J, Waxman SG. Astrocytes within multiple sclerosis lesions upregulate sodium channel Nav1.5. Brain 2010;133:835-846.

Blakemore WF. Observations on oligodendrocyte degeneration, the resolution of status spongiosus and remyelination in cuprizone intoxication in mice. J Neurocytol 1972;1:413-426.

Bo L, Dawson TM, Wesselingh S, Mork S, Choi S, Kong PA, Hanley D, Trapp BD. Induction of nitric oxide synthase in demyelinating regions of multiple sclerosis brains. Ann Neurol 1994;36:778-786.

Boissy AR, Cohen JA. Multiple sclerosis symptom management. Expert Rev Neurother 2007;7:1213-1222.

Bolanos JP, Almeida A, Stewart V, Peuchen S, Land JM, Clark JB, Heales SJ. Nitric oxide-mediated mitochondrial damage in the brain: mechanisms and implications for neurodegenerative diseases. J Neurochem 1997;68:2227-2240.

Booss J, Esiri MM, Tourtellotte WW, Mason DY. Immunohistological analysis of T lymphocyte subsets in the central nervous system in chronic progressive multiple sclerosis. J Neurol Sci 1983;62:219-232.

Bredt DS, Snyder SH. Isolation of nitric oxide synthetase, a calmodulin-requiring enzyme. Proc Natl Acad Sci U S A 1990;87:682-685.

Brenner T, Brocke S, Szafer F, Sobel RA, Parkinson JF, Perez DH, Steinman L. Inhibition of nitric oxide synthase for treatment of experimental autoimmune encephalomyelitis. J Immunol 1997;158:2940-2946.

Brown DA, Sawchenko PE. Time course and distribution of inflammatory and neurodegenerative events suggest structural bases for the pathogenesis of experimental autoimmune encephalomyelitis. J Comp Neurol 2007;502:236-260.

Brown GC, Borutaite V. Nitric oxide inhibition of mitochondrial respiration and its role in cell death. Free Radic Biol Med 2002;33:1440-1450.

Brown RF, Jackson GD, Martin T, Westbrook RF, Pollard JD, Westland KW. Bacterial lipopolysaccharide induces a conduction block in the sciatic nerves of rats. Lab Anim Sci 1999;49:62-69.

Bruck W, Porada P, Poser S, Rieckmann P, Hanefeld F, Kretzschmar HA, Lassmann H. Monocyte/macrophage differentiation in early multiple sclerosis lesions. Ann Neurol 1995;38:788-796.

Brundin L, Morcos E, Olsson T, Wiklund NP, Andersson M. Increased intrathecal nitric oxide formation in multiple sclerosis; cerebrospinal fluid nitrite as activity marker. Eur J Neurol 1999;6:585-590.

Buljevac D, Flach HZ, Hop WC, Hijdra D, Laman JD, Savelkoul HF, van Der Meche FG, van Doorn PA, Hintzen RQ. Prospective study on the relationship between infections and multiple sclerosis exacerbations. Brain 2002;125:952-960.

Carnegie PR. Properties, structure and possible neuroreceptor role of the encephalitogenic protein of human brain. Nature 1971;229:25-28.

Centonze D, Muzio L, Rossi S, Cavasinni F, De C, V, Bergami A, Musella A, D'Amelio M, Cavallucci V, Martorana A, Bergamaschi A, Cencioni MT, Diamantini

A, Butti E, Comi G, Bernardi G, Cecconi F, Battistini L, Furlan R, Martino G. Inflammation triggers synaptic alteration and degeneration in experimental autoimmune encephalomyelitis. J Neurosci 2009;29:3442-3452.

Cerasa A, Fera F, Gioia MC, Liguori M, Passamonti L, Nicoletti G, Vercillo L, Paolillo A, Clodomiro A, Valentino P, Quattrone A. Adaptive cortical changes and the functional correlates of visuo-motor integration in relapsing-remitting multiple sclerosis. Brain Res Bull 2006;69:597-605.

Chabas D, Baranzini SE, Mitchell D, Bernard CC, Rittling SR, Denhardt DT, Sobel RA, Lock C, Karpuj M, Pedotti R, Heller R, Oksenberg JR, Steinman L. The influence of the proinflammatory cytokine, osteopontin, on autoimmune demyelinating disease. Science 2001;294:1731-1735.

Chalk JB, McCombe PA, Pender MP. Conduction abnormalities are restricted to the central nervous system in experimental autoimmune encephalomyelitis induced by inoculation with proteolipid protein but not with myelin basic protein. Brain 1994;117 (Pt 5):975-986.

Chalk JB, McCombe PA, Pender MP. Restoration of conduction in the spinal roots correlates with clinical recovery from experimental autoimmune encephalomyelitis. Muscle Nerve 1995;18:1093-1100.

Chang MW, Young MS, Lin MT. An inclined plane system with microcontroller to determine limb motor function of laboratory animals. J Neurosci Methods 2008;168:186-194.

Charcot JM. Lectures on diseases of the nervous system. London: New Sydenham Society . 1877.
Ref Type: Unpublished Work

Cheng X, Pang CC. Increased vasoconstriction to noradrenaline by 1400W, inhibitor of iNOS, in rats with streptozotocin-induced diabetes. Eur J Pharmacol 2004;484:263-268.

Chiba A, Nakanishi H, Hiruma S, Satou T, Hashimoto S, Chichibu S. Magnetically induced motor evoked potentials and H-reflex during nembutal and ketamine anesthesia administration in rats. Res Commun Mol Pathol Pharmacol 1998;101:43-57.

Choi YB, Lipton SA. Redox modulation of the NMDA receptor. Cell Mol Life Sci 2000;57:1535-1541.

Cleeter MW, Cooper JM, rley-Usmar VM, Moncada S, Schapira AH. Reversible inhibition of cytochrome c oxidase, the terminal enzyme of the mitochondrial respiratory chain, by nitric oxide. Implications for neurodegenerative diseases. FEBS Lett 1994;345:50-54.

Compston A, Coles A. Multiple sclerosis. Lancet 2002;359:1221-1231.

Confavreux C. Infections and the risk of relapse in multiple sclerosis. Brain 2002;125:933-934.

Cowden WB, Cullen FA, Staykova MA, Willenborg DO. Nitric oxide is a potential down-regulating molecule in autoimmune disease: inhibition of nitric oxide production renders PVG rats highly susceptible to EAE. J Neuroimmunol 1998;88:1-8.

Cross AH, Keeling RM, Goorha S, San M, Rodi C, Wyatt PS, Manning PT, Misko TP. Inducible nitric oxide synthase gene expression and enzyme activity correlate with disease activity in murine experimental autoimmune encephalomyelitis. J Neuroimmunol 1996;71:145-153.

Cross AH, Manning PT, Keeling RM, Schmidt RE, Misko TP. Peroxynitrite formation within the central nervous system in active multiple sclerosis. J Neuroimmunol 1998;88:45-56.

Cross AH, Misko TP, Lin RF, Hickey WF, Trotter JL, Tilton RG. Aminoguanidine, an inhibitor of inducible nitric oxide synthase, ameliorates experimental autoimmune encephalomyelitis in SJL mice. J Clin Invest 1994;93:2684-2690.

D'Arcangelo G, Grassi F, Ragozzino D, Santoni A, Tancredi V, Eusebi F. Interferon inhibits synaptic potentiation in rat hippocampus. Brain Res 1991;564:245-248.

Davis FA. Axonal conduction studies based on some considerations of temperature effects in multiple sclerosis. Electroencephalogr Clin Neurophysiol 1970;28:281-286.

Davis FA, Jacobson S. Altered thermal sensitivity in injured and demyelinated nerve. A possible model of temperature effects in multiple sclerosis. J Neurol Neurosurg Psychiatry 1971;34:551-561.

Davis SL, Wilson TE, White AT, Frohman EM. Thermoregulation in multiple sclerosis. J Appl Physiol 2010;109:1531-1537.

Deakin AM, Payne AN, Whittle BJ, Moncada S. The modulation of IL-6 and TNF-alpha release by nitric oxide following stimulation of J774 cells with LPS and IFN-gamma. Cytokine 1995;7:408-416.

Deguchi K, Takeuchi H, Miki H, Yamada A, Touge T, Terada S, Nishioka M. Electrophysiological follow-up of acute and chronic experimental allergic encephalomyelitis in the Lewis rat. Eur Arch Psychiatry Clin Neurosci 1992;242:1-5.

Denham S, Rowland IJ. Inhibition of the reactive proliferation of lymphocytes by activated macrophages: the role of nitric oxide. Clin Exp Immunol 1992;87:157-162.

Ding M, Wong JL, Rogers NE, Ignarro LJ, Voskuhl RR. Gender differences of inducible nitric oxide production in SJL/J mice with experimental autoimmune encephalomyelitis. J Neuroimmunol 1997;77:99-106.

Dodd F, Capranica RR. A comparison of anesthetic agents and their effects on the response properties of the peripheral auditory system. Hear Res 1992;62:173-180.

Edwards S, Zvartau M, Clarke H, Irving W, Blumhardt LD. Clinical relapses and disease activity on magnetic resonance imaging associated with viral upper respiratory tract infections in multiple sclerosis. J Neurol Neurosurg Psychiatry 1998;64:736-741.

Eikelenboom MJ, Killestein J, Kragt JJ, Uitdehaag BM, Polman CH. Gender differences in multiple sclerosis: cytokines and vitamin D. J Neurol Sci 2009;286:40-42.

Encinas JA, Lees MB, Sobel RA, Symonowicz C, Weiner HL, Seidman CE, Seidman JG, Kuchroo VK. Identification of genetic loci associated with paralysis, inflammation and weight loss in mouse experimental autoimmune encephalomyelitis. Int Immunol 2001;13:257-264.

Endo T, Tominaga T, Olson L. Cortical changes following spinal cord injury with emphasis on the Nogo signaling system. Neuroscientist 2009;15:291-299.

Engelhardt B. Immune cell entry into the central nervous system: involvement of adhesion molecules and chemokines. J Neurol Sci 2008;274:23-26.

Felts PA, Baker TA, Smith KJ. Conduction in segmentally demyelinated mammalian central axons. J Neurosci 1997;17:7267-7277.

Fenyk-Melody JE, Garrison AE, Brunnert SR, Weidner JR, Shen F, Shelton BA, Mudgett JS. Experimental autoimmune encephalomyelitis is exacerbated in mice lacking the NOS2 gene. J Immunol 1998;160:2940-2946.

Fischbeck KH, Simon RP. Neurological manifestations of accidental hypothermia. Ann Neurol 1981;10:384-387.

Fletcher JM, Lalor SJ, Sweeney CM, Tubridy N, Mills KH. T cells in multiple sclerosis and experimental autoimmune encephalomyelitis. Clin Exp Immunol 2010;162:1-11.

Ford AL, Goodsall AL, Hickey WF, Sedgwick JD. Normal adult ramified microglia separated from other central nervous system macrophages by flow cytometric sorting. Phenotypic differences defined and direct ex vivo antigen presentation to myelin basic protein-reactive CD4+ T cells compared. J Immunol 1995;154:4309-4321.

Fossier P, Blanchard B, Ducrocq C, Leprince C, Tauc L, Baux G. Nitric oxide transforms serotonin into an inactive form and this affects neuromodulation. Neuroscience 1999;93:597-603.

Friese MA, Fugger L. Pathogenic CD8(+) T cells in multiple sclerosis. Ann Neurol 2009;66:132-141.

Fuhr P, Borggrefe-Chappuis A, Schindler C, Kappos L. Visual and motor evoked potentials in the course of multiple sclerosis. Brain 2001;124:2162-2168.

Fuhr P, Kappos L. Evoked potentials for evaluation of multiple sclerosis. Clin Neurophysiol 2001;112:2185-2189.

Gambert S, Ricquier D. Mitochondrial thermogenesis and obesity. Curr Opin Clin Nutr Metab Care 2007;10:664-670.

Garvey EP, Oplinger JA, Furfine ES, Kiff RJ, Laszlo F, Whittle BJ, Knowles RG. 1400W is a slow, tight binding, and highly selective inhibitor of inducible nitric-oxide synthase in vitro and in vivo. J Biol Chem 1997;272:4959-4963.

Giovannoni G. Cerebrospinal fluid and serum nitric oxide metabolites in patients with multiple sclerosis. Mult Scler 1998;4:27-30.

Giovannoni G, Cutter GR, Lunemann J, Martin R, Munz C, Sriram S, Steiner I, Hammerschlag MR, Gaydos CA. Infectious causes of multiple sclerosis. Lancet Neurol 2006;5:887-894.

Goss-Sampson MA, Kriss A. Effects of pentobarbital and ketamine-xylazine anaesthesia on somatosensory, brainstem auditory and peripheral sensory-motor responses in the rat. Lab Anim 1991;25:360-366.

Greer GG, Rietschel ET. Lipid A-induced tolerance and hyperreactivity to hypothermia in mice. Infect Immun 1978;19:357-368.

Grigoriadis N, Hadjigeorgiou GM. Virus-mediated autoimmunity in Multiple Sclerosis. J Autoimmune Dis 2006;3:1.

Guzman NJ, Fang MZ, Tang SS, Ingelfinger JR, Garg LC. Autocrine inhibition of Na+/K(+)-ATPase by nitric oxide in mouse proximal tubule epithelial cells. J Clin Invest 1995;95:2083-2088.

Hampton DW, Anderson J, Pryce G, Irvine KA, Giovannoni G, Fawcett JW, Compston A, Franklin RJ, Baker D, Chandran S. An experimental model of secondary progressive multiple sclerosis that shows regional variation in gliosis, remyelination, axonal and neuronal loss. J Neuroimmunol 2008;201-202:200-211.

Hanak SE, Reilly EM, Wotanis J, Zhu B, Pulicicchio C, Monagle-Strucko K, Wettstein JG, Black MD. An electrophysiological model of spinal transmission deficits in mouse experimental autoimmune encephalomyelitis. J Pharmacol Exp Ther 2004;308:214-220.

Hansen LA, Pender MP. Hypothermia due to an ascending impairment of shivering in hyperacute experimental allergic encephalomyelitis in the Lewis rat. J Neurol Sci 1989;94:231-240.

He BP, Wen W, Strong MJ. Activated microglia (BV-2) facilitation of TNF-alpha-mediated motor neuron death in vitro. J Neuroimmunol 2002;128:31-38.

Heininger K, Fierz W, Schafer B, Hartung HP, Wehling P, Toyka KV. Electrophysiological investigations in adoptively transferred experimental autoimmune encephalomyelitis in the Lewis rat. Brain 1989;112 (Pt 2):537-552.

Hilton AA, Slavin AJ, Hilton DJ, Bernard CC. Characterization of cDNA and genomic clones encoding human myelin oligodendrocyte glycoprotein. J Neurochem 1995;65:309-318.

HODGKIN AL, KATZ B. The effect of temperature on the electrical activity of the giant axon of the squid. J Physiol 1949;109:240-249.

Hume AL, Waxman SG. Evoked potentials in suspected multiple sclerosis: diagnostic value and prediction of clinical course. J Neurol Sci 1988;83:191-210.

Hur EM, Youssef S, Haws ME, Zhang SY, Sobel RA, Steinman L. Osteopontin-induced relapse and progression of autoimmune brain disease through enhanced survival of activated T cells. Nat Immunol 2007;8:74-83.

Ignarro LJ. Biological actions and properties of endothelium-derived nitric oxide formed and released from artery and vein. Circ Res 1989;65:1-21.

Imitola J, Chitnis T, Khoury SJ. Cytokines in multiple sclerosis: from bench to bedside. Pharmacol Ther 2005;106:163-177.

Jackson SJ, Lee J, Nikodemova M, Fabry Z, Duncan ID. Quantification of myelin and axon pathology during relapsing progressive experimental autoimmune encephalomyelitis in the Biozzi ABH mouse. J Neuropathol Exp Neurol 2009;68:616-625.

Jafarian-Tehrani M, Louin G, Royo NC, Besson VC, Bohme GA, Plotkine M, Marchand-Verrecchia C. 1400W, a potent selective inducible NOS inhibitor, improves histopathological outcome following traumatic brain injury in rats. Nitric Oxide 2005;12:61-69.

Jansson M, Panoutsakopoulou V, Baker J, Klein L, Cantor H. Cutting edge: Attenuated experimental autoimmune encephalomyelitis in eta-1/osteopontin-deficient mice. J Immunol 2002;168:2096-2099.

Kahl KG, Zielasek J, Uttenthal LO, Rodrigo J, Toyka KV, Schmidt HH. Protective role of the cytokine-inducible isoform of nitric oxide synthase induction and nitrosative stress in experimental autoimmune encephalomyelitis of the DA rat. J Neurosci Res 2003;73:198-205.

Kallmann BA, Fackelmann S, Toyka KV, Rieckmann P, Reiners K. Early abnormalities of evoked potentials and future disability in patients with multiple sclerosis. Mult Scler 2006;12:58-65.

Kantarci O, Wingerchuk D. Epidemiology and natural history of multiple sclerosis: new insights. Curr Opin Neurol 2006;19:248-254.

Kapoor R, Davies M, Blaker PA, Hall SM, Smith KJ. Blockers of sodium and calcium entry protect axons from nitric oxide-mediated degeneration. Ann Neurol 2003;53:174-180.

Karpus WJ, Kennedy KJ. MIP-1alpha and MCP-1 differentially regulate acute and relapsing autoimmune encephalomyelitis as well as Th1/Th2 lymphocyte differentiation. J Leukoc Biol 1997;62:681-687.

Karwacki Z, Kowianski P, Morys J. General anaesthesia in rats undergoing experiments on the central nervous system. Folia Morphol (Warsz) 2001;60:235-242.

Kopp LA, Yost CS, Kindler CH. Anaesthetic mechanisms: update on the challenge of unravelling the mystery of anaesthesia. Eur J Anaesthesiol 2009;26:807-820.

Koprowski H, Zheng YM, Heber-Katz E, Fraser N, Rorke L, Fu ZF, Hanlon C, Dietzschold B. In vivo expression of inducible nitric oxide synthase in experimentally induced neurologic diseases. Proc Natl Acad Sci U S A 1993;90:3024-3027.

Kubes P, Suzuki M, Granger DN. Nitric oxide: an endogenous modulator of leukocyte adhesion. Proc Natl Acad Sci U S A 1991;88:4651-4655.

Kurenny DE, Moroz LL, Turner RW, Sharkey KA, Barnes S. Modulation of ion channels in rod photoreceptors by nitric oxide. Neuron 1994;13:315-324.

Laszlo F, Evans SM, Whittle BJ. Aminoguanidine inhibits both constitutive and inducible nitric oxide synthase isoforms in rat intestinal microvasculature in vivo. Eur J Pharmacol 1995;272:169-175.

Lehning EJ, Doshi R, Isaksson N, Stys PK, LoPachin RM, Jr. Mechanisms of injury-induced calcium entry into peripheral nerve myelinated axons: role of reverse sodium-calcium exchange. J Neurochem 1996;66:493-500.

Lenhardt R. The effect of anesthesia on body temperature control. Front Biosci (Schol Ed) 2010;2:1145-1154.

Li Z, Chapleau MW, Bates JN, Bielefeldt K, Lee HC, Abboud FM. Nitric oxide as an autocrine regulator of sodium currents in baroreceptor neurons. Neuron 1998;20:1039-1049.

Linington C, Lassmann H. Antibody responses in chronic relapsing experimental allergic encephalomyelitis: correlation of serum demyelinating activity with antibody titre to the myelin/oligodendrocyte glycoprotein (MOG). J Neuroimmunol 1987;17:61-69.

Linker RA, Mohr A, Cepek L, Gold R, Prange H. Core hypothermia in multiple sclerosis: case report with magnetic resonance imaging localization of a thalamic lesion. Mult Scler 2006;12:112-115.

Lipton HL, Liang Z, Hertzler S, Son KN. A specific viral cause of multiple sclerosis: one virus, one disease. Ann Neurol 2007;61:514-523.

Lublin FD, Reingold SC. Defining the clinical course of multiple sclerosis: results of an international survey. National Multiple Sclerosis Society (USA) Advisory Committee on Clinical Trials of New Agents in Multiple Sclerosis. Neurology 1996;46:907-911.

Lundmark F, Duvefelt K, Iacobaeus E, Kockum I, Wallstrom E, Khademi M, Oturai A, Ryder LP, Saarela J, Harbo HF, Celius EG, Salter H, Olsson T, Hillert J. Variation in interleukin 7 receptor alpha chain (IL7R) influences risk of multiple sclerosis. Nat Genet 2007;39:1108-1113.

MacMicking JD, Willenborg DO, Weidemann MJ, Rockett KA, Cowden WB. Elevated secretion of reactive nitrogen and oxygen intermediates by inflammatory leukocytes in hyperacute experimental autoimmune encephalomyelitis: enhancement by the soluble products of encephalitogenic T cells. J Exp Med 1992;176:303-307.

Mahad D, Lassmann H, Turnbull D. Review: Mitochondria and disease progression in multiple sclerosis. Neuropathol Appl Neurobiol 2008;34:577-589.

Mahad DJ, Ransohoff RM. The role of MCP-1 (CCL2) and CCR2 in multiple sclerosis and experimental autoimmune encephalomyelitis (EAE). Semin Immunol 2003;15:23-32.

Marletta MA. Nitric oxide synthase structure and mechanism. J Biol Chem 1993;268:12231-12234.

Marques KB, Santos LM, Oliveira AL. Spinal motoneuron synaptic plasticity during the course of an animal model of multiple sclerosis. Eur J Neurosci 2006;24:3053-3062.

Marshall JC. Lipopolysaccharide: an endotoxin or an exogenous hormone? Clin Infect Dis 2005;41 Suppl 7:S470-S480.

Matsumoto Y, Park IK, Hiraki K, Ohtani S, Kohyama K. Role of pathogenic T cells and autoantibodies in relapse and progression of myelin oligodendrocyte glycoprotein-induced autoimmune encephalomyelitis in LEW.1AV1 rats. Immunology 2009;128:e250-e261.

Matsushima GK, Morell P. The neurotoxicant, cuprizone, as a model to study demyelination and remyelination in the central nervous system. Brain Pathol 2001;11:107-116.

Matthews WB, Small DG. Serial recording of visual and somatosensory evoked potentials in multiple sclerosis. J Neurol Sci 1979;40:11-21.

Merrill JE, Ignarro LJ, Sherman MP, Melinek J, Lane TE. Microglial cell cytotoxicity of oligodendrocytes is mediated through nitric oxide. J Immunol 1993;151:2132-2141.

Miller SD, Eagar TN. Functional role of epitope spreading in the chronic pathogenesis of autoimmune and virus-induced demyelinating diseases. Adv Exp Med Biol 2001;490:99-107.

Mohr DC, Hart SL, Julian L, Cox D, Pelletier D. Association between stressful life events and exacerbation in multiple sclerosis: a meta-analysis. BMJ 2004;328:731.

Moncada S, Higgs EA. Nitric oxide and the vascular endothelium. Handb Exp Pharmacol 2006;213-254.

Moreau T, Coles A, Wing M, Isaacs J, Hale G, Waldmann H, Compston A. Transient increase in symptoms associated with cytokine release in patients with multiple sclerosis. Brain 1996;119 (Pt 1):225-237.

Muller DM, Pender MP, Greer JM. A neuropathological analysis of experimental autoimmune encephalomyelitis with predominant brain stem and cerebellar involvement and differences between active and passive induction. Acta Neuropathol 2000;100:174-182.

Murray PD, McGavern DB, Lin X, Njenga MK, Leibowitz J, Pease LR, Rodriguez M. Perforin-dependent neurologic injury in a viral model of multiple sclerosis. J Neurosci 1998;18:7306-7314.

Nave KA, Trapp BD. Axon-glial signaling and the glial support of axon function. Annu Rev Neurosci 2008;31:535-561.

Nogai A, Siffrin V, Bonhagen K, Pfueller CF, Hohnstein T, Volkmer-Engert R, Bruck W, Stadelmann C, Kamradt T. Lipopolysaccharide injection induces relapses of experimental autoimmune encephalomyelitis in nontransgenic mice via bystander activation of autoreactive CD4+ cells. J Immunol 2005;175:959-966.

O'Connor P, Marchetti P, Lee L, Perera M. Evoked potential abnormality scores are a useful measure of disease burden in relapsing-remitting multiple sclerosis. Ann Neurol 1998;44:404-407.

Okuda Y, Nakatsuji Y, Fujimura H, Esumi H, Ogura T, Yanagihara T, Sakoda S. Expression of the inducible isoform of nitric oxide synthase in the central nervous system of mice correlates with the severity of actively induced experimental allergic encephalomyelitis. J Neuroimmunol 1995;62:103-112.

Okuda Y, Sakoda S, Fujimura H, Yanagihara T. Nitric oxide via an inducible isoform of nitric oxide synthase is a possible factor to eliminate inflammatory cells from the central nervous system of mice with experimental allergic encephalomyelitis. J Neuroimmunol 1997;73:107-116.

Okuda Y, Sakoda S, Fujimura H, Yanagihara T. Aminoguanidine, a selective inhibitor of the inducible nitric oxide synthase, has different effects on experimental allergic encephalomyelitis in the induction and progression phase. J Neuroimmunol 1998;81:201-210.

Ou P, Wolff SP. Aminoguanidine: a drug proposed for prophylaxis in diabetes inhibits catalase and generates hydrogen peroxide in vitro. Biochem Pharmacol 1993;46:1139-1144.

Ousman SS, Tomooka BH, van Noort JM, Wawrousek EF, O'Connor KC, Hafler DA, Sobel RA, Robinson WH, Steinman L. Protective and therapeutic role for alphaB-crystallin in autoimmune demyelination. Nature 2007;448:474-479.

Pantano P, Mainero C, Caramia F. Functional brain reorganization in multiple sclerosis: evidence from fMRI studies. J Neuroimaging 2006;16:104-114.

Papadopoulos D, Pham-Dinh D, Reynolds R. Axon loss is responsible for chronic neurological deficit following inflammatory demyelination in the rat. Exp Neurol 2006;197:373-385.

Park HJ, Won CK, Pyun KH, Shin HC. Interleukin 2 suppresses afferent sensory transmission in the primary somatosensory cortex. Neuroreport 1995;6:1018-1020.

Paterson PY. Transfer of allergic encephalomyelitis in rats by means of lymph node cells. J Exp Med 1960;111:119-136.

Paterson PY. Experimental allergic encephalomyelitis: role of fibrin deposition in immunopathogenesis of inflammation in rats. Fed Proc 1976;35:2428-2434.

Pender MP. Demyelination and neurological signs in experimental allergic encephalomyelitis. J Neuroimmunol 1987;15:11-24.

Pender MP. The pathophysiology of acute experimental allergic encephalomyelitis induced by whole spinal cord in the Lewis rat. J Neurol Sci 1988a;84:209-222.

Pender MP. The pathophysiology of myelin basic protein-induced acute experimental allergic encephalomyelitis in the Lewis rat. J Neurol Sci 1988b;86:277-289.

Pender MP. Recovery from acute experimental allergic encephalomyelitis in the Lewis rat. Early restoration of nerve conduction and repair by Schwann cells and oligodendrocytes. Brain 1989;112 (Pt 2):393-416.

Pender MP. Ascending Impairment of Nociception in Rats with Experimental Allergic Encephalomyelitis. Journal of the Neurological Sciences 1986a;75:317-328.

Pender MP. Conduction block due to demyelination at the ventral root exit zone in experimental allergic encephalomyelitis. Brain Res 1986b;367:398-401.

Pender MP, Sears TA. Involvement of the Dorsal Root Ganglion in Acute Experimental Allergic Encephalomyelitis in the Lewis Rat. Journal of the Neurological Sciences 1986;72:231-242.

Pender MP, Sears TA. Conduction block in the peripheral nervous system in experimental allergic encephalomyelitis. Nature 1982;296:860-862.

Pender MP, Sears TA. The pathophysiology of acute experimental allergic encephalomyelitis in the rabbit. Brain 1984;107 (Pt 3):699-726.

Piani D, Frei K, Do KQ, Cuenod M, Fontana A. Murine brain macrophages induced NMDA receptor mediated neurotoxicity in vitro by secreting glutamate. Neurosci Lett 1991;133:159-162.

Pitt D, Werner P, Raine CS. Glutamate excitotoxicity in a model of multiple sclerosis. Nat Med 2000;6:67-70.

Qin L, Wu X, Block ML, Liu Y, Breese GR, Hong JS, Knapp DJ, Crews FT. Systemic LPS causes chronic neuroinflammation and progressive neurodegeneration. Glia 2007;55:453-462.

Rabins PV, Brooks BR, O'Donnell P, Pearlson GD, Moberg P, Jubelt B, Coyle P, Dalos N, Folstein MF. Structural brain correlates of emotional disorder in multiple sclerosis. Brain 1986;109 (Pt 4):585-597.

Raivich G, Banati R. Brain microglia and blood-derived macrophages: molecular profiles and functional roles in multiple sclerosis and animal models of autoimmune demyelinating disease. Brain Res Brain Res Rev 2004;46:261-281.

Ramagopalan SV, Knight JC, Ebers GC. Multiple sclerosis and the major histocompatibility complex. Curr Opin Neurol 2009;22:219-225.

Rasmussen S, Wang Y, Kivisakk P, Bronson RT, Meyer M, Imitola J, Khoury SJ. Persistent activation of microglia is associated with neuronal dysfunction of callosal projecting pathways and multiple sclerosis-like lesions in relapsing--remitting experimental autoimmune encephalomyelitis. Brain 2007;130:2816-2829.

Redford EJ, Kapoor R, Smith KJ. Nitric oxide donors reversibly block axonal conduction: demyelinated axons are especially susceptible. Brain 1997;120 (Pt 12):2149-2157.

Riise T, Mohr DC, Munger KL, Rich-Edwards JW, Kawachi I, Ascherio A. Stress and the risk of multiple sclerosis. Neurology 2011;76:1866-1871.

Rivers TM. Observations on attempts to produce acute disseminated encephalomyelitis in monkeys. J Exp Med 1933;58:39-53.

Rutkove SB. Effects of temperature on neuromuscular electrophysiology. Muscle Nerve 2001;24:867-882.

Ruuls SR, Van Der LS, Sontrop K, Huitinga I, Dijkstra CD. Aggravation of experimental allergic encephalomyelitis (EAE) by administration of nitric oxide (NO) synthase inhibitors. Clin Exp Immunol 1996;103:467-474.

Salle JY, Hugon J, Tabaraud F, Boulesteix JM, Vallat JM, Dumas M, Poser CM. Improvement in motor evoked potentials and clinical course post-steroid therapy in multiple sclerosis. J Neurol Sci 1992;108:184-188.

Salter M, Knowles RG, Moncada S. Widespread tissue distribution, species distribution and changes in activity of Ca(2+)-dependent and Ca(2+)-independent nitric oxide synthases. FEBS Lett 1991;291:145-149.

Schubart A. Aspects of the immunobiology of myelin oligodendrocyte glycoprotein (MOG)- induced experimental autoimmune encephalomyelitis (EAE). 26-10-2001. Ref Type: Thesis/Dissertation

Sedel F, Bechade C, Vyas S, Triller A. Macrophage-derived tumor necrosis factor alpha, an early developmental signal for motoneuron death. J Neurosci 2004;24:2236-2246.

Serres S, Anthony DC, Jiang Y, Broom KA, Campbell SJ, Tyler DJ, van Kasteren SI, Davis BG, Sibson NR. Systemic inflammatory response reactivates immune-mediated lesions in rat brain. J Neurosci 2009;29:4820-4828.

Sharma JN, Al-Omran A, Parvathy SS. Role of nitric oxide in inflammatory diseases. Inflammopharmacology 2007;15:252-259.

Sicher SC, Vazquez MA, Lu CY. Inhibition of macrophage Ia expression by nitric oxide. J Immunol 1994;153:1293-1300.

Sim FJ, Zhao C, Penderis J, Franklin RJ. The age-related decrease in CNS remyelination efficiency is attributable to an impairment of both oligodendrocyte progenitor recruitment and differentiation. J Neurosci 2002;22:2451-2459.

Skundric DS. Experimental models of relapsing-remitting multiple sclerosis: current concepts and perspective. Curr Neurovasc Res 2005;2:349-362.

Skundric DS, Dai R, Zakarian VL, Bessert D, Skoff RP, Cruikshank WW, Kurjakovic Z. Anti-IL-16 therapy reduces CD4+ T-cell infiltration and improves paralysis and histopathology of relapsing EAE. J Neurosci Res 2005;79:680-693.

Smith KJ. Sodium channels and multiple sclerosis: roles in symptom production, damage and therapy. Brain Pathol 2007;17:230-242.

Smith KJ. Conduction properties of central demyelinated and remyelinated axons, and their relation to symptom production in demyelinating disorders. Eye (Lond) 1994;8 (Pt 2):224-237.

Smith KJ, Blakemore WF, McDonald WI. Central remyelination restores secure conduction. Nature 1979;280:395-396.

Smith KJ, Hall SM. Factors directly affecting impulse transmission in inflammatory demyelinating disease: recent advances in our understanding. Curr Opin Neurol 2001;14:289-298.

Smith KJ, Kapoor R, Hall SM, Davies M. Electrically active axons degenerate when exposed to nitric oxide. Ann Neurol 2001;49:470-476.

Smith KJ, Lassmann H. The role of nitric oxide in multiple sclerosis. Lancet Neurol 2002;1:232-241.

Solomon AJ, Whitham RH. Multiple sclerosis and vitamin D: a review and recommendations. Curr Neurol Neurosci Rep 2010;10:389-396.

Stanley GP, Pender MP. The pathophysiology of chronic relapsing experimental allergic encephalomyelitis in the Lewis rat. Brain 1991;114 (Pt 4):1827-1853.

Steinman L. Immune therapy for autoimmune diseases. Science 2004;305:212-216.

Stoll G, Muller S, Schmidt B, van der MP, Jung S, Toyka KV, Hartung HP. Localization of interferon-gamma and Ia-antigen in T cell line-mediated experimental autoimmune encephalomyelitis. Am J Pathol 1993;142:1866-1875.

Storch MK, Stefferl A, Brehm U, Weissert R, Wallstrom E, Kerschensteiner M, Olsson T, Linington C, Lassmann H. Autoimmunity to myelin oligodendrocyte glycoprotein in rats mimics the spectrum of multiple sclerosis pathology. Brain Pathol 1998;8:681-694.

Strassmann G, Fong M, Kenney JS, Jacob CO. Evidence for the involvement of interleukin 6 in experimental cancer cachexia. J Clin Invest 1992;89:1681-1684.

Stromnes IM, Goverman JM. Active induction of experimental allergic encephalomyelitis. Nat Protoc 2006;1:1810-1819.

Stuehr DJ, Marletta MA. Induction of nitrite/nitrate synthesis in murine macrophages by BCG infection, lymphokines, or interferon-gamma. J Immunol 1987;139:518-525.

Stys PK, Waxman SG, Ransom BR. Na(+)-Ca2+ exchanger mediates Ca2+ influx during anoxia in mammalian central nervous system white matter. Ann Neurol 1991;30:375-380.

Su KG, Banker G, Bourdette D, Forte M. Axonal degeneration in multiple sclerosis: the mitochondrial hypothesis. Curr Neurol Neurosci Rep 2009;9:411-417.

Tancredi V, D'Arcangelo G, Grassi F, Tarroni P, Palmieri G, Santoni A, Eusebi F. Tumor necrosis factor alters synaptic transmission in rat hippocampal slices. Neurosci Lett 1992;146:176-178.

Thomsen LL, Scott JM, Topley P, Knowles RG, Keerie AJ, Frend AJ. Selective inhibition of inducible nitric oxide synthase inhibits tumor growth in vivo: studies with 1400W, a novel inhibitor. Cancer Res 1997;57:3300-3304.

Tracey KJ, Wei H, Manogue KR, Fong Y, Hesse DG, Nguyen HT, Kuo GC, Beutler B, Cotran RS, Cerami A, . Cachectin/tumor necrosis factor induces cachexia, anemia, and inflammation. J Exp Med 1988;167:1211-1227.

Trapp BD, Nave KA. Multiple sclerosis: an immune or neurodegenerative disorder? Annu Rev Neurosci 2008;31:247-269.

Tuohy VK, Yu M, Yin L, Kawczak JA, Johnson JM, Mathisen PM, Weinstock-Guttman B, Kinkel RP. The epitope spreading cascade during progression of experimental autoimmune encephalomyelitis and multiple sclerosis. Immunol Rev 1998;164:93-100.

Uhthoff. Untersuchungen Uber Die Bei Der Multiplen Herdsklerose Vorkommenden Augenstorungen. Arch Psychiair Nervenkrank 1890;21:53-116.

Van Dam AM, Bauer J, Man AHW, Marquette C, Tilders FJ, Berkenbosch F. Appearance of inducible nitric oxide synthase in the rat central nervous system after rabies virus infection and during experimental allergic encephalomyelitis but not after peripheral administration of endotoxin. J Neurosci Res 1995;40:251-260.

van d, V, Hinton DR, Incardonna F, Hofman FM. Extensive peroxynitrite activity during progressive stages of central nervous system inflammation. J Neuroimmunol 1997;77:1-7.

Varma TK, Lin CY, Toliver-Kinsky TE, Sherwood ER. Endotoxin-induced gamma interferon production: contributing cell types and key regulatory factors. Clin Diagn Lab Immunol 2002;9:530-543.

Vogt J, Paul F, Aktas O, Muller-Wielsch K, Dorr J, Dorr S, Bharathi BS, Glumm R, Schmitz C, Steinbusch H, Raine CS, Tsokos M, Nitsch R, Zipp F. Lower motor neuron loss in multiple sclerosis and experimental autoimmune encephalomyelitis. Ann Neurol 2009;66:310-322.

WAKSMAN BH, ADAMS RD. Allergic neuritis: an experimental disease of rabbits induced by the injection of peripheral nervous tissue and adjuvants. J Exp Med 1955;102:213-236.

Watanabe M, Toyama Y, Nishiyama A. Differentiation of proliferated NG2-positive glial progenitor cells in a remyelinating lesion. J Neurosci Res 2002;69:826-836.

Waxman SG. Demyelination in spinal cord injury. J Neurol Sci 1989;91:1-14.

Waxman SG. Clinical course and electrophysiology of multiple sclerosis. Adv Neurol 1988;47:157-184.

Waxman SG, Black JA, Ransom BR, Stys PK. Anoxic injury of rat optic nerve: ultrastructural evidence for coupling between Na+ influx and Ca(2+)-mediated injury in myelinated CNS axons. Brain Res 1994;644:197-204.

Waxman SG, Ritchie JM. Molecular dissection of the myelinated axon. Ann Neurol 1993;33:121-136.

Weiss N, Hasboun D, Demeret S, Fontaine B, Bolgert F, Lyon-Caen O, Chabas D. Paroxysmal hypothermia as a clinical feature of multiple sclerosis. Neurology 2009;72:193-195.

White KD, Scoones DJ, Newman PK. Hypothermia in multiple sclerosis. J Neurol Neurosurg Psychiatry 1996;61:369-375.

Willenborg DO, Staykova M, Fordham S, O'Brien N, Linares D. The contribution of nitric oxide and interferon gamma to the regulation of the neuro-inflammation in experimental autoimmune encephalomyelitis. J Neuroimmunol 2007;191:16-25.

Witte ME, Geurts JJ, de Vries HE, van d, V, van HJ. Mitochondrial dysfunction: a potential link between neuroinflammation and neurodegeneration? Mitochondrion 2010;10:411-418.

Wolswijk G, Balesar R. Changes in the expression and localization of the paranodal protein Caspr on axons in chronic multiple sclerosis. Brain 2003;126:1638-1649.

Xiao BG, Zhang GX, Ma CG, Link H. The cerebrospinal fluid from patients with multiple sclerosis promotes neuronal and oligodendrocyte damage by delayed production of nitric oxide in vitro. J Neurol Sci 1996;142:114-120.

Youl BD, Turano G, Miller DH, Towell AD, MacManus DG, Moore SG, Jones SJ, Barrett G, Kendall BE, Moseley IF, . The pathophysiology of acute optic neuritis. An association of gadolinium leakage with clinical and electrophysiological deficits. Brain 1991;114 (Pt 6):2437-2450.

Zabaleta ME, Bianco NE, De Sanctis JB. serum nitric oxide products in patients with multiple sclerosis: relationship with clinical activity. Med Sci Res 1998;26:373-374.

Zandieh S, Hopf R, Redl H, Schlag MG. The effect of ketamine/xylazine anesthesia on sensory and motor evoked potentials in the rat. Spinal Cord 2003;41:16-22.

Zhao W, Tilton RG, Corbett JA, McDaniel ML, Misko TP, Williamson JR, Cross AH, Hickey WF. Experimental allergic encephalomyelitis in the rat is inhibited by aminoguanidine, an inhibitor of nitric oxide synthase. J Neuroimmunol 1996;64:123-133.

Zhou HH, Jin TT, Qin B, Turndorf H. Suppression of spinal cord motoneuron excitability correlates with surgical immobility during isoflurane anesthesia. Anesthesiology 1998;88:955-961.

Zhou HH, Mehta M, Leis AA. Spinal cord motoneuron excitability during isoflurane and nitrous oxide anesthesia. Anesthesiology 1997;86:302-307.

Zhu B, Luo L, Moore GR, Paty DW, Cynader MS. Dendritic and synaptic pathology in experimental autoimmune encephalomyelitis. Am J Pathol 2003;162:1639-1650.

Zielasek J, Jung S, Gold R, Liew FY, Toyka KV, Hartung HP. Administration of nitric oxide synthase inhibitors in experimental autoimmune neuritis and experimental autoimmune encephalomyelitis. J Neuroimmunol 1995;58:81-88.